AD-A151 176 DEVELOPMENT OF A DYNAMIC FINITE ELEMENT MODEL FOR UNRESTRAINED FLEXIBLE S..(U) MARYLAND UNIV COLLEGE PARK DEPT OF AEROSPACE ENGINEERING E R CHRISTENSEN ET AL. 1/2

UNCLASSIFIED OCT 84 AFOSR-TR-85-0183 AFOSR-82-0296 F/G 12/1 NL

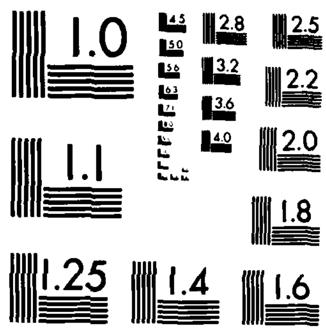
1.0
1.1
1.25
1.4
1.6
1.8
2.0
2.2
2.5
2.8
3.2
3.6
4.0

AFOSR-TR- 85-0183

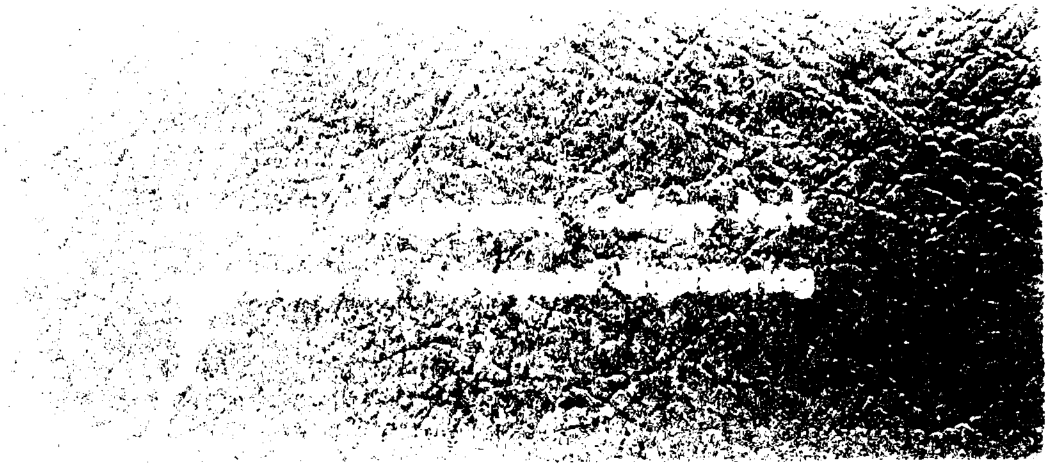

DEVELOPMENT OF A DYNAMIC FINITE ELEMENT MODEL FOR UNRESTRAINED FLEXIBLE STRUCTURES

E. R. Christensen
S. W. Lee

Department of Aerospace Engineering
University of Maryland
College Park, Maryland 20742

October 1984

Prepared for

AIR FORCE OFFICE OF SCIENTIFIC RESEARCH
UNITED STATES AIR FORCE
UNDER

GRANT NO. AFOSR-82-0296

Unclassified

SECURITY CLASSIFICATION OF THIS PAGE (When Data Entered)

REPORT DOCUMENTATION PAGE		READ INSTRUCTIONS BEFORE COMPLETING FORM
1. REPORT NUMBER AFOSR-TR- 85-0183	2. GOVT ACCESSION NO.	3. RECIPIENT'S CATALOG NUMBER
4. TITLE (and Subtitle) Development of a Dynamic Finite Element Model for Unrestrained Flexible Structures		5. TYPE OF REPORT & PERIOD COVERED Final Sept. 1, 1982 - June 30, 1984
		6. PERFORMING ORG. REPORT NUMBER
7. AUTHOR(s) E. R. Christensen, S. W. Lee		8. CONTRACT OR GRANT NUMBER(s) AFOSR-82-0296
9. PERFORMING ORGANIZATION NAME AND ADDRESS Department of Aerospace Engineering, University of Maryland, College Park, MD 20742		10. PROGRAM ELEMENT, PROJECT, TASK AREA & WORK UNIT NUMBERS 61102F 2307/B1
11. CONTROLLING OFFICE NAME AND ADDRESS Air Force Office of Scientific Research /NA, Bldg. 410, Bolling AFB, DC 20332-6448		12. REPORT DATE Oct. 1984
		13. NUMBER OF PAGES 141
14. MONITORING AGENCY NAME & ADDRESS (if different from Controlling Office)		15. SECURITY CLASS. (of this report) Unclassified
		15a. DECLASSIFICATION/DOWNGRADING SCHEDULE

16. DISTRIBUTION STATEMENT (of this Report)

Approved for public release; distribution unlimited.

17. DISTRIBUTION STATEMENT (of the abstract entered in Block 20, if different from Report)

18. SUPPLEMENTARY NOTES

19. KEY WORDS (Continue on reverse side if necessary and identify by block number)

Finite element method
Unrestrained flexible structures
Space structures
Large deflection
Three dimensional beam element

20. ABSTRACT (Continue on reverse side if necessary and identify by block number)

An efficient finite element model and solution technique have been developed for the analysis of unrestrained flexible structures undergoing large elastic deformations coupled with gross nonsteady translational and rotational motions with respect to an inertial reference frame. The nonlinear coupled differential equations resulting from the finite element approximation are integrated timewise using an implicit-explicit split operator numerical integration scheme which treats the stability sensitive terms of the equation

DD FORM 1 JAN 73 1473 EDITION OF 1 NOV 65 IS OBSOLETE

S/N 0102-014-6601

Unclassified

SECURITY CLASSIFICATION OF THIS PAGE (When Data Entered)

20. Cont.

implicitly while the rest of the equation is treated explicitly. The motion of simple spacecraft structures consisting of flexible beams attached to rigid masses and including the effect of control forces has been studied using three-node eighteen-degree-of-freedom three dimensional beam elements based on the total Lagrangian description.

AFOSR TR

DEVELOPMENT OF A DYNAMIC FINITE ELEMENT MODEL FOR UNRESTRAINED FLEXIBLE STRUCTURES

E. R. Christensen
S. W. Lee

Department of Aerospace Engineering
University of Maryland
College Park, Maryland 20742

October, 1984

PREPARED FOR

Air Force Office of Scientific Research

United States Air Force

UNDER

Grant No. AFOSR-82-0296

APPROVED FOR PUBLIC RELEASE; DISTRIBUTION UNLIMITED.

ACKNOWLEDGEMENT

This research task was supported by the U.S. Air Force Office of Scientific Research (Grant No. AFOSR-82-0296) with Dr. Anthony K. Amos as the program monitor.

The work was conducted by the Department of Aerospace Engineering, University of Maryland, College Park, Maryland.

The bulk of computing time was provided by the Computer Science Center of the University of Maryland.

ABSTRACT

An efficient finite element model and solution technique have been developed for the analysis of unrestrained flexible structures undergoing large elastic deformations coupled with gross nonsteady translational and rotational motions with respect to an inertial reference frame. The nonlinear coupled differential equations resulting from the finite element approximation are integrated timewise using an implicit-explicit split operator numerical integration scheme which treats the stability sensitive terms of the equation implicitly while the rest of the equation is treated explicitly. The motion of simple spacecraft structures consisting of flexible beams attached to rigid masses and including the effect of control forces has been studied using three-node eighteen-degree-of-freedom three dimensional beam elements based on the total Lagrangian description.

Additional keywords: Space structures, equations of motion, Stiffness matrix, flexible spacecraft.

TABLE OF CONTENTS

CHAPTER			Page

LIST OF TABLES

LIST OF FIGURES

The velocity vector is defined as follows:

$$\dot{\underline{u}} = \lim_{\Delta t \to 0} \frac{\Delta \underline{u}}{\Delta t} \tag{2.11}$$

Substituting eq. (2.10) into eq. (2.11),

$$\dot{\underline{u}} = \lim_{\Delta t \to 0} \underline{N}^* \frac{\Delta \underline{q}}{\Delta t} \tag{2.12}$$

But

$$\dot{\underline{q}} = \lim_{\Delta t \to 0} \frac{\Delta \underline{q}}{\Delta t} \tag{2.13}$$

Thus $\dot{\underline{u}} = \underline{N}^* \dot{\underline{q}}$ (2.14)

Similarly,

$$\ddot{\underline{u}} = \underline{N}^* \ddot{\underline{q}} + \dot{\underline{N}}^* \dot{\underline{q}} \approx \underline{N}^* \ddot{\underline{q}} \tag{2.15}$$

noting that $\dot{\underline{N}}^* \dot{\underline{q}}$ is either zero for solid elements or very small in the case of beam, plate, or shell elements.

2.4 Conservation of Linear Momentum

If $\underline{F}_T$ is the sum total of applied forces on the body, then conservation of linear momentum requires that the following equation be satisfied:

$$\frac{d}{dt} \int_V \rho \frac{d\underline{R}}{dt} dv = \int_V \rho \frac{d^2\underline{R}}{dt^2} dv = \underline{F}_T \tag{2.16}$$

In eq. (2.16), the integral is defined over the original undeformed configuration. Substituting the expression for acceleration eq. (2.8) into eq. (2.16) and using eqs. (2.14) and (2.15), eq. (2.16) becomes

$$M(\dot{\underline{V}}_o + \underline{\overline{\Omega}}\, V_o) + \underline{P}^T \ddot{\underline{q}} + \underline{G}\, \dot{\underline{\Omega}} + 2\, \underline{\overline{\Omega}}\, \underline{P}^T \dot{\underline{q}} + \underline{f}_c = \underline{F}_T \tag{2.17}$$

$$\bar{\underline{A}} = \begin{bmatrix} 0 & -A_3 & A_2 \\ A_3 & 0 & -A_1 \\ -A_2 & A_1 & 0 \end{bmatrix} \qquad (2.7b)$$

where

Applying equations (2.7) to equation (2.6), the cross products can be replaced as follows:

$$\frac{d^2\underline{R}}{dt^2} = \dot{\underline{V}}_o + \bar{\underline{\Omega}}\,\underline{V}_o + \ddot{\underline{u}} + \dot{\bar{\underline{\Omega}}}\,\underline{r} + 2\bar{\underline{\Omega}}\,\dot{\underline{u}} + \bar{\underline{\Omega}}^2\,\underline{r} \qquad (2.8)$$

2.3 Finite Element Expression for Velocity and Acceleration

In the finite element method, the structure being analyzed is divided into a finite number of sections or elements. Within each element the exact displacement $\underline{u}$ is approximated by polynomials containing unknown constants which generally represent the displacement at a finite number of points or nodes within the element and on its boundaries. It is these nodal displacements which are solved for. For time dependent problems, the displacement $\underline{u}$ can be written in an incremental form as

$$\underline{u} = {}^t\underline{u} + \Delta\underline{u} \qquad (2.9)$$

In equation (2.9), ${}^t\underline{u}$ represents the value of $\underline{u}$ at time t while $\Delta\underline{u}$ is the change in displacement between time t and t + Δt. In the finite element formulation the value of $\Delta\underline{u}$ within each element can be expressed as

$$\Delta\underline{u} = \underline{N}^* \;\Delta\underline{q} \qquad (2.10)$$

Here $\Delta\underline{q}$ is the nodal displacement vector and $\underline{N}^*$ is the matrix of shape functions and is a function of a set of local coordinates within each element as well as the initial angular displacements. The determination of $\underline{N}^*$ is given in Chapter III.

In order to express the motion in terms of the rotating body axes, it is necessary to express the acceleration of point P in terms of body axis coordinates. Thus the following expression for the acceleration is used:

$$\frac{d^2\underline{R}}{dt^2} = \frac{d\underline{V}_o}{dt} + \ddot{\underline{r}} + \dot{\underline{\Omega}} \times \underline{r} + 2\, \underline{\Omega} \times \dot{\underline{r}} + \underline{\Omega} \times (\underline{\Omega} \times \underline{r}) \tag{2.2}$$

where $\frac{d\underline{V}_o}{dt}$ = the acceleration of the origin of the body axis

$\dot{\underline{r}}$ = the velocity of the material point p relative to the body axis

$\ddot{\underline{r}}$ = the acceleration of the material point P relative to the body axis

$\dot{\underline{\Omega}} \times \underline{r}$ = the "tangential" acceleration

$2\underline{\Omega} \times \dot{\underline{r}}$ = the Coriolis acceleration

$\underline{\Omega} \times (\underline{\Omega} \times \underline{r})$ = the centripetal acceleration

In terms of the body axis coordinates,

$$\frac{d\underline{V}_o}{dt} = \dot{\underline{V}}_o + \underline{\Omega} \times \underline{V}_o \tag{2.3}$$

Also note that since $\dot{\underline{r}}_o = \ddot{\underline{r}}_o = 0$,

$$\dot{\underline{r}} = \dot{\underline{u}} \tag{2.4}$$

$$\ddot{\underline{r}} = \ddot{\underline{u}} \tag{2.5}$$

Substituting equations (2.3) - (2.5) into equation (2.2),

$$\frac{d^2\underline{R}}{dt^2} = \dot{\underline{V}}_o + \underline{\Omega} \times \underline{V}_o + \ddot{\underline{u}} + \dot{\underline{\Omega}} \times \underline{r} + 2\underline{\Omega} \times \dot{\underline{u}} + \underline{\Omega} \times (\underline{\Omega} \times \underline{r}) \tag{2.6}$$

In order to simplify equation (2.6) a bit, the cross products can be replaced by matrix products. If $\underline{A}$ and $\underline{B}$ are any 3-vectors, then

$$\underline{A} \times \underline{B} = \bar{\underline{A}}\, \underline{B} \tag{2.7}$$

CHAPTER II

EQUATIONS OF MOTION

2.1 Introduction

For elastic structures undergoing gross translational and angular motion as well as small or large elastic deformations the motion can be described by the following three sets of equations:

1. The conservation of linear momentum which is a vector equation describing the gross translational motion.
2. The conservation of angular momentum which is a vector equation describing the gross rotational motion.
3. The principle of virtual work which describes the deformations.

If the structure is very flexible, the deformed configuration may be quite different from the original undeformed configuration. Thus the elastic deformations will be coupled with the gross translations and rotations, especially if the applied loads are deformation or velocity dependent.

2.2 Geometry and Kinematics

Consider the deformable body pictured in Fig. 1. A set of mutually orthogonal axes, x_1, x_2, and x_3 are fixed in the undeformed body at point O. Point O is located a distance $\underline{R}_0$ from a set of mutually orthogonal inertial axes X_1, X_2, X_3, centered at point C. The body axes are translating with velocity $\underline{V}_0$ and rotating with angular velocity $\underline{\Omega}$ relative to the inertial axes. A point P located a distance $\underline{r}_0$ from O displaces by $\underline{u}$ to point P' as the body deforms so that it is now a distance $\underline{r}$ from O. Point P' is located a distance $\underline{R}$ from C where $\underline{R}$ is as follows:

$$\underline{R} = \underline{R}_0 + \underline{r} = \underline{R}_0 + \underline{r}_0 + \underline{u} \tag{2.1}$$

flexible structures which are undergoing large elastic deformations coupled with gross nonsteady rigid body translational and rotational motions with respect to an inertial reference.

The formation and solution scheme used for this research can be briefly described as follows. The governing equations of motion are derived using momentum conservation principles and the principle of virtual work. The finite element approximation is applied to the equations of motion and a matrix form of those equations is obtained. The resulting set of second order matrix differential equations is solved timewise by direct numerical time integration using an implicit-explicit split operator scheme. This scheme treats the terms which control the stability of the solution implicitly while the terms which are less sensitive to stability are treated explicitly. The solution technique developed is tested on simple spacecraft consisting of long slender uniform beams attached to a rigid mass and modeled by three dimensional beam elements. The effects of control forces on the motion of the spacecraft are also considered.

not the associated modal generalized forces vanish identically. McDonough [3] considered the formulation of the global equations of motion of an unrestrained deformable body using translating and rotating reference frames. The motion of the body (including deformations) is of unrestricted magnitude in the analysis. Fraejis de Veubeke [4] considered the motion of a flexible body undergoing arbitrarily large rotations with respect to an inertial frame. The motion was split into a mean rigid body motion and a relative motion taking into account the deformtions. This mean rigid body motion is chosen so as to minimize the mean square of relative displacements. Kane and Levinson [5,6] considered different methods for formulating the equations of motion for complex flexible spacecraft. These methods included momentum principles, D'Alembert's Principle, and Lagrange's equations, among others. They also developed an algorithm for producing numerical simulations of large motions of a nonuniform flexible cantilever beam in orbit using the finite element method. Santini [7] has studied the stability of both nonspinning and spinning flexible spacecraft in a gravitational field by the superposition of a rigid motion plus a combination of structural modes. Other investigtors [8-17] have also studied these types of problems using both general analyses or in connection with more specific types of flexible spacecraft. It appears however that, in spite of the progress made in the analysis of such problems, little attention has been paid to the development of the finite element method for the dynamics of unrestrained structures undergoing large elastic deformations coupled with nonsteady gross translational and rotational motions.

With these problems in mind, the objective of this research is to use the finite element method to determine the time response of unrestrained

CHAPTER I

INTRODUCTION

In order to predict the motion of many types of flexible spacecraft, it is necessary to accurately simulate the time response of an unrestrained structure which is undergoing large elastic deformations as well as gross nonsteady rigid body translations and rotations. For such structures, the large elastic deformations are coupled with the rigid body motions resulting in a complicated set of nonlinear differential equations. Such spacecraft may be simple enough to be modeled as rigid bodies supporting flexible beams or they may be more complicated structures consisting of frames, plates and shells in combination with one or more rigid bodies. For example, consider a large space structure consisting of a frame made up of long, slender, flexible beams connected to one or more rigid masses. If such a spacecraft were to execute a sudden rotational maneuver or reorientation, then large elastic deformations coupled with rigid body motion would occur. An accurate time response analysis of the motion of the structure would be necessary in order to predict the orientation of the structure especially if it were necessary to determine the pointing accuracy of any sensors which may be attached to the spacecraft.

Extensive research has been done in the field of the dynamics of flexible spacecraft. The motion of unrestrained flexible structures has been discussed by Bisplinghoff and Ashley [1] who considered small vibrations of aircraft structures using a modal technique. Ashley [2] also studied gravitational excitation of very simple elastic spacecraft under the restriction of infinitesimal elastic displacements as well as categorizing typical free-free structural configurations according to whether or

$\underline{\phi}$	A vector the components of which are the time integrals of $\underline{\Omega}$
ψ, θ, ζ	Euler angles
$\underline{\Omega}$	Body axis angular velocity
ω	Circular frequency
ω_d	Damped natural frequency
ω_{max}	Maximum natural frequency
Ω_o	A reference angular velocity

${}^{0}\underline{u}_o$	Initial displacement of the $\underline{a}_1,\underline{a}_2,\underline{a}_3$ axes
V	Volume of the undeformed body
$\underline{V}_o$	Body axis velocity
$\underline{V}_T$	Velocity of the beam tip
x_1,x_2,x_3	Body axis coordinates
X_1,X_2,X_3	Inertial axis coordinates
x,y,z	The $\underline{a}_1,\underline{a}_2,\underline{a}_3$ axis coordinates

GREEK SYMBOLS

α	A factor used in computing orientation angles
β	Shear factor A factor used in computing orientation angles The angle between the orbital radius vector and the x_1 axis
γ	A scalar constant Angle between angular velocity vector and x_1 axis
δ	Variational operator
$\Delta\underline{\varepsilon}$	Linear portion of incremental Green strain vector
$\Delta\underline{\varepsilon}^{\ell}$	Local $\Delta\underline{\varepsilon}$ vector
$\Delta\underline{\eta}$	Nonlinear portion of incremental Green strain vector
$\Delta\underline{\eta}^{\ell}$	Local $\Delta\underline{\eta}$ vector
θ	Orientation angles
$\theta_1,\theta_2,\theta_3$	Space-three: 1-2-3 angles
${}^{0}\theta_i$	Initial Value of θ_i
$\Delta\theta_i$	Incremental change in θ_i
θ_{Ref}	A reference orientation angle
λ	Precession rate
μ	Gravitational gradient damping parameter
μ_o	Gravitational constant of the Earth
ξ	The normalized local coordinates along the beam axis
ξ_d	Damping constant
ρ	Mass density

$\underline{r}$	Body axis position vector of a material point at time t
$\underline{R}_o$	Inertial position vector of the body axis origin
$\underline{r}_o$	Body axis position vector of a material point at time t = 0
$\underline{r}_G$	Instantaneous center of mass location in body axis coordinates
$\underline{r}_p$	Position vector of a point in the cross section of the undeformed beam in terms of the $\underline{a}_1, \underline{a}_2, \underline{a}_3$ axes
$\underline{r}'_p$	Position vector of a point in the cross section of the deformed beam in terms of the $\underline{a}'_1, \underline{a}'_2, \underline{a}'_3$ axes.
$\underline{r}_T$	Position vector of the beam tip
$\underline{S}$	Second Pyola-Kirchhoff stress vector
$\Delta\underline{S}$	Incremental Pyola-Kirchhoff stress vector
${}^0\underline{S}$	Initial Pyola-Kirchhoff stress vector
$\underline{S}^\ell$	Local Pyola-Kirchhoff stress vector
${}^0\underline{S}^\ell$	Local initial Pyola-Kirchhoff stress vector
${}^0\underline{S}_o, {}^0\underline{S}_y, {}^0\underline{S}_z$	The constant, y, and z components of ${}^0\underline{S}$
S_σ	Portion of the body surface over which tractions are applied
t	Time
$\underline{T}$	Transformation matrix between the local and global coordinates
$\underline{\mathbf{T}}$	Applied surface force vector
Δt	Time step increment
T_{MOM}	Time period during which a moment is applied
t_n	Time at state n
T_o	A time period
Tol	Convergence tolerance
$\underline{u}$	Displacement of a material point
${}^0\underline{u}$	Initial displacement vector
$\Delta\underline{u}$	Incremental displacement vector
$\underline{u}_o$	Displacement of the $\underline{a}_1, \underline{a}_2, \underline{a}_3$ axes

$\underline{M}_{cent}$	Moment due to centrifugal force
$\underline{M}_{cent_R}$	Moment due to the centrifugal force acting on the rigid mass
$\underline{M}_{cor}$	Moment due to the Coriolis force
$\underline{M}_G$	Generalized mass matrix Applied moment due to the gravitational gradient
m_R	Mass of the rigid mass
$\underline{M}_T$	Total of applied moments about the inertial axes
$\underline{m}_T$	A vector representing the right hand side of the momentum equation
$\underline{M}_o$	Total of applied moment about the body axes
$\underline{M}_o,\underline{M}_y,\underline{M}_z$	The constant, y, and z components of the mass matrix
$\underline{M}_\theta$	A matrix relating the angular velocities to the time derivatives of the orientation angles
N	Total number of elements
n	Refers to the state of the body at $t = t_n$
$\underline{N}^*$	Matrix of shape functions
$\underline{N}^*_o,\underline{N}^*_y,\underline{N}^*_z$	The constant, y, and z components of the shape function matrix
p	Gravity gradient frequency
$\underline{P}$	Matrix coupling the nodal acceleration with the body axis acceleration
$\underline{P}_s$	Matrix of initial stresses
$\underline{P}_{s_o},\underline{P}_{s_y},\underline{P}_{s_z}$	The constant, y, and z components of the $\underline{P}_s$ matrix
$\underline{P}_o$	A submatrix of $\underline{P}_s$
$\underline{q}$	Nodal displacement vector
$\Delta\underline{q}$	Incremental nodal displacement vector
${}^o\underline{q}$	Initial nodal displacement vector
$\underline{q}_G$	Generalized nodal displacement vector
$\tilde{\underline{q}}_G$	Predicted value of generalized nodal displacements
$\underline{R}$	Inertial position vector of a material point at time t

G	Shear modulus
$\underline{G}$	Matrix of the instantaneous center of mass of the body
$\underline{H}$	Coupling inertia matrix between the nodal acceleration and the angular acceleration of the body axes
$\underline{H}_A$	Angular momentum vector
$\underline{H}_D$	Angular momentum due to the displacements of the beam
$\underline{H}_{D_o}$	The value of $\underline{H}_D$ at $t = T_o$
H_j	The $j^{\underline{th}}$ Gaussian integration point weighting factor
h_o, h_{o_y}, h_{o_z}	Parameters used in calculating the $\underline{D}_\varepsilon$ matrix
I_B	Mass moment of inertia of the beam
I_R	Mass moment of inertia of the rigid body
$\underline{I}_T$	Instantaneous mass moment of inertia matrix
I_{yy}, I_{zz}	Undeformed beam element area moments of inertia
$\underline{I}_3$	The 3 x 3 identity matrix
$\underline{J}$	Jacobian Matrix
$\underline{K}$	Basic stiffness matrix
$\underline{K}_E$	Total elastic stiffness matrix
$\underline{K}_{GE}$	Generalized stiffness matrix
$\underline{K}_G^*$	Effective stiffness matrix
$\underline{K}_s$	Initial stress stiffness matrix
K_T, K_W	Control force constants
ℓ	Beam element length
L_β	Control constant
L_{ij}	Element of the Jacobian matrix
o_ℓ, y_ℓ, z_ℓ	Parameters used in calculating the $\underline{D}_\varepsilon$ matrix
M	Total mass of the body
$\underline{M}$	Mass matrix
M_c	Control constant

$\underline{D}_{\varepsilon}$	The matrix relating the $\underline{\Delta\varepsilon}$ vector to the derivatives of the incremental displacements
$\underline{D}_{\varepsilon o}, \underline{D}_{\varepsilon y}, \underline{D}_{\varepsilon z}$	The constant, y, and z components of the $\underline{D}_{\varepsilon}$ matrix
E_1, E_o	Young's modulus
$\underline{E}$	Green strain vector
E_{ij}	The ij$\underline{th}$ Component of the Green strain tensor
${}^{0}\underline{E}$	Green strain vector at state i
$\Delta\underline{E}$	Incremental change in the Green strain vector
ΔE_{ij}	Incremental change in ij$\underline{th}$ component of the Green strain tensor
$\delta\underline{E}$	The virtual Green strain vector
δE_{ij}	The ij$\underline{th}$ component of the virtual Green strain tensor
$\underline{E}^{\ell}$	The local Green strain vector
$\underline{F}$	Applied body and inertial force vector
$\underline{F}_B$	Nodal applied body force vector
$\underline{F}_b$	Applied body force term excluding inertia terms
$\underline{F}_c$	Force vector in displacement equation due to centripetal acceleration Applied control force
$\underline{f}_c$	Force vector in linear momentum equation due to the centripetal acceleration
$\underline{F}_G$	Generalized force vector
$\underline{F}_G^*$	Effective force vector
$\underline{F}_q$	A vector representing the right hand side of the displacement equation
$\underline{F}_s$	Initial stress force vector
$\underline{F}_T$	Vector of applied forces
$\underline{f}_T$	A vector representing the right hand side of the linear momentum equation
$\underline{F}_o$	Vector of applied nodal forces

LIST OF SYMBOLS

A	Undeformed beam element cross-sectional area
a_i	The $i^{\underline{th}}$ gaussian integration point
A_n	Higher order terms in the virtual work integral
$\underline{A}$	The matrix which relates the derivatives of the displacements to the nodal displacement vector
$\underline{A}_o, \underline{A}_y, \underline{A}_z$	The constant, y and z components of the $\underline{A}$ matrix
$\underline{a}_1, \underline{a}_2, \underline{a}_3$	A set of mutually orthogonal axes fixed in the undeformed beam
$\underline{a}_1', \underline{a}_2', \underline{a}_3'$	A set of mutually orthogonal axes fixed in the deformed beam
${}^0\underline{a}_1', {}^0\underline{a}_2', {}^0\underline{a}_3'$	The values of $\underline{a}_1', \underline{a}_2', \underline{a}_3'$ for state i
$\underline{B}$	Matrix which relates the incremental nodal displacements with the incremental strains
$\underline{B}_i$	The $i^{\underline{th}}$ component of the $\underline{B}$ matrix
$\underline{B}^{\ell}$	The local $\underline{B}$ matrix
$\underline{B}_s$	Matrix which relates the incremental nodal displacements to the initial stresses
$\underline{B}_{s_i}$	The $i^{\underline{th}}$ component of the $\underline{B}_s$ matrix
$\underline{B}_s^{\ell}$	The local $\underline{B}_s$ matrix
$\underline{C}$	The gyroscopic matrix The material property matrix
$\underline{C}_o, \underline{C}_y, \underline{C}_z$	The constant, y and z components of the gyroscopic matrix
$\underline{C}^{\ell}$	The local material property matrix
$\underline{C}_D$	Direction cosine matrix
$\underline{D}$	The y component of the matrix of orientation angles
$\underline{d}$	A vector the components of which are the time integrals of $\underline{V}_o$
$\underline{D}^k$	The $k^{\underline{th}}$ partition of the $\underline{A}$ matrix
$\underline{D}_o^k, \underline{D}_y^k, \underline{D}_z^k$	The constant, y, and z components of the $\underline{D}^k$ matrix

where

$$\underline{M} = \int_V \rho \, dv = \text{Total mass of body} \tag{2.18}$$

$$\underline{P}^T = \sum_{i=1}^{N} \int_{V_i} \rho \, \underline{N}^* \, dv \tag{2.19}$$

$$\underline{G} = - \int_V \rho \, \underline{\bar{r}} \, dv \tag{2.20}$$

$$\underline{f}_c = \underline{\bar{\Omega}}^2 \int_V \rho \, \underline{r} \, dv \tag{2.21}$$

The nodal accelerations $\ddot{\underline{q}}$ are coupled with the translation of the body axes and the $\underline{P}$ matrix represents the mass of the finite elements in the coupling terms. Note that $\underline{P}$ is the summation or assembly over all N finite elements. The elements of the $\underline{G}$ matrix represent the location of the instantaneous center of mass. The $\underline{f}_c$ vector is the force due to the centripetal acceleration. Details of the $\underline{P}$, $\underline{G}$, and $\underline{f}_c$ matrices are given in Appendix C. Rewriting eq. (2.18) with all the acceleration terms grouped together results in the following:

$$\underline{P}^T \ddot{\underline{q}} + \underline{G}^T \dot{\underline{\Omega}} + M \dot{\underline{V}}_o = \underline{f}_T \tag{2.22}$$

where

$$\underline{f}_T = \underline{F}_T - M \underline{\bar{\Omega}} \, \underline{V}_o - 2 \, \underline{\bar{\Omega}} \, \underline{P}^T \dot{\underline{q}} - \underline{f}_c \tag{2.23}$$

2.5 Conservation of Angular Momentum

If $\underline{M}_T$ is the sum total of the applied moments about the inertial axes, then the conservation of angular momentum requires that the following equation be satisfied:

$$\frac{d}{dt} \int_V \left(\underline{R} \times \frac{d\underline{R}}{dt}\right) dv = \int_V \rho\left(\underline{R} \times \frac{d^2\underline{R}}{dt^2}\right) dv = \underline{M}_T \tag{2.24}$$

Substituting eq. (2.1) into eq. (2.24) and using eq. (2.16), eq. (2.24) becomes

$$\underline{M}_T = \underline{R}_o \times \underline{F}_T + \int_V \rho\left(\underline{r} \times \frac{d^2\underline{R}}{dt^2}\right) dv \tag{2.25}$$

But the applied moment about the inertal axes can also be written in the following form:

$$\underline{M}_T = \underline{M}_o + \underline{R}_o \times \underline{F}_T \tag{2.26}$$

Here $\underline{M}_o$ represents the applied moment about the body axes. Thus equation (2.25) reduces to

$$\underline{M}_o = \int_V \rho \left(r \times \frac{d^2\underline{R}}{dt^2}\right) dv \tag{2.27}$$

Now, substituting eq. (2.8) for the accelerations into eq. (2.27), and using eqs. (2.18) - (2.21), eq. (2.27) becomes as follows:

$$\underline{M}_o = \underline{G}^T \dot{\underline{V}}_o + \underline{G}^T \overline{\underline{\Omega}}\, \underline{V}_o + \underline{H}^T \ddot{\underline{q}} + \underline{I}_T \dot{\underline{\Omega}} + \underline{M}_{cor} + \underline{M}_{cent} \tag{2.28}$$

where

$$\underline{I}_T = - \int_V \rho\, \overline{\underline{r}}^2\, dv \tag{2.29}$$

$$\underline{H}^T = \sum_{i=1}^{N} \int_{V_i} \rho\, \overline{\underline{r}}\, \underline{N}^*\, dv \tag{2.30}$$

$$\underline{M}_{cor} = 2 \int_V \rho \, \underline{\bar{r}} \, \underline{\bar{\Omega}} \, \underline{\dot{u}} \, dv \tag{2.31}$$

$$\underline{M}_{cent} = \int_V \rho \, \underline{\bar{r}} \, \underline{\bar{\Omega}}^2 \, \underline{r} \, dv \tag{2.32}$$

The $\underline{I}_T$ matrix represents the instantaneous moment of inertia matrix of the entire structure. The $\underline{H}^T$ matrix represents the distributed moment of inertia matrix of the finite elements and when multipled by the nodal acceleration vector $\underline{\ddot{q}}$ provides the coupling term between the rotary inertia due to the elastic displacements and the rotation of the body axes. The $\underline{M}_{cor}$ and $\underline{M}_{cent}$ vectors represent moments due to the Coriolis and centrifugal forces respectively. Details of $\underline{I}_T$, $\underline{H}$, $\underline{M}_{cor}$ and $\underline{M}_{cent}$ are provided in Appendix C. Expressing eq. (2.28) in a form similar to eq. (2.23) results in the following:

$$\underline{H}^T \underline{\ddot{q}} + \underline{I}_T \underline{\dot{\Omega}} + \underline{G} \, \underline{\dot{V}}_o = \underline{m}_T \tag{2.33}$$

where

$$\underline{m}_T = \underline{M}_o - \underline{G} \, \underline{\bar{\Omega}} \, \underline{V}_o - \underline{M}_{cor} - \underline{M}_{cent} \tag{2.34}$$

2.6 Principle of Virtual Work

The principle of virtual work is used to describe the elastic displacements of the structure. Using tensor notation, the principle of virtual work for a solid body undergoing large deformations can be written as follows:

$$\int_V \underline{S} : \delta\underline{E} \, dv - \int_V \underline{F} \cdot \delta\underline{u} \, dv - \int_{S_\sigma} \underline{T} \cdot \delta\underline{u} \, ds = 0 \tag{2.35}$$

The first integral represents the virtual work done by the internal forces where $\underline{S}$ is the second Pyola-Kirchhoff stress tensor and $\delta\underline{E}$ is the virtual Green strain tensor. The second integral represents the virtual work done by the body force $\underline{F}$. The virtual displacement is represented by $\delta\underline{u}$. The third integral represents the virtual work done by the applied surface tractions $\underline{T}$. The portion of the surface over which the tractions are applied is S_σ.

Now, consider the second integral in eq. (2.35). The body forces acting on the body are as follows:

$$\underline{F} = -\rho \frac{d^2\underline{R}}{dt^2} + \underline{F}_b \tag{2.36}$$

The first term represents the inertia force while $\underline{F}_b$ represents any other applied body forces such as gravity. If eq. (2.36) is substituted into eq. (2.35) and if eqs. (2.8), (2.10), (2.14), (2.15), (2.18) - (2.21), and (2.29) - (2.32) are used, then the second integral in eq. (2.35) becomes as follows for a single element:

$$-\int_V \underline{F} \cdot \delta\underline{u}dv = \delta\underline{q}^T (\underline{M}\,\ddot{\underline{q}} + \underline{H}\,\dot{\underline{\Omega}} + \underline{P}\,\dot{\underline{V}}_0 + \underline{C}\,\dot{\underline{q}} + \underline{P}\,\overline{\underline{\Omega}}\,\underline{V}_0 + \underline{F}_c - \underline{F}_B) \tag{2.37}$$

where

$$\underline{M} = \int_V \rho\, \underline{N}^{*T} \underline{N}^* \, dv \tag{2.38}$$

$$\underline{C} = 2\int_V \rho\, \underline{N}^{*T} \overline{\underline{\Omega}}\, \underline{N}^* \, dv \tag{2.39}$$

$$\underline{F}_c = \int_V \rho\, \underline{N}^{*T} \overline{\underline{\Omega}}^2 (\underline{r}_0 + \underline{u})\, dv \tag{2.40}$$

$$\underline{F}_B = \int_V \underline{N}^{*T} \underline{F}_b \, dv \tag{2.41}$$

Note that $\underline{M}$ is the usual consistent mass matrix. The $\underline{C}$ matrix is the gyroscopic matrix which is skew-symmetric and represents the contribution of the Coriolis acceleration to the inertia force. The $\underline{F}_c$ vector is the force vector due to the centrifugal force. Finally, $\underline{F}_B$ is the applied force term due to gravity. Details of eqs. (2.38)-(2.41) are given in Appendix D. In addition, the volume integrals are evaluated over the original undeformed volume.

The third integral in eq. (2.35) is treated in the standard fashion for finite elements.

$$\int_{S_\sigma} \underline{\bar{T}} \cdot \delta\underline{u} \, ds = \delta\underline{q}^T \underline{F}_o \tag{2.42}$$

Here $\underline{F}_o$ is the vector of applied forces at the nodes which result from the applied tractions.

2.6.1 The Elastic Stiffness Matrix

The application of the finite element approximation and a trapezoidal rule integration to the first integral in the principle of virtual work leads to a system of nonlinear equations that can be solved by Newton-Raphson iteration. With this iteration in mind, the displacements $\underline{u}$, the second Pyola-Kirchhoff stress and the Green strain tensor $\underline{E}$ are written in incremental form as

$$\underline{u} = {}^{o}\underline{u} + \Delta\underline{u} \tag{2.43a}$$

$$\underline{S} = {}^{o}\underline{S} + \Delta\underline{S} \tag{2.43b}$$

$$\underline{E} = {}^{o}\underline{E} + \Delta\underline{E} \tag{2.43c}$$

where $\underset{\sim}{{}^{\circ}u}$ = Displacement vector at state i

$\underset{\sim}{{}^{\circ}S}$ = Second Pyola-Kirchoff stress vector at state i

$\underset{\sim}{{}^{\circ}E}$ = Green strain vector at state i

$\Delta\underset{\sim}{u}$ = Incremental change in $\underset{\sim}{u}$ between states i and i + 1

$\Delta\underset{\sim}{S}$ = Incremental change in $\underset{\sim}{S}$ between states i and i + 1

$\Delta\underset{\sim}{E}$ = Incremental change in $\underset{\sim}{E}$ between states i and i + 1

Note that i refers to the i^{th} iteration in the Newton-Raphson iteration. Substituting eq. (2.43) into the first integral in eq. (2.35),

$$\int_V \delta\underset{\sim}{E}^T \underset{\sim}{S}\, dV = \int_V \delta\, \underset{\sim}{E}^T\, {}^{\circ}\underset{\sim}{S}\, dV + \int_V \delta\, \underset{\sim}{E}^T\, \Delta\underset{\sim}{S}\, dV \tag{2.44}$$

The constitutive law may be written as

$$\Delta\underset{\sim}{S} = \underset{\sim}{C}\, \Delta\underset{\sim}{E} \tag{2.45}$$

where $\underset{\sim}{C}$ = Material property matrix

The material property matrix $\underset{\sim}{C}$ may in general depend upon state n. All the materials considered here, however, are linearly elastic which results in the $\underset{\sim}{C}$ matrix being constant.

Substituting eq. (2.45) into eq. (2.44),

$$\int_V \delta\, \underset{\sim}{E}^T\, \underset{\sim}{S}\, dV = \int_V \delta\, \underset{\sim}{E}^{T}\, {}^{\circ}\underset{\sim}{S}\, dV + \int_V \delta\, \underset{\sim}{E}^T\, \underset{\sim}{C}\, \Delta\underset{\sim}{E}\, dV \tag{2.46}$$

Now, using tensor notation, the Green strain tensor can be written as:

$$E_{ij} = \frac{1}{2}\left(\frac{\partial u_i}{\partial X_j} + \frac{\partial u_j}{\partial X_i} + \frac{\partial u_k}{\partial X_i}\frac{\partial u_k}{\partial X_j}\right) \tag{2.47}$$

also
$$\delta E_{ij} = \frac{1}{2}\left(\frac{\partial \delta u_i}{\partial X_j} + \frac{\partial \delta u_j}{\partial X_i} + \frac{\partial u_k}{\partial X_i}\frac{\partial \delta u_k}{\partial X_j} + \frac{\partial u_k}{\partial X_j}\frac{\partial \delta u_k}{\partial X_i}\right) \tag{2.48}$$

and $\quad u_i = {}^{\circ}u_i + \Delta u_i \qquad (2.49)$

Substituting equation (2.49) into equations (2.47) and (2.48) results in

$$E_{ij} = {}^{\circ}E_{ij} + \Delta E_{ij} \qquad (2.50)$$

$$\delta E_{ij} = \delta\varepsilon_{ij} + \delta\eta_{ij} \qquad (2.51)$$

where $\quad {}^{\circ}E_{ij} = \frac{1}{2}\left(\frac{\partial{}^{\circ}u_i}{\partial X_j} + \frac{\partial{}^{\circ}u_j}{\partial X_i} + \frac{\partial{}^{\circ}u_k}{\partial X_i}\frac{\partial{}^{\circ}u_k}{\partial X_j}\right) \qquad (2.52)$

$$\Delta E_{ij} = \Delta\varepsilon_{ij} + \Delta\eta_{ij} \qquad (2.53)$$

$$\Delta\varepsilon_{ij} = \frac{1}{2}\left(\frac{\partial\Delta u_i}{\partial X_j} + \frac{\partial\Delta u_j}{\partial X_i} + \frac{\partial{}^{\circ}u_k}{\partial X_i}\frac{\partial\Delta u_k}{\partial X_j} + \frac{\partial{}^{\circ}u_k}{\partial X_j}\frac{\partial\Delta u_k}{\partial X_i}\right) \qquad (2.54)$$

$$\delta\varepsilon_{ij} = \frac{1}{2}\left(\frac{\partial\delta u_i}{\partial X_j} + \frac{\partial\delta u_j}{\partial X_i} + \frac{\partial{}^{\circ}u_k}{\partial X_i}\frac{\partial\delta u_k}{\partial X_j} + \frac{\partial{}^{\circ}u_k}{\partial X_j}\frac{\partial\delta u_k}{\partial X_i}\right) \qquad (2.55)$$

$$\Delta\eta_{ij} = \frac{1}{2}\frac{\partial\Delta u_k}{\partial X_i}\frac{\partial\Delta u_k}{\partial X_j} \qquad (2.56)$$

$$\delta\eta_{ij} = \frac{1}{2} = \left(\frac{\partial\Delta u_k}{\partial X_i}\frac{\partial\delta u_k}{\partial X_j} + \frac{\partial\Delta u_k}{\partial X_j}\frac{\partial\delta u_k}{\partial X_i}\right) \qquad (2.57)$$

Note that $\Delta\eta_{ij}$ is quadratic in Δu_i. Now, substituting equations (2.51) and (2.53) into equation (2.46) and using matrix notation results in

$$\int_V \delta\underline{E}^T\,\underline{S}\,dv = \int_V \delta\underline{\varepsilon}^T\,\underline{C}\,\Delta\underline{\varepsilon}\,dv + \int_V \delta\underline{\eta}^{T\,\circ}\underline{S}\,dv + \int_V \delta\underline{\varepsilon}^{T\,\circ}\underline{S}\,dV + A_n \qquad (2.58)$$

where A_n = Higher order terms, i.e., terms nonlinear in $\Delta\underline{u}$.

2.6.2 Finite Element Approximation

The finite element approximation to the incremental displacements between iteration steps i and i + 1 is as follows:

$$\Delta\underline{u} = \underline{N}^* \, \Delta\underline{q} \tag{2.59}$$

where $\underline{N}^*$ = Shape function matrix dependent upon state i

$\Delta\underline{q}$ = Nodal displacement between states i and i + 1

The virtual displacement $\delta\underline{u}$ can thus be expressed as follows:

$$\delta\underline{u} = \underline{N}^* \, \delta\underline{q} \tag{2.60}$$

Also, as will be shown in Chapter 3, it is possible to express the incremental strains $\Delta\underline{\varepsilon}$ within each element as follows:

$$\Delta\underline{\varepsilon} = \underline{B} \, \Delta\underline{q} \tag{2.61}$$

Also, $$\delta\underline{\varepsilon} = \underline{B} \, \delta\underline{q} \tag{2.62}$$

where $$\Delta\underline{\varepsilon}^T = \lfloor \Delta\varepsilon_{11} \;\; \Delta\varepsilon_{22} \;\; \Delta\varepsilon_{33} \;\; 2\Delta\varepsilon_{12} \;\; 2\Delta\varepsilon_{13} \;\; 2\Delta\varepsilon_{23} \rfloor \tag{2.63}$$

In addition, it will be shown that

$$\delta\underline{n}^{T\,o}\underline{S} = \delta\underline{q}^T \, \underline{B}_S \, \Delta\underline{q} \tag{2.64}$$

If equations (2.61) - (2.64) are substituted into the integrals on the right-hand side of equation (2.58), these integrals, when taken over the volume of the ith element become:

$$\int_{v_i} \delta\underline{\varepsilon}^T \, \underline{C} \, \Delta\underline{\varepsilon} \, dv = \delta\underline{q}^T \left(\int_{v_i} \underline{B}^T \, \underline{C} \, \underline{B} \, dv \right) \Delta\underline{q} = \delta\underline{q}^T \, \underline{K}_i \, \Delta\underline{q} \tag{2.65}$$

$$\int_{v_i} \delta \underline{\eta}^T \, {}^o\underline{S} \, dv = \delta \underline{q}^T \left(\int_{v_i} \underline{B}_S \, dv \right) \Delta \underline{q} = \delta \underline{q}^T \, \underline{K}_{s_i} \, \Delta \underline{q} \tag{2.66}$$

$$\int_{v_i} \delta \, \underline{\varepsilon}^T \, {}^o\underline{S} \, dv = \delta \underline{q}^T \left(\int_{v_i} \underline{B}^T \, {}^o\underline{S} \, dv \right) = \delta \underline{q}^T \, \underline{F}_{s_i} \tag{2.67}$$

where $$\underline{K}_i = \int_{v_i} \underline{B}^T \, \underline{C} \, \underline{B} \, dV = \text{element basic stiffness matrix} \tag{2.68}$$

$$\underline{K}_{s_i} = \int_{v_i} \underline{B}_s \, dV = \text{element initial stress stiffness matrix} \tag{2.69}$$

$$\underline{F}_{s_i} = \int_{v_i} \underline{B}^T \, {}^o\underline{S} \, dV = \text{element initial stress force vector} \tag{2.70}$$

Thus, if the higher order terms A_n are neglected, the virtual work expression, equation (2.58), becomes when summed over all N elements,

$$\int_{v} \delta \underline{E}^T \underline{S} \, dv = \sum_{i=1}^{N} \delta \underline{q}_i^T [(\underline{K}_i + \underline{K}_{s_i}) \, \Delta \underline{q}_i + \underline{F}_{s_i}] \tag{2.71}$$

Assembling the elements in the usual way,

$$\int_{v} \delta \underline{E}^T \underline{S} \, dv = \delta \underline{q}^T \, (\underline{K}_E \, \Delta \underline{q} + \underline{F}_S) \tag{2.72}$$

where $\underline{K}_E = \underline{K} + \underline{K}_S$ = Total global elastic stiffness matrix (2.73)

$\underline{F}_S$ = Global initial stress force vector (2.74)

Finally, by using eqs. (2.71), (2.42), and (2.37), the virtual work expression can now be written as follows:

$$\underline{M}\,\ddot{\underline{q}} + \underline{H}\,\dot{\underline{\Omega}} + \underline{P}\,\dot{\underline{V}}_o + \underline{C}\,\dot{\underline{q}} + \underline{K}_E\,\Delta\underline{q} = \underline{F}_q \tag{2.75}$$

where $\underline{F}_q = \underline{F}_o + \underline{F}_B - \underline{F}_c - \underline{F}_s - \underline{P}\,\overline{\underline{\Omega}}\,\underline{V}_o$ (2.76)

Thus, Eq. (2.75), (2.33) and (2.22) are the three sets of nonlinear coupled equations of motion for the unrestrained system shown in Fig. 1.

The next section developes the element stiffness matrices and initial stress force vector for the three node, 18 degree of freedom beam element.

CHAPTER III

DEVELOPMENT OF THE STIFFNESS MATRIX FOR THE THREE NODE BEAM ELEMENT

3.1 The Three Node 18 Degree-of-Freedom Beam Element Geometry

In Figure 2 is shown a section of the beam both before and after deformation. It is assumed that during the large deflection that there can be large rotations but that the strains remain small. Also, it is assumed that there is no warping of the cross section, i.e., plane sections remain plane. The following quantities are then defined:

$\underline{a}_1$, $\underline{a}_2$, $\underline{a}_3$ - a set of mutually orthogonal axes in the undeformed beam, centered at point 0 with $\underline{a}_1$ tangent to the reference line (beam axis)

$\underline{a}_1'$, $\underline{a}_2'$, $\underline{a}_3'$ - a set of mutual orthogonal axes in the deformed beam centered at 0' with $\underline{a}_2'$ and $\underline{a}_3'$ lying in the deformed cross-sectional plane

$\underline{X}_o$ - Position vector of point 0

$\underline{X} = \underline{X}_o + \underline{r}_p$ = Position vector of a general point P in the plane of the cross-section

$\underline{u}_o$ = Displacement of point 0

$\underline{u}$ = Displacement of point P

Note that both $\underline{a}_2'$ and $\underline{a}_3'$ as well as $\underline{a}_2$ and $\underline{a}_3$ remain in the cross-sectional plane because of the assumption that plane sections remain plane. Thus $\underline{a}_1'$, $\underline{a}_2'$, and $\underline{a}_3'$ represents the orientation of the $\underline{a}_1$, $\underline{a}_2$, $\underline{a}_3$ axes after their rotation due to the deformations.

From the geometry in Figure 2,

$$\underline{u} = \underline{u}_o + \underline{r}_p' - \underline{r}_p \tag{3.1}$$

Next, define a local coordinate system, x, y, z, such that x, y, and z are the $\underline{a}_1$, $\underline{a}_2$, and $\underline{a}_3$ coordinates respectively. Thus,

$$\underline{r}_p = y\,\underline{a}_2 + z\,\underline{a}_3 \tag{3.2}$$

and

$$\underline{X} = \underline{X}_o + \underline{r}_p \tag{3.3}$$

Also, because the cross section only translates and rotates (and doesn't distort),

$$\underline{r}'_p = y\,\underline{a}'_2 + z\,\underline{a}'_3 \tag{3.4}$$

Substituting equations (3.2) and (3.4) into equation (3.1) yields,

$$\underline{u} = \underline{u}_o + (\underline{a}'_2 - \underline{a}_2)\,y + (\underline{a}'_3 - \underline{a}_3)\,z \tag{3.5}$$

In the Total Lagrangian description all variables are referred to the original undeformed configuration. Thus, it is necessary to determine $\underline{a}'_2$ and $\underline{a}'_3$ in terms of $\underline{a}_1$, $\underline{a}_2$ and $\underline{a}_3$. In order to do that, a way of describing the rotations must be found. There are many well known ways of doing this, probably the best known way being Euler angles (Fig. 3a). Another way of doing this is by using space-three or body-three angles (Figs. 3b, 3c) [34]. In the space-three 1-2-3 description, $\underline{a}_1$, $\underline{a}_2$ and $\underline{a}_3$ are rotated successively about three separate axes as follows:

1. First, rotate by an amount θ_1 about the <u>original</u> $\underline{a}_1$ axis.
2. Next, rotate the new configuration θ_2 about the <u>original</u> $\underline{a}_2$ axis.
3. Finally, rotate the last configuration θ_3 about the <u>original</u> $\underline{a}_3$ axis.

The body-three 1-2-3 sequence is similar except that instead of rotating about the original axes, the rotation is about the body axes. It is also possible to use sequences other than 1-2-3, for example, a space-three 2-3-1, or body-three 1-3-2 or any sequence which results in the required orientation is possible. In the case of a 1-2-1 or 3-1-3 sequence or any sequence in which there is a rotation about only two axes, the rotation would be referred to as a space-two or body-two rotation. Note that the Euler angles correspond to a body-two 3-1-3 rotation.

For the purpose of this research, the space-three 1-2-3 rotation sequence was chosen to describe the rotations because it seemed the most straight forward and because none of the others offered any particular advantages over it.

Once a method for describing the rotations is chosen, the relationship between $\underline{a}_1'$, $\underline{a}_2'$, $\underline{a}_3'$ and $\underline{a}_1$, $\underline{a}_2$, $\underline{a}_3$ can be determined. For the space-three 1-2-3, this is as follows:

$$\underline{a}_1' = \cos\theta_2 \cos\theta_3 \, \underline{a}_1 + \cos\theta_2 \sin\theta_3 \, \underline{a}_2 - \sin\theta_2 \, \underline{a}_3 \tag{3.6a}$$

$$\begin{aligned}\underline{a}_2' = {} & (\sin\theta_1 \sin\theta_2 \cos\theta_3 - \sin\theta_3 \cos\theta_1) \, \underline{a}_1 + (\sin\theta_1 \sin\theta_2 \sin\theta_3 \\ & + \cos\theta_3 \cos\theta_1) \, \underline{a}_2 + \sin\theta_1 \cos\theta_2 \, \underline{a}_3\end{aligned} \tag{3.6b}$$

$$\begin{aligned}\underline{a}_3' = {} & (\cos\theta_1 \sin\theta_2 \cos\theta_3 + \sin\theta_3 \sin\theta_1) \, \underline{a}_1 + (\cos\theta_1 \sin\theta_2 \sin\theta_3 \\ & - \cos\theta_3 \sin\theta_1) \, \underline{a}_2 + \cos\theta_1 \cos\theta_2 \, \underline{a}_3\end{aligned} \tag{3.6c}$$

Next, the displacements and rotations are written in incremental form

$$\underline{u} = {}^{\circ}\underline{u} + \Delta\underline{u} \tag{3.7}$$

$$\underline{u}_0 = {}^{\circ}\underline{u}_0 + \Delta\underline{u}_0 \tag{3.8}$$

$$\theta_k = {}^{\circ}\theta_k + \Delta\theta_k, \quad k = 1,2,3 \tag{3.9}$$

If equations (3.6), (3.8) and (3.9) are substituted into equation (3.5) and higher order terms are neglected then the following results:

$$°\underline{u} = °\underline{u}_o + y\,(°\underline{a}_2' - \underline{a}_2) + z\,(°\underline{a}_3' - \underline{a}_3) \tag{3.10}$$

$$\Delta\underline{u} = \Delta\underline{u}_o + (y\,\underline{D} + z\,\underline{E})\;\Delta\underline{\theta} \tag{3.11}$$

where $°\underline{a}_i' = \underline{a}_i'\,(°\theta_1,\ °\theta_2,\ °\theta_3) \qquad i = 1,2,3$

$$\Delta\underline{\theta}^T = \lfloor \Delta\theta_1\ \ \Delta\theta_2\ \ \Delta\theta_3 \rfloor$$

$$\underline{D} = \underline{D}\,(°\theta_1,\ °\theta_2,\ °\theta_3)$$

$$\underline{E} = \underline{E}\,(°\theta_1,\ °\theta_2,\ °\theta_3)$$

The elements of the 3 x 3 matrices $\underline{D}$ and $\underline{E}$ as well as expressions for $°\underline{a}_i' - \underline{a}_i$, i = 2,3 are given in Appendix A.

3.2 Finite Element Approximation

The three node eighteen degree of freedom element is pictured in Figure 4. The local coordinates ξ, y, z are normalized such that the origin is at the center and the ξ coordinate varies between -1 at one end of the beam and +1 at the other end. The transformation between the global coordinates and the local coordinates is thus as follows:

$$\underline{X} = \sum_{i=1}^{3} N_i(\xi)\,\underline{X}_{oi} + y\,\underline{a}_2 + z\,\underline{a}_3 \tag{3.12}$$

Here $\underline{X}_{oi}$ are the coordinates of the three nodes and $N_i(\xi)$ are the shape functions which are

$$N_1(\xi) = \frac{1}{2}\,\xi\,(\xi - 1) \tag{3.13a}$$

$$N_2(\xi) = 1 - \xi^2 \tag{3.13b}$$

Thus the integral is first evaluated over the original cross-sectional area of the undeformed beam element A_i and then along its length ℓ_i. Next, eq. (3.83) is substituted into eq. (3.85) and the various matrix products and area integrals carried out. It is assumed that the longitudinal axis of the beam is through its centroid and that the cross section is symmetric. The following equation then results:

$$\underline{K}_i = \int_{\ell_i} [A\, (\underline{B}_o^\ell)^T\, \underline{C}^\ell\, \underline{B}_o^\ell + I_{zz}\, (\underline{B}_1^\ell)^T\, \underline{C}^\ell\, \underline{B}_1^\ell + I_{yy}\, (\underline{B}_2^\ell)^T\, \underline{C}^\ell\, \underline{B}_2^\ell]\, d\ell \quad (3.86)$$

where $$A = \int_{A_i} dA \quad (3.87)$$

$$I_{zz} = \int_{A_i} y^2\, dA \quad (3.88)$$

$$I_{yy} = \int_{A_i} z^2\, dA \quad (3.89)$$

Note that A, I_{zz}, and I_{yy} are merely the area and area moments of inertia of the beam cross-section. The integration along the length of the beam is done numerically using Gaussian integration [28]:

$$\underline{K}_i = \sum_{j=1}^{n} \{[A\, (\underline{B}_o^\ell)^T\, \underline{C}^\ell\, \underline{B}_o^\ell + I_{zz}\, (\underline{B}_1^\ell)^T\, \underline{C}^\ell\, \underline{B}_1^\ell + I_{yy}\, (\underline{B}_2^\ell)^T\, \underline{C}^\ell\, \underline{B}_2^\ell]\, |\underline{J}|\}_{\xi=a_j}\, H_j \quad (3.90)$$

The a_j are the Gaussian integration points and H_j represents the weighting factors while n is the number of integration points used. Since the

For an isotropic material, the local 3 x 3 matrix of material properties is then

$$\underline{C}^{\ell} = \begin{bmatrix} E & 0 & 0 \\ 0 & \beta G & 0 \\ 0 & 0 & \beta G \end{bmatrix} \tag{3.81}$$

Here E is the Young's modulus of the material, G is the shear modulus, and β is the shear correction factor. For an isotropic material with rectangular cross section, β is equal to 5/6.

3.7 Calculation of the Stiffness Matrix and Initial Stress Force Vector

It is now possible to calculate the element stiffness matrices and initial stress force vector as given by eqs. (3.46) - (3.49). First, note that the local $\underline{B}$ matrices are formed via eqs. (3.44) as follows:

$$\underline{B}_i^{\ell} = \underline{T}\,\underline{B}_i, \qquad i = 0,1,2 \tag{3.82}$$

Thus $$\underline{B}^{\ell} = \underline{B}_0^{\ell} + y\,\underline{B}_1^{\ell} + z\,\underline{B}_2^{\ell} \tag{3.83}$$

Also note that before the $\underline{B}_s$ matrices can be formed, it is necessary to transform the stresses from the local coordinates using eq. (3.40):

$$^{\circ}\underline{S} = \underline{T}^T\,{}^{\circ}\underline{S}^{\ell} \tag{3.84}$$

The $\underline{P}_{s_i}$ matrices can then be formed using the elements of the $^{\circ}\underline{S}$ vector from which in turn the $\underline{B}_{s_i}$ matrices can be formed. To calculate the stiffness matrix, first note that the volume integral in eq. (3.46) can be written as follows:

$$\underline{K}_i = \int_{V_i} (\underline{B}^{\ell})^T\,\underline{C}^{\ell}\,\underline{B}^{\ell}\,dV = \int_{\ell_i}\int_{A_i} (\underline{B}^{\ell})^T\,\underline{C}^{\ell}\,\underline{B}^{\ell}\,dA\,d\ell \tag{3.85}$$

along its length. Thus, in a manner analogous to eq. (3.70), the ${}^{o}\underline{S}_o$ vector can be written as

$$ {}^{o}\underline{S} = {}^{o}\underline{S}_o + y\ {}^{o}\underline{S}_y + z\ {}^{o}\underline{S}_z \tag{3.77} $$

also,

$$ \underline{P}_s = \underline{P}_{so} + y\ \underline{P}_{sy} + z\ \underline{P}_{sz} \tag{3.78} $$

Finally, if eqs. (3.59) and (3.78) are substituted into eq. (3.76) and the matrix products carried out, the following expression for $\underline{B}_s$ results:

$$ \underline{B}_s = \underline{B}_{so} + y\ \underline{B}_{s1} + z\ \underline{B}_{s2} + yz\ \underline{B}_{s3} + y^2\ \underline{B}_{s4} + z^2\ \underline{B}_{s5} \tag{3.79} $$

where

$$ \underline{B}_{so} = \underline{A}_o^T\ \underline{P}_{so}\ \underline{A}_o \tag{3.79a} $$

$$ \underline{B}_{s1} = \underline{A}_y^T\ \underline{P}_{so}\ \underline{A}_o + \underline{A}_o^T\ \underline{P}_{sy}\ \underline{A}_o + \underline{A}_o^T\ \underline{P}_{so}\ \underline{A}_y \tag{3.79b} $$

$$ \underline{B}_{s2} = \underline{A}_z^T\ \underline{P}_{so}\ \underline{A}_o + \underline{A}_o^T\ \underline{P}_{sz}\ \underline{A}_o + \underline{A}_o^T\ \underline{P}_{so}\ \underline{A}_z \tag{3.79c} $$

$$ \underline{B}_{s3} = \underline{A}_o^T(\underline{P}_{sy}\underline{A}_z+\underline{P}_{sz}\underline{A}_y) + \underline{A}_y^T(\underline{P}_{so}\underline{A}_z+\underline{P}_{sz}\underline{A}_o) + \underline{A}_z^T(\underline{P}_{so}\underline{A}_y+\underline{P}_{so}\underline{A}_z) \tag{3.79d} $$

$$ \underline{B}_{s4} = \underline{A}_y^T\ \underline{P}_{so}\ \underline{A}_y + \underline{A}_o^T\ \underline{P}_{sy}\ \underline{A}_y + \underline{A}_y^T\ \underline{P}_{sy}\ \underline{A}_o \tag{3.79e} $$

$$ \underline{B}_{s5} = \underline{A}_z^T\ \underline{P}_{so}\ \underline{A}_z + \underline{A}_o^T\ \underline{P}_{sz}\ \underline{A}_z + \underline{A}_z^T\ \underline{P}_{sz}\ \underline{A}_o \tag{3.79f} $$

3.6 The Material Property Matrix

The material property matrix $\underline{C}$ will in general depend upon the state of the structure and as such it is a function of time. All of the materials considered here, however, are linearly elastic which results in the $\underline{C}$ matrix being constant. The form of the local incremental stress strain relation is as follows:

$$ \Delta\underline{S}^{\ell} = \underline{C}^{\ell}\ \Delta\underline{\varepsilon}^{\ell} \tag{3.80} $$

$$\underline{B} = \underline{B}_0 + y\,\underline{B}_1 + z\,\underline{B}_2 \tag{3.70}$$

Next it is necessary to determine the form of the $\underline{B}_s$ matrix. From eq. (2.67),

$$\delta\underline{n}^{T\,\circ}\underline{S} = \delta\underline{q}^T\,\underline{B}_s\,\Delta\underline{q} \tag{3.71}$$

Using the expression for $\delta\underline{n}$ given in eq. (2.57) it is possible to show that the following is true:

$$\delta\underline{n}^{T\,\circ}\underline{S} = \{\frac{\partial\delta u}{\partial X}\}^T\;\underline{P}_s\;\{\frac{\partial\Delta u}{\partial X}\} \tag{3.72}$$

where

$$\underline{P}_s = \begin{bmatrix} \underline{p}_o & \underline{0} & \underline{0} \\ \underline{0} & \underline{p}_o & \underline{0} \\ \underline{0} & \underline{0} & \underline{p}_o \end{bmatrix} \tag{3.73}$$

$$\underline{p}_o = \begin{bmatrix} {}^\circ S_{11} & {}^\circ S_{12} & {}^\circ S_{13} \\ {}^\circ S_{12} & {}^\circ S_{22} & {}^\circ S_{23} \\ {}^\circ S_{13} & {}^\circ S_{23} & {}^\circ S_{33} \end{bmatrix} \tag{3.74}$$

Thus, using eqs. (3.58) and (3.63), eq. (3.72) can be written as

$$\delta\underline{n}^{T\,\circ}\underline{S} = \delta\underline{q}^T\,\underline{A}^T\,\underline{P}_s\,\underline{A}\,\Delta\underline{q} \tag{3.75}$$

or $$\underline{B}_s = \underline{A}^T\,\underline{P}_s\,\underline{A} \tag{3.76}$$

Since the incremental stresses at each step are calculated by using the constitutive law eq. (2.45) and are dependent upon the strains $\Delta\underline{\varepsilon}$, it follows that ${}^\circ\underline{S}$ will vary over the cross section of the beam as well as

$$\frac{\partial\,{}^{o}u}{\partial z} = \sum_{i=1}^{3} N_i(\xi)\ ({}^{o}\underline{a}_3' - \underline{a}_3)_i \tag{3.66}$$

Using eqs. (3.64) - (3.66) as well as eq. (3.52), the elements of the expanded $\underline{D}_\varepsilon$ matrix can be obtained.

$$\underline{D}_\varepsilon = \underline{D}_{\varepsilon o} + y\ \underline{D}_{\varepsilon y} + z\ \underline{D}_{\varepsilon z} \tag{3.67}$$

The terms of $\underline{D}_{\varepsilon o}$, $\underline{D}_{\varepsilon y}$ and $\underline{D}_{\varepsilon z}$ are given in detail in Appendix B.

Now we are prepared to calculate the $\underline{B}$ matrix given in eqs. (2.61) and (2.62). Substitute eqs. (3.58), (3.59), and (3.67) into eq. (3.50) and perform the matrix multiplications to obtain the following:

$$\Delta\underline{\varepsilon} = \underline{B}\ \Delta\underline{q} \tag{3.68}$$

where $$\underline{B} = \underline{B}_o + y\ \underline{B}_1 + z\ \underline{B}_2 + yz\ \underline{B}_3 + y^2\ \underline{B}_4 + z^2\ \underline{B}_5 \tag{3.69}$$

$$\underline{B}_o = \underline{D}_{\varepsilon o}\ \underline{A}_o \tag{3.69a}$$

$$\underline{B}_1 = \underline{D}_{\varepsilon y}\ \underline{A}_o + \underline{D}_{\varepsilon o}\ \underline{A}_y \tag{3.69b}$$

$$\underline{B}_2 = \underline{D}_{\varepsilon z}\ \underline{A}_o + \underline{D}_{\varepsilon o}\ \underline{A}_z \tag{3.69c}$$

$$\underline{B}_3 = \underline{D}_{\varepsilon z}\ \underline{A}_y + \underline{D}_{\varepsilon y}\ \underline{A}_z \tag{3.69d}$$

$$\underline{B}_4 = \underline{D}_{\varepsilon y}\ \underline{A}_y \tag{3.69e}$$

$$\underline{B}_5 = \underline{D}_{\varepsilon z}\ \underline{A}_z \tag{3.69f}$$

Because they are fairly insignificnt and add unnecessarily to the complexity of the stiffness matrix, the higher order terms yz $\underline{B}_3$, y^2 $\underline{B}_4$ and z^2 $\underline{B}_5$ are neglected. Thus the $\underline{B}$ matrix can be written as follows:

and $$\underline{A}_o = \begin{bmatrix} \underline{J}^{-1} & \underline{D}_o^1 \\ \underline{J}^{-1} & \underline{D}_o^2 \\ \underline{J}^{-1} & \underline{D}_o^3 \end{bmatrix} \tag{3.60}$$

$$\underline{A}_y = \begin{bmatrix} \underline{J}^{-1} & \underline{D}_y^1 \\ \underline{J}^{-1} & \underline{D}_y^2 \\ \underline{J}^{-1} & \underline{D}_y^3 \end{bmatrix} \tag{3.61}$$

$$\underline{A}_z = \begin{bmatrix} \underline{J}^{-1} & \underline{D}_z^1 \\ \underline{J}^{-1} & \underline{D}_z^2 \\ \underline{J}^{-1} & \underline{D}_z^3 \end{bmatrix} \tag{3.62}$$

It should also be noted that an expression similar to eq. (3.58) holds for $\{\frac{\partial \delta \underline{u}}{\partial \underline{X}}\}$. Thus,

$$\{\frac{\partial \delta \underline{u}}{\partial \underline{X}}\} = \underline{A}\ \delta \underline{q} \tag{3.63}$$

The next thing needed to do is to determine the elements of the $\underline{D}_\varepsilon$ matrix. This will require the evaluation of derivatives like $\frac{\partial\, {}^\circ\underline{u}}{\partial \underline{X}}$. These terms can be determined by first differentiating the expression for ${}^\circ\underline{u}$ given in Eq. (3.14) as follows:

$$\frac{\partial\, {}^\circ\underline{u}}{\partial \xi} = \sum_{i=1}^{3} \frac{\partial N_i}{\partial \xi}\, {}^\circ\underline{u}_{o_i} + \sum_{i=1}^{3} \frac{\partial N_i}{\partial \xi} [y\ ({}^\circ\underline{a}_2' - \underline{a}_2)_i + z\ ({}^\circ\underline{a}_3' - \underline{a}_3)_i] \tag{3.64}$$

$$\frac{\partial\, {}^\circ\underline{u}}{\partial y} = \sum_{i=1}^{3} N_i(\xi)\ ({}^\circ\underline{a}_2' - \underline{a}_2)_i \tag{3.65}$$

The next step in the derivation is to express the vector of derivatives $\{\frac{\partial \Delta \underline{u}}{\partial \underline{X}}\}$ in terms of the nodal displacements $\Delta \underline{q}$. This can be done by differentiating the expression for the finite element approximation to $\Delta \underline{u}$ given in eq. (3.15).

$$\frac{\partial \Delta \underline{u}}{\partial \xi} = \sum_{i=1}^{3} \frac{\partial N_i}{\partial \xi} \Delta \underline{u}_{o_i} + \sum_{i=1}^{3} \frac{\partial N_i}{\partial \xi} (y \underline{D}_i + z \underline{E}_i) \Delta \underline{\theta}_i \tag{3.53}$$

$$\frac{\partial \Delta \underline{u}}{\partial y} = \sum_{i=1}^{3} N_i(\xi) \underline{D}_i \Delta \underline{\theta}_i \tag{3.54}$$

$$\frac{\partial \Delta \underline{u}}{\partial z} = \sum_{i=1}^{3} N_i(\xi) \underline{E}_i \Delta \underline{\theta}_i \tag{3.55}$$

By using eqs. (3.53) - (3.55) as well as eq. (3.24), it now becomes possible to write $\{\frac{\partial \Delta \underline{u}}{\partial \underline{X}}\}$ as follows:

$$\{\frac{\partial \Delta \underline{u}}{\partial \underline{X}}\} = \begin{bmatrix} \underline{J}^{-1} & \underline{D}^{1} \\ \underline{J}^{-1} & \underline{D}^{2} \\ \underline{J}^{-1} & \underline{D}^{3} \end{bmatrix} \Delta \underline{q} \tag{3.56}$$

where $\underline{D}^k = \underline{D}_o^k (\xi) + y \underline{D}_y^k (\xi) + z \underline{D}_z^k (\xi); \quad k = 1,2,3$ (3.57)

The elements of $\underline{D}^k$ are composed of the elements from the $\underline{D}_i$ and $\underline{E}_i$ matrices, as well as terms from the shape functions N_i and their derivatives. The exact composition of the $\underline{D}^k$ matrix is given in appendix B. Equation (3.56) can be rewritten as follows:

$$\{\frac{\partial \Delta \underline{u}}{\partial \underline{X}}\} = \underline{A} \Delta \underline{q} \tag{3.58}$$

where $\underline{A} = \underline{A}_o + y \underline{A}_y + z \underline{A}_z$ (3.59)

$$\underline{K}_{s_i} = \int_{v_i} \underline{B}_S^{\ell} \, dV \tag{3.48}$$

$$\underline{F}_{s_i} = \int_{v_i} (\underline{B}^{\ell})^{T\,\circ}\underline{S}^{\ell} \, dv \tag{3.49}$$

3.5 Calculation of the $\underline{B}$ and $\underline{B}_S$ Matrices

The calculation of the $\underline{B}$ and $\underline{B}_S$ matrices used in the integrals of equations (3.46) - (3.49) is now considered. The incremental strain $\Delta\varepsilon_{ij}$ given in eq. (2.59), when written in vector form as in eq. (2.66), can be expressed as the following matrix product:

$$\Delta\underline{\varepsilon} = \underline{D}_{\varepsilon} \left\{\frac{\partial\Delta\underline{u}}{\partial\underline{X}}\right\} \tag{3.50}$$

where
$$\left\{\frac{\partial\Delta\underline{u}}{\partial\underline{X}}\right\} = \left\lfloor \frac{\partial\Delta u_1}{\partial X_1} \; \frac{\partial\Delta u_1}{\partial X_2} \; \frac{\partial\Delta u_1}{\partial X_3} \; \frac{\partial\Delta u_2}{\partial X_1} \; \frac{\partial\Delta u_2}{\partial X_2} \; \frac{\partial\Delta u_2}{\partial X_3} \; \frac{\partial\Delta u_3}{\partial X_1} \; \frac{\partial\Delta u_3}{\partial X_2} \; \frac{\partial\Delta u_3}{\partial X_3} \right\rfloor \tag{3.51}$$

$$\underline{D}_{\varepsilon} = \begin{bmatrix}
1+\frac{\partial^\circ u_1}{\partial X_1} & 0 & 0 & \frac{\partial^\circ u_2}{\partial X_1} & 0 & 0 & \frac{\partial^\circ u_3}{\partial X_1} & 0 & 0 \\
0 & \frac{\partial^\circ u_1}{\partial X_2} & 0 & 0 & 1+\frac{\partial^\circ u_2}{\partial X_2} & 0 & 0 & \frac{\partial^\circ u_3}{\partial X_2} & 0 \\
0 & 0 & \frac{\partial^\circ u_1}{\partial X_3} & 0 & 0 & \frac{\partial^\circ u_2}{\partial X_3} & 0 & 0 & 1+\frac{\partial^\circ u_3}{\partial X_3} \\
\frac{\partial^\circ u_1}{\partial X_2} & 1+\frac{\partial^\circ u_1}{\partial X_1} & 0 & 1+\frac{\partial^\circ u_2}{\partial X_2} & \frac{\partial^\circ u_2}{\partial X_1} & 0 & \frac{\partial^\circ u_3}{\partial X_2} & \frac{\partial^\circ u_3}{\partial X_1} & 0 \\
\frac{\partial^\circ u_1}{\partial X_3} & 0 & 1+\frac{\partial^\circ u_1}{\partial X_1} & \frac{\partial^\circ u_2}{\partial X_3} & 0 & \frac{\partial^\circ u_2}{\partial X_1} & 1+\frac{\partial^\circ u_3}{\partial X_3} & 0 & \frac{\partial^\circ u_3}{\partial X_1} \\
0 & \frac{\partial^\circ u_1}{\partial X_3} & \frac{\partial^\circ u_1}{\partial X_2} & 0 & \frac{\partial^\circ u_2}{\partial X_3} & 1+\frac{\partial^\circ u_2}{\partial X_2} & 0 & 1+\frac{\partial^\circ u_3}{\partial X_3} & \frac{\partial^\circ u_3}{\partial X_2}
\end{bmatrix} \tag{3.52}$$

where

$$(\underline{E}^{\ell})^T = \lfloor E_{11}^{\ell} \; 2E_{12}^{\ell} \; 2E_{13}^{\ell} \rfloor$$

The elements of $\underline{T}$ are given in Appendix A. Since all the other quantities involved in equation (3.34) are tensors, similar expressions hold for them also.

$$\Delta\underline{\varepsilon}^{\ell} = \underline{T} \; \Delta\underline{\varepsilon} \tag{3.37}$$

$$\delta\underline{\varepsilon}^{\ell} = \underline{T} \; \delta\underline{\varepsilon} \tag{3.38}$$

$$\delta\underline{\eta}^{\ell} = \underline{T} \; \delta\underline{\eta} \tag{3.39}$$

$${}^{o}\underline{S}^{\ell} = \underline{T}\,{}^{o}\underline{S} \tag{3.40}$$

Next, substitute equations (2.64) - (2.66) into equations (3.37) - (3.40)

$$\Delta\underline{\varepsilon}^{\ell} = \underline{B}^{\ell} \; \Delta\underline{q} \tag{3.41}$$

$$\delta\underline{\varepsilon}^{\ell} = \underline{B}^{\ell} \; \delta\underline{q} \tag{3.42}$$

$$(\delta\underline{\eta}^{\ell})^{T}\,{}^{o}\underline{S}^{\ell} = \delta\underline{q}^{T} \; \underline{B}_{S}^{\ell} \; \Delta\underline{q} \tag{3.43}$$

where $$\underline{B}^{\ell} = \underline{T} \; \underline{B} \tag{3.44}$$

$$\underline{B}_{S}^{\ell} = \underline{B}_{S} \tag{3.45}$$

Finally, the stiffness matrices and the initial stress force vector, equations (2.73)-(2.75), become,

$$\underline{K}_{i} = \int_{v_i} (\underline{B}^{\ell})^T \; \underline{C}^{\ell} \; \underline{B}^{\ell} \, dv \tag{3.46}$$

3.4 Assumptions on Stress and the Transformation Matrix

The following assumptions have been made concerning the local stresses in the beam:

$$| S_{22}^{\ell} | \quad | S_{33}^{\ell} | \quad | S_{23}^{\ell} | \quad << \quad | S_{11}^{\ell} |$$

Here the ℓ superscript refers to the local $\underline{a}_1$, $\underline{a}_2$, $\underline{a}_3$ coordinate system. The S_{22}^{ℓ}, S_{33}^{ℓ}, and S_{23}^{ℓ} stresses are thus considered small enough to be neglected.

Since the virtual work integral is a scalar, it is invariant under any coordinate transformation.

$$\int_V \delta\, \underline{E}^{\ell T}\, \underline{S}^{\ell}\, dv = \int_V \delta\, \underline{E}^T\, \underline{S}\, dv \tag{3.34}$$

The transformation from local to global coordinates using tensor notation is as follows:

$$E_{rs}^{\ell} = (\underline{i}_p \cdot \underline{a}_r)(\underline{i}_q \cdot \underline{a}_s)\, E_{pq} \tag{3.35}$$

where $\quad i$ = global unit vectors

For example,

$$E_{11}^{\ell} = a_{11}^2\, E_{11} + a_{12}^2\, E_{22} + a_{13}^2\, E_{33} + 2a_{11}\, a_{12}\, E_{12}$$

$$+ 2a_{11}\, a_{13}\, E_{13} + 2a_{12}\, a_{13}\, E_{23}$$

Similar expressions hold for E_{12}^{ℓ} and E_{13}^{ℓ}. A transformation matrix $\underline{T}$ can thus be defined relating the local and global strain components:

$$\underline{E}^{\ell} = \underline{T}\, \underline{E} \tag{3.36}$$

$$\frac{\partial \underline{X}}{\partial \xi} = \frac{\ell}{2}\, \underline{a}_1 \tag{3.28a}$$

$$\frac{\partial \underline{X}}{\partial y} = \underline{a}_2 \tag{3.28b}$$

$$\frac{\partial \underline{X}}{\partial z} = \underline{a}_3 \tag{3.28c}$$

Thus, the Jacobian matrix is as follows:

$$\underline{J} = \begin{bmatrix} \frac{\ell}{2}\, a_{11} & \frac{\ell}{2}\, a_{12} & \frac{\ell}{2}\, a_{13} \\ a_{21} & a_{22} & a_{23} \\ a_{31} & a_{32} & a_{33} \end{bmatrix} \tag{3.29}$$

To determine $\underline{J}^{-1}$, it is first necessary to evaluate the determinate of the Jacobian. First, note that

$$|\,\underline{J}\,| = \frac{\ell}{2}\, \underline{a}_1 \cdot (\underline{a}_2 \times \underline{a}_3) \tag{3.30}$$

But $\quad \underline{a}_2 \times \underline{a}_3 = \underline{a}_1 \qquad (3.31)$

Thus $\quad |\,\underline{J}\,| = \frac{\ell}{2}\, \underline{a}_1 \cdot \underline{a}_1 \qquad (3.32)$

and $\quad |\,\underline{J}\,| = \frac{\ell}{2} \qquad (3.33)$

This expression for the determinant of the Jacobian will prove useful in the evaulation of various integrals.

$$\text{or} \quad \begin{Bmatrix} \frac{\partial}{\partial \xi} \\ \frac{\partial}{\partial y} \\ \frac{\partial}{\partial z} \end{Bmatrix} = \underline{J} \begin{Bmatrix} \frac{\partial}{\partial X_1} \\ \frac{\partial}{\partial X_2} \\ \frac{\partial}{\partial X_3} \end{Bmatrix} \tag{3.23}$$

where $\underline{J}$= Jocabian matrix

Solving for the desired derivative,

$$\begin{Bmatrix} \frac{\partial}{\partial X_1} \\ \frac{\partial}{\partial X_2} \\ \frac{\partial}{\partial X_3} \end{Bmatrix} = \underline{J}^{-1} \begin{Bmatrix} \frac{\partial}{\partial \xi} \\ \frac{\partial}{\partial y} \\ \frac{\partial}{\partial z} \end{Bmatrix} \tag{3.24}$$

In order to evaluate the Jacobian, equation (3.12) is used.

$$\underline{X} = \sum_{i=1}^{3} N_i(\xi)\, \underline{X}_{oi} + y\, \underline{a}_2 + z\, \underline{a}_3 \tag{3.25}$$

For straight beams, however,

$$\underline{X}_{o2} = \underline{X}_{o1} + \frac{\ell}{2}\, \underline{a}_1 \tag{3.26a}$$

$$\underline{X}_{o3} = \underline{X}_{o1} + \ell\, \underline{a}_1 \tag{3.26b}$$

where ℓ = Length of the beam element

Substituting equations (3.26) into (3.12) and using the expressions for the shape functions given in equations (3.13) results in

$$\underline{X} = \underline{X}_{o1} + \frac{\ell}{2}(\xi+1)\, \underline{a}_1 + y\, \underline{a}_2 + z\, \underline{a}_3 \tag{3.27}$$

Using equation (3.27) to evaluate the derivatives in the Jacobian,

$$\Delta \underline{u} = \underline{N}^* \; \Delta \underline{q} \tag{3.17}$$

where
$$\underline{N}^* = \underline{N}^*_o + y\,\underline{N}^*_y + z\,\underline{N}^*_z \tag{3.18}$$

$$\underline{N}^*_o = [N_1 \underline{I}_3 \;\; \underline{0} \;\; N_2 \underline{I}_3 \;\; \underline{0} \;\; N_3 \underline{I}_3] \tag{3.19}$$

$$\underline{N}^*_y = [\underline{0} \;\; N_1 \underline{D}_1 \;\; \underline{0} \;\; N_2 \underline{D}_2 \;\; \underline{0} \;\; N_3 \underline{D}_3] \tag{3.20}$$

$$\underline{N}^*_z = [\underline{0} \;\; N_1 \underline{E}_1 \;\; \underline{0} \;\; N_2 \underline{E}_2 \;\; \underline{0} \;\; N_3 \underline{E}_3] \tag{3.21}$$

Note that $\underline{N}^*_o$, $\underline{N}^*_y$ and $\underline{N}^*_z$ are 3 x 18 matrices since $\underline{I}_3$ is the 3 x 3 identity matrix and $\underline{0}$ is the 3 x 3 null matrix.

3.3 Derivatives and the Jacobian

In order to evaluate the integrals in the virtual work expression, it is necessary to evaluate terms that include derivatives with respect to $\underline{X}$. Since the displacements are expressed in terms of the local coordinates, it is necessary to find an expression which relates derivatives with respect to the local coordinates to derivatives with respect to $\underline{X}$. This can be done using the chain rule as follows:

$$\left\{ \begin{matrix} \dfrac{\partial}{\partial \xi} \\[2ex] \dfrac{\partial}{\partial y} \\[2ex] \dfrac{\partial}{\partial z} \end{matrix} \right\} = \begin{bmatrix} \dfrac{\partial X_1}{\partial \xi} & \dfrac{\partial X_2}{\partial \xi} & \dfrac{\partial X_3}{\partial \xi} \\[2ex] \dfrac{\partial X_1}{\partial y} & \dfrac{\partial X_2}{\partial y} & \dfrac{\partial X_3}{\partial y} \\[2ex] \dfrac{\partial X_1}{\partial z} & \dfrac{\partial X_2}{\partial z} & \dfrac{\partial X_3}{\partial z} \end{bmatrix} \left\{ \begin{matrix} \dfrac{\partial}{\partial X_1} \\[2ex] \dfrac{\partial}{\partial X_2} \\[2ex] \dfrac{\partial}{\partial X_3} \end{matrix} \right\} \tag{3.22}$$

$$N_3(\xi) = \frac{1}{2}\,\xi\,(\xi + 1) \tag{3.13c}$$

In the finite element approximation the displacements within each element are assumed in terms of the shape functions as follows:

$$°\underline{u} = \sum_{i=1}^{3} N_i(\xi)\ °\underline{u}_{oi} + y \sum_{i=1}^{3} N_i(\xi)\ (°\underline{a}_2' - \underline{a}_2)_i + z \sum_{i=1}^{3} N_i(\xi)(°\underline{a}_3' - \underline{a}_3)_i \tag{3.14}$$

$$\Delta\underline{u} = \sum_{i=1}^{3} N_i(\xi)\ \Delta\underline{u}_{oi} + \sum_{i=1}^{3} N_i(\xi)\ (y\ \underline{D}_i + z\ \underline{E}_i)\ \Delta\underline{\theta}_i \tag{3.15}$$

Figure 4 shows the 18 degrees of freedom for the 3 node beam element used here. The subscript i refers to the appropriate node and the displacements are expressed in terms of the nodal displacements. Thus, for i = 1,2,3,

$$°\underline{u}_{oi} = °\underline{u}_o\ (\underline{X}_{oi})$$

$$\Delta\underline{u}_{oi} = \Delta\underline{u}_o\ (\underline{X}_{oi})$$

$$\Delta\underline{\theta}_i = \Delta\underline{\theta}\ (\underline{X}_{oi})$$

$$\underline{D}_i = \underline{D}\ (°\theta_{1_i},\ °\theta_{2_i},\ °\theta_{3_i})$$

$$\underline{E}_i = \underline{E}\ (°\theta_{1_i},\ °\theta_{2_i},\ °\theta_{3_i})$$

Now the displacements need to be expressed in the form of equation (2.10). To do this, define the nodal incremental displacement vector $\underline{q}$ as follows:

$$\Delta\underline{q}^T = \lfloor \Delta\underline{u}_{o1}^T,\ \Delta\underline{\theta}_1^T,\ \Delta\underline{u}_{o2}^T,\ \Delta\underline{\theta}_2^T,\ \Delta\underline{u}_{o3}^T,\ \Delta\underline{\theta}_3^T \rfloor \tag{3.16}$$

Rewriting equation (3.15) in terms of equation (3.16) and using matrix notation, expressions in eq. (3.90) are no higher than 4th order polynomials, a three-point numerical integration would give exact results. However, these beam elements allow transverse shear deformations similar to a Timoshenko beam. It is well known that when the finite element approximation is applied to such beams which have a large length to thickness ratio that exact integration results in overly constrained equations which leads to inaccurate results [36]. One remedy to this situation is to use reduced integration [29,30]. Therefore a two point integration (n = 2) was chosen for eq. (3.90). For n = 2 the Gaussian integration points are $a_1 = -1/\sqrt{3}$ and $a_2 = 1/\sqrt{3}$ while $H_1 = H_2 = 1$. Also, from eq. (3.33), $|\underline{J}| = \ell/2$. Thus, eq. (3.86) becomes

$$\underline{K}_i = \frac{\ell}{2} \sum_{j=1}^{2} \{[A\ (\underline{B}_0^\ell)^T\ \underline{C}^\ell\ \underline{B}_0^\ell + I_{zz}\ (\underline{B}_1^\ell)^T\ \underline{C}^\ell\ \underline{B}_1^\ell + I_{yy}\ (\underline{B}_2^\ell)^T\ \underline{C}^\ell\ \underline{B}_2^\ell]_{\xi=a_j} \tag{3.91}$$

The initial stiffness matrix and force vector are calculated in a simliar manner. If eq. (3.79) is substituted into eq. (3.48) and the integrals are evaluated as in eq. (3.85), the following results are obtained (again using 2-point numerical integration):

$$\underline{K}_{s_i} = \frac{\ell}{2} \sum_{j=1}^{2} (A\ \underline{B}_{s_0} + I_{zz}\ \underline{B}_{s_4} + I_{yy}\ \underline{B}_{s_5})_{\xi=a_j} \tag{3.92}$$

Finally, if eq. (3.83) and (3.77) are substituted into the expression for the initial stress force vector given in Eq. (3.49) and the integrals evaluated as above, the result is as follows:

$$\underline{F}_{s_i} = \frac{\ell}{2} \sum_{j=1}^{2} [A\ (\underline{B}_0^\ell)^T\ {}^\circ\underline{S}_0 + I_{zz}\ (\underline{B}_1^\ell)^T\ {}^\circ\underline{S}_y + I_{yy}\ (\underline{B}_2^\ell)^T\ {}^\circ\underline{S}_z]_{\xi=a_i} \tag{3.93}$$

The element stiffness matrices and force vectors are assembled in the usual way to obtain the global stiffness matrix and initial stress force vector.

CHAPTER IV

NUMERICAL TIME INTEGRATION SOLUTION SCHEME

4.1 Introduction

There are many methods which can be used for the numerical time integration of equations (2.17), (2.22), and (2.75). Generally speaking, these methods can be classified as either explicit or implicit schemes. For any of these schemes the time variations of $\underline{q}$ and $\dot{\underline{q}}$ are discretized using an m-step, one-derivative, linear multistep difference operator

$$\underline{q}_{n+1} = \sum_{i=o}^{p} a_i \, \underline{q}_{n-i} + \Delta t \sum_{i=-1}^{p} b_i \, \dot{\underline{q}}_{n-i} \tag{4.1a}$$

$$\dot{\underline{q}}_{n+1} = \sum_{i=o}^{m} c_i \, \dot{\underline{q}}_{n-i} + \Delta t \sum_{i=-1}^{m} d_i \, \ddot{\underline{q}}_{n-i} \tag{4.1b}$$

where $\underline{q}_{n-i} = \underline{q}(t_{n-i})$

$\dot{\underline{q}}_{n-i} = \dot{\underline{q}}(t_{n-i})$

$\ddot{\underline{q}}_{n-i} = \ddot{\underline{q}}(t_{n-i})$

Δt = time increment = $t_{n+1} - t_n$

In any particular application of equations (4.1), any of the scalar constants, a_i, b_i, c_i or d_i may be zero. If both b_{-1} and d_{-1} are zero then the solution scheme is classified as explicit. If either of b_{-1} or d_{-1} are nonzero then the scheme is an implicit one and equations (4.1) will generally be solvable only by an iterative procedure unless the differential equation is linear. In this case it is possible to solve explicitly for $\underline{q}_{n+1}$.

Explicit schemes are computationally simplier than implicit schemes since they don't involve the solution of an implicit equation. However, with explicit methods it can be shown [31,32] that the stability of the solution is dependent upon the time increment Δt. For linear systems, the maximum time step for a stable solution is related to the highest natural frequency of the system as follows:

$$\Delta t \leq \gamma/\omega_{max} \tag{4.2}$$

Here γ is a scalar constant dependent upon the a_i - d_i and ω_{max} is the highest frequency of the system. For nonlinear systems, the natural frequencies of the system generally change with time as the configuration of the system changes. Equation (4.2) however, will still be true. For certain "stiff" systems with widely varying natural frequencies, the time step necessary for stability can be so small that it becomes computationally time consuming.

Implicit schemes, on the other hand, generally have much less stringent stability requirements. In fact, some methods (e.g. Newmark's method) are unconditionally stable with no time step limitations. The accuracy of the solution then becomes the only limitation on the time step size.

For the example problems discussed in this research, a three node beam element is used. For small displacements, this is essentially a Timoshenko beam. The natural frequencies for a linear cantilevered beam modelled by these elements are shown in Tables 1 and 2 as a function of the shear factor chosen. As is obvious from Tables 1 and 2, using these beam elements will result in a stiff system. The very high frequencies are associated with the shear modes of the beam and even through they are only a small component of the beam response, they control the stability of the numerical solution. Even when very small shear factors are used, the high frequencies due to shear will result in unacceptably small time steps for stability. Thus even though we are interested in nonlinear solutions, the linear solution clearly indicates that an implicit scheme is necessary.

Probably one of the most straight-forward and widely used implicit schemes is the Newmark method or trapezoidal rule [33]. However, most structural dynamics problems involve second order differential equations which include only symmetric matrices whereas the problem here includes a nonsymmetric gyroscopic matrix $\underline{C}$. If the Newmark (or any other strictly implicit method) is used it would result in having to invert a nonsymmetric matrix which involves a good deal more computational time than inverting a symmetric matrix. In addition, many of the terms in the linear and angular momentum equations are nonlinear ones involving the displacements. It would be preferable to treat these terms as equivalent "force" terms to be moved to the right hand side of the equations. So what is really needed is a solution scheme which treats some of the terms in the equations explicitly and some of them implicitly. Such a scheme is the implicit-explicit split operator method [25]. In this method terms such as the $\underline{C}$ matrix are treated explicitly and terms which control the stability of the solution, such as the elastic stiffness matrix, are treated implicitly.

4.2 The Time Integration Method

Consider again equations (2.17), (2.22), and (2.75) with all the terms to be treated implicitly kept on the left hand side and all explicit terms moved to the right hand side of the equations.

$$\underline{M}(\underline{q})\,\ddot{\underline{q}} + \underline{P}(\underline{q})\,\dot{\underline{V}}_o + \underline{H}(\underline{q})\,\dot{\underline{\Omega}} + \underline{K}_E(\underline{q})\,\Delta\underline{q} = \underline{F}_q\,(\underline{R}_o,\underline{V}_o,\underline{\Omega},\underline{q}) - \underline{C}(\underline{\Omega},\underline{q})\dot{\underline{q}} \quad (4.3)$$

$$\underline{P}^T(\underline{q})\ \ddot{\underline{q}} + \underline{M}\ \dot{\underline{V}}_o + \underline{G}(\underline{q})\ \dot{\underline{\Omega}} = \underline{f}_T\ (\underline{R}_o, \underline{V}_o, \underline{\Omega}, \underline{q}, \dot{\underline{q}}) \tag{4.4}$$

$$\underline{H}^T(\underline{q})\ \ddot{\underline{q}} + \underline{G}^T(\underline{q})\ \underline{V}_o + \underline{I}_T(\underline{q})\ \dot{\underline{\Omega}} = \underline{m}_T\ (\underline{R}_o, \underline{V}_o, \underline{\Omega}, \underline{q}, \dot{\underline{q}}) \tag{4.5}$$

Now, replace these three equations by a single "generalized" equation as follows:

$$\underline{M}_G\ \ddot{\underline{q}}_G + \underline{K}_{GE}\ \Delta\underline{q}_G = \underline{F}_G \tag{4.6}$$

where
$$\underline{q}_G = \begin{Bmatrix} \underline{q} \\ \underline{d} \\ \underline{\phi} \end{Bmatrix} \tag{4.7}$$

$$\underline{M}_G = \begin{bmatrix} \underline{M}(\underline{q}) & \underline{P}(\underline{q}) & \underline{H}(\underline{q}) \\ \underline{P}^T(\underline{q}) & M\underline{I}_3 & \underline{G}(\underline{q}) \\ \underline{H}^T(\underline{q}) & \underline{G}^T(\underline{q}) & \underline{I}_T(\underline{q}) \end{bmatrix} \tag{4.8}$$

$$\underline{K}_{GE} = \begin{bmatrix} \underline{K}_E(q) & \underline{0} & \underline{0} \\ \underline{0} & \underline{0} & \underline{0} \\ \underline{0} & \underline{0} & \underline{0} \end{bmatrix} \tag{4.9}$$

$$\underline{F}_G = \begin{Bmatrix} \underline{F}_q\ (\underline{q}_G, \dot{\underline{q}}_G) - \underline{C}\ (\underline{q}_G, \dot{\underline{q}}_G)\ \dot{\underline{q}} \\ \underline{f}_T\ (\underline{q}_G, \dot{\underline{q}}_G) \\ \underline{m}_T\ (\underline{q}_G, \dot{\underline{q}}_G) \end{Bmatrix} \tag{4.10}$$

The variable $\underline{d}$ is a "translational" variable the components of which are the time integrals of $\underline{V}_o$. Similarly, $\underline{\phi}$ is a "rotational" variable the components of which are the time integrals of $\underline{\Omega}$. Thus,

$$\dot{\underline{d}} = \underline{V}_o \tag{4.11}$$

$$\dot{\underline{\phi}} = \underline{\Omega} \tag{4.12}$$

Assuming all the variables in eq. (4.6) are known at time $t = t_n$, the equation at time $t_{n+1} = t_n + \Delta t$ is written as

$$\underline{M}_G^{n+1} \ddot{\underline{q}}_G^{n+1} + \underline{K}_{GE}^{n+1} \Delta\underline{q}_G^{n+1} = \underline{F}_G^{n+1} \tag{4.13}$$

where $$\underline{q}_G^{n+1} = \underline{q}_G (t_{n+1}) \tag{4.14}$$

$$\underline{M}_G^{n+1} = \underline{M}_G (\underline{q}_G^{n+1}) \tag{4.15}$$

$$\underline{K}_{GE}^{n+1} = \underline{K}_{GE} (\underline{q}_G^{n+1}) \tag{4.16}$$

$$\underline{F}_G^{n+1} = \underline{F}_G (\underline{q}_G^{n+1}, \dot{\underline{q}}_G^{n+1}) \tag{4.17}$$

using the trapezoidal rule,

$$\underline{q}_G^{n+1} = \underline{q}_G^{n} + \frac{\Delta t}{2} (\dot{\underline{q}}_G^{n} + \dot{\underline{q}}_G^{n+1}) \tag{4.18}$$

$$\dot{\underline{q}}_G^{n+1} = \dot{\underline{q}}_G^{n} + \frac{\Delta t}{2} (\ddot{\underline{q}}_G^{n} + \ddot{\underline{q}}_G^{n+1}) \tag{4.19}$$

Combining eqs. (4.18) and (4.19) results in the following:

$$\ddot{\underline{q}}_G^{n+1} = \frac{4}{(\Delta t)^2} (\underline{q}_G^{n+1} - \underline{q}_G^{n}) - \frac{4}{\Delta t} \dot{\underline{q}}_G^{n} - \ddot{\underline{q}}_G^{n} \tag{4.20}$$

Substituting eq. (4.20) into eq. (4.13) yields

$$\underline{M}_G^{n+1} \left[\frac{4}{(\Delta t)^2} (\underline{q}_G^{n+1} - \underline{q}_G^{n}) - \frac{4}{\Delta t} \dot{\underline{q}}_G^{n} - \ddot{\underline{q}}_G^{n}\right] + \underline{K}_{GE}^{n+1} \Delta\underline{q}_G^{n+1} = \underline{F}_G^{n+1} \tag{4.21}$$

The above equation is the linearized form of a nonlinear equation and can be solved by Newton-Raphson iteration. Letting subscript i represent the i-th iteration number, eq. (4.21) becomes

$$\underline{M}_{G_i}^{n+1} \left[\frac{4}{(\Delta t)^2} (\underline{q}_{G_{i+1}}^{n+1} - \underline{q}_G^n) - \frac{4}{\Delta t} \dot{\underline{q}}_G^n - \ddot{\underline{q}}_G^n\right] + \underline{K}_{G_{Ei}}^{n+1} \Delta\underline{q}_{G_i}^{n+1} = \underline{F}_{G_i}^{n+1} \tag{4.22}$$

where

$$\Delta\underline{q}_{G_i}^{n+1} = \underline{q}_{G_{i+1}}^{n+1} - \underline{q}_{G_i}^{n+1} \tag{4.23}$$

Rewriting eq. (4.22) a bit results in the following:

$$\underline{M}_{G_i}^{n+1} \left[\frac{4}{(\Delta t)^2} (\underline{q}_{G_{i+1}}^{n+1} - \underline{q}_{G_i}^{n+1} + \underline{q}_{G_i}^{n+1} - \underline{q}_G^n) - \frac{4}{\Delta t} \dot{\underline{q}}_G^n - \ddot{\underline{q}}_G^n\right]$$

$$+ \underline{K}_{GE_i}^{n+1} (\underline{q}_{G_{i+1}}^{n+1} - \underline{q}_{G_i}^{n+1}) = \underline{F}_{G_i}^{n+1} \tag{4.24}$$

Then, after rearranging a few terms, eq. (4.24) becomes

$$[\underline{K}_{GE_i}^{n+1} + \frac{4}{(\Delta t)^2} \underline{M}_{G_i}^{n+1}] \Delta\underline{q}_{G_i}^{n+1} = \underline{F}_{G_i}^{n+1} - \underline{M}_{G_i}^{n+1} \left[\frac{4}{(\Delta t)^2} (\underline{q}_{G_i}^{n+1} - \underline{q}_G^n\right.$$

$$\left. - \frac{4}{\Delta t} \dot{\underline{q}}_G^n - \ddot{\underline{q}}_G^n\right] \tag{4.25}$$

Using eq. (4.20) and rewriting some of the terms a bit, eq. (4.25) becomes

$$\underline{K}_{G_i}^{*} \Delta\underline{q}_{G_i}^{n+1} = \underline{F}_{G_i}^{*} \tag{4.26}$$

where $$\underline{K}_{G_i}^{*} = \underline{K}_{GE_i}^{n+1} + \frac{4}{(\Delta t)^2} \underline{M}_{G_i}^{n+1} \tag{4.27}$$

$$\underline{F}_{G_i}^{*} = \underline{F}_{G_i}^{n+1} - \underline{M}_{G_i}^{n+1} \ddot{\underline{q}}_{G_i}^{n+1} \tag{4.28}$$

Thus by the use of the trapezoidal rule the dynamic equation of eq. (4.13) has been reduced to the static equation of eq. (4.26). The $\underline{K}_G^*$ matrix is called the effective stiffness matrix and $\underline{F}_G^*$ is the effective force vector.

The iteration starts with i = 1 and proceeds until $\Delta \underline{q}_{G_i}^{n+1}$ converges to within a required tolerance, that is, until

$$\left\| \frac{\Delta \underline{q}_{G_i}^{n+1}}{\underline{q}_{G_i}^{n+1} - \underline{q}_G^n} \right\| \leq \text{Tol} \tag{4.29}$$

where Tol is a given tolerance. For the problems considered in this work, Tol=0.01.

4.3 Starting the Iterations

The difficulty that now arises is how to start the iterations. The simplest way of doing this is to use the state of the structure at time t_n as a first approximation to the state of the structure at time t_{n+1}. Thus,

$$\underline{q}_{G_1}^{n+1} = \underline{q}_G^n \tag{4.30}$$

$$\underline{M}_{G_1}^{n+1} = \underline{M}_G^n \tag{4.31}$$

$$\underline{K}_{GE_1}^{n+1} = \underline{K}_{GE}^n \tag{4.32}$$

This approximation is fine for the mass and stiffness matrices since they change slowly with time, but what about the terms in $\underline{F}_G^{n+1}$ which involve $\underline{q}_G^{n+1}$ and $\dot{\underline{q}}_G^{n+1}$? None of these terms have been treated implicitly using eq. (4.18) as was done for the acceleration and elastic stiffness terms. The reason for this, as stated previously, was because many of these terms are nonlinear or involve nonsymmetric matrices. In addition, the stability of the solution cannot be guaranteed if these terms are predicted using eq. (4.30) [25]. To ensure stability, reference [25] indicates that when a trapizoidal rule is used for the implicit part, the following explicit "predictors" for use in the first iteration of $\underline{F}_G^{n+1}$ must be used:

$$\tilde{\dot{\underline{q}}}_G^{n+1} = \dot{\underline{q}}_G^n + \frac{\Delta t}{2} \ddot{\underline{q}}_G^n \tag{4.33}$$

$$\tilde{\underline{q}}_G^{n+1} = \underline{q}_G^n + \Delta t\ \dot{\underline{q}}_G^n + \frac{(\Delta t)^2}{4} \ddot{\underline{q}}_G^n \tag{4.34}$$

Thus, $$\underline{F}_{G_1}^{n+1} = \underline{F}_G\ (\tilde{\underline{q}}_G^{n+1},\ \tilde{\dot{\underline{q}}}_G^{n+1}) \tag{4.35}$$

Note that eqs. (4.34) and (4.35) are obtained by setting $\ddot{\underline{q}}_G^{n+1} = 0$ in eqs. (4.18) and (4.19). Eqs. (4.30) - (4.32) and (4.35) thus are used in the first iteration of eqn. (4.26). The entire iteration process is summarized in Table 3. The solution scheme described in the previous pages used the regular Newton-Raphson iteration. A modified Newton-Raphson iteration in which the $\underline{K}_G^*$ matrix is kept constant throughout the iterations could also be used. This could result in a computational savings since $\underline{K}_G^*$ need be decomposed only once; however, a larger number of iterations will generally be necessary than for the regular Newton-Raphson iteration.

4.4 Spacecraft Angular Orientation Determination

In order to determine the orientation of the spacecraft at a given time, it is necessry to determine the angular transformation between the inertial axes and the rotating body axes. As shown in a previous section, this transformation can be represented in many different ways, including Euler angles or space-three: 1-2-3 angles. Let this set of three orientation angles be represented by the vector $\underline{\theta}$ which is of course a function of time. These orientation angles are related to the body axis angular velocity as follows [34]:

$$\dot{\underline{\theta}} = \underline{M}_\Theta\ (\underline{\theta})\ \underline{\Omega} \tag{4.36}$$

The $\underline{M}_\Theta$ matrix is a 3 x 3 matrix whose elements are functions of the orientation angles $\underline{\Theta}$. For space-three angles,

$$\underline{\Theta}^T = \lfloor \Theta_1 \ \Theta_2 \ \Theta_3 \rfloor \qquad (4.37)$$

and

$$\underline{M}_\Theta = \frac{1}{\cos\Theta_2} \begin{bmatrix} \cos\Theta_2 & \sin\Theta_1 \sin\Theta_2 & \cos\Theta_1 \sin\Theta_2 \\ 0 & \cos\Theta_1 \cos\Theta_2 & -\sin\Theta_1 \cos\Theta_2 \\ 0 & \sin\Theta_1 & \cos\Theta_1 \end{bmatrix} \qquad (4.38)$$

For Euler angles,

$$\underline{\Theta}^T = [\psi \ \theta \ \phi] \qquad (4.39)$$

$$\underline{M}_\Theta = \frac{1}{\sin\theta} \begin{bmatrix} \sin\phi & \cos\phi & 0 \\ \cos\phi\sin\theta & -\sin\phi\sin\theta & 0 \\ -\sin\phi\cos\theta & -\cos\phi\cos\theta & \sin\theta \end{bmatrix} \qquad (4.40)$$

Notethat for time periods when $\cos\Theta_2 = 0$, space-three angles cannot be used and Euler angles cannot be used if $\sin\theta = 0$. Thus it is necessary to calculate both space-three and Euler (or any other description) so that if one formula fails at a given time, the other can be used.

It is necessary to solve eq. (4.36) numerically and this can be done using the following integration scheme:

$$\underline{\Theta}_{n+1} = \underline{\Theta}_n + \frac{\Delta t}{2} \underline{M}_\Theta (\underline{\Omega}_n + \underline{\Omega}_{n+1}) \qquad (4.41)$$

Both $\underline{\Omega}_n$ and $\underline{\Omega}_{n+1}$ will have been previously calculated. Once the new $\underline{\Theta}$ has been calculated, it becomes possible to determine the direction cosine matrix $\underline{C}_D$ which relates the inertial coordinates to the body axis coordinates as follows:

$$\underline{X}_{INERTIAL} = \underline{C}_D \, \underline{X}_{BODY} \tag{4.42}$$

The elements of the $\underline{C}_D$ matrix for space-three angles are given below:

$$C_{D_{11}} = \cos\theta_2 \cos\theta_3 \tag{4.43a}$$

$$C_{D_{12}} = \sin\theta_1 \sin\theta_2 \cos\theta_3 - \sin\theta_3 \cos\theta_1 \tag{4.43b}$$

$$C_{D_{13}} = \cos\theta_1 \sin\theta_2 \cos\theta_3 + \sin\theta_3 \sin\theta_1 \tag{4.43c}$$

$$C_{D_{21}} = \cos\theta_2 \sin\theta_3 \tag{4.43d}$$

$$C_{D_{22}} = \sin\theta_1 \sin\theta_2 \sin\theta_3 + \cos\theta_3 \cos\theta_1 \tag{4.43e}$$

$$C_{D_{23}} = \cos\theta_1 \sin\theta_2 \sin\theta_3 - \cos\theta_3 \sin\theta_1 \tag{4.43f}$$

$$C_{D_{31}} = -\sin\theta_2 \tag{4.43g}$$

$$C_{D_{32}} = \sin\theta_1 \cos\theta_2 \tag{4.43h}$$

$$C_{D_{33}} = \cos\theta_1 \cos\theta_2 \tag{4.43i}$$

The elements of the $\underline{C}_D$ matrix for Euler angles are also given as follows:

$$C_{D_{11}} = \cos\phi \cos\psi - \sin\phi \cos\theta \sin\psi \tag{4.44a}$$

$$C_{D_{12}} = -\sin\phi \cos\psi - \cos\phi \cos\theta \sin\psi \tag{4.44b}$$

$$C_{D_{13}} = \sin\theta \sin\psi \tag{4.44c}$$

$$C_{D_{21}} = \cos\phi \sin\psi + \sin\phi \cos\theta \cos\psi \tag{4.44d}$$

$$C_{D_{22}} = -\sin\phi \sin\psi + \cos\phi \cos\theta \cos\psi \tag{4.44e}$$

$$C_{D_{23}} = -\sin\theta \cos\psi \tag{4.44f}$$

$$C_{D_{31}} = \sin\phi \sin\theta \tag{4.44g}$$

$$C_{D_{32}} = \cos\phi \sin\theta \tag{4.44h}$$

$$C_{D_{33}} = \cos\theta \tag{4.44i}$$

Once eq. (4.41) has been solved for $\underline{\Theta}$, then the $\underline{C}_D$ can be calculated using either Eq. (4.43) or (4.44) depending upon whether space-three or Euler angles have been computed in eq. (4.41). The $\underline{C}_D$ matrix can then be used to determine the orientation angles that weren't calculated in eq. (6) [34]. For example, suppose eq. (4.41) is used to solve for the space-three angles and then eqs. (4.43) are used to calcualte $\underline{C}_D$. Since $\underline{C}_D$ must be the same for any orientation angle used, the Euler angles could be calculated by solving for ψ, θ, and ϕ in eqs. (4.44). The reverse is, of course, also true, i.e., given $\underline{C}_D$, the angles Θ_1, Θ_2, and Θ_3 can be solved for in eqs. (4.43). Table 4 summarizes the entire procedure as well as providing more details on solving for the orientation angles given in the $\underline{C}_D$ matrix.

CHAPTER FIVE

NUMERICAL RESULTS

5.1 Gravitational Forces and Moments

The method developed in the previous sections is now used to analyze several example problems. The first four examples involve the analysis of structures which are rotating with large enough angular velocities that most of the response occurs in a short time period of a minute or less. Examples 2-4 involve spacecraft which rotate in this fashion. For these spacecraft, the moment caused by the gravitational gradient is small and can be neglected. Also, the spacecraft will move very little along the orbital path during the short time periods which are of interest in these problems. The spacecraft is thus treated as though it is in a force free environment (except for any applied control forces). In example 5, the geometry of the spacecraft is such that moments due to the gravitational gradient are important and the time periods of interest are relatively long, up to an hour. Thus it is necessary to obtain an expression for the force and moment due to gravity.

In Fig. 1, let the inertial axes be located at the center of the earth C and let $\underline{R}_o$ be the position vector of the orbiting spacecraft. Neglecting any small changes in $\underline{R}_o$ due to deformations,

$$\underline{F}_T = - \frac{\mu_o M \underline{R}_o}{R_o^{\,3}} \tag{5.1}$$

where

μ_o = Gravitational constant of the Earth

M = Spacecraft mass

The element body force term eq. (2.43) in the principle of virtual work, thus becomes as follows:

$\omega_d = \omega\sqrt{1 - \xi_d^2}$ = Damped natural frequency

I_{33} = Total spacecraft moment of inertia

For a given I_{33}, the values of the control constants are determined by the values of ω and ξ_d which are in turn determined by the desired percent overshoot and rise time of the response,

$$\xi_d = -\sqrt{\frac{\ell n\ p}{\pi^2 + \ell n^2\ p}} \tag{5.23}$$

$$\omega t_r = \frac{1}{\sqrt{1 - \xi_d^2}}\ [\mathrm{Tan}^{-1}\ (-\frac{\sqrt{1 - \xi_d^2}}{\xi_d}) + \pi] \tag{5.24}$$

where p = Percent overshoot of the response

t_r = Response rise time; the time at which θ first equals θ_{ref}

For $p = 0.01$ and $t_r = 5$ sec, the following results:

$\xi_d = 0.82609$

$\omega = 0.902472$ rad/sec

$K_T = 0.814456\ I_{33}$

$K_W = 1.49103\ I_{33}$

Using the spacecraft parameters given in figure 20 results in $I_{33} = 15{,}122$ slug-ft^2, $K_T = 12{,}316$ ft-lb/rad, and $K_W = 22{,}547$ ft-lb-sec. A value of $\theta_{Ref} = 20^\circ$ was chosen as the reference angle.

Since the spacecraft is symmetric, only half of it need be modeled. The motion was studied using both one and two beam elements with a time step size of $\Delta t = 0.1$ second. In addition, two values of Young's modulus were used, $E = E_o$ and $E = 0.5\ E_o$. The rotation angle for both the rigid

5.5 Example 4 - Spacecraft Rotating to a Specified Orientation

In examples 2 and 3 the motion of a rotating spacecraft with prescribed angular velocity was analyzed. In this example the more realistic problem of a spacecraft rotating to a specified angular orientation using an applied control moment is considered. The spacecraft is the simple symmetric dipole pictured in figure 20 and is originally at rest until a control moment that is proportional to the angular change desired is applied at the center of the rigid mass. To provide damping, the control moment is also proportional to the angular velocity. The control moment is thus as follows:

$$M = -K_T\,(\theta-\theta_{ref})\ -K_W\,\Omega$$

where K_T, K_W = Control constants

θ = Rotation angle

θ_{ref} = Reference angle through which the spacecraft is to be rotated

If a sensor or some other form of instrument for which pointing accuracy is important is attached to the spacecraft, it becomes important to have a good estimation of how $\theta(t)$ varies with time.

The rigid body solution for this problem is the usual damped sinusoidal response typical of underdamped second-order control systems,

$$\theta_{Rigid} = \theta_{Ref}\,\{1 - e^{-\xi_d \omega t}\,[\cos \omega_d\, t + \frac{\xi_d}{1 - \xi_d^2} \sin \omega_d\, t]\} \quad (5.22)$$

where $\omega^2 = K_T/I_{33}$ = Circular frequency

$\xi_d = K_W/2\omega I_{33}$ = Damping constant

$$\Omega_3 = \Omega_0 \sin\gamma \cos\lambda\,(t-T_0) \tag{5.20c}$$

where $$\lambda = \left(\frac{I_{22} - I_{11}}{I_{22}}\right) \Omega_0 \cos\gamma \tag{5.21}$$

For the elastic spacecraft, the inertias of the rigid body are chosen such that $I_{22} = I_{33} > I_{11}$ in the undeformed structure. One beam element is used to represent each beam and a time step size of $\Delta t = 0.1$ second was used in the numerical integration.

The angular velocities of the elastic spacecraft are compared to the rigid body case in figures 17-19. The elastic response for Ω_1 is much closer to the rigid body case than the responses for the Ω_2 and Ω_3 components are. The three dimensional elastic deformations are coupled with each other as well as with the angular velocities causing a very complicated response. The state of the spacecraft at any given time would be very different from that predicted by rigid body dynamics alone.

5.4 Example 3 - Three Dimensional Precessing Spacecraft

In this example the same spacecraft as in example 2 is subjected to out of plane rotations. As pictured in Fig. 16, the spacecraft is "spun-up" about a line in the x_1-x_3 plane by applying a moment during the time period $0 \leq t \leq T_0$ which results in the following angular velocity:

$$\Omega_1 = \begin{cases} \Omega_0 \cos\gamma \left[6\left(\frac{t}{T_0}\right)^5 - 15\left(\frac{t}{T_0}\right)^4 + 10\left(\frac{t}{T_0}\right)^3\right] \text{ rad/sec} & 0 \leq t \leq T_0 \\ \text{Free Variable} & t > T_0 \end{cases} \quad (5.19a)$$

$$\Omega_2 = \begin{cases} \Omega_1(t) \tan\gamma & 0 \leq t \leq T_0 \\ \text{Free Variable} & t > T_0 \end{cases} \quad (5.19b)$$

$$\Omega_3 = \begin{cases} 0 & 0 \leq t \leq T_0 \\ \text{Free Variable} & t \geq T_0 \end{cases} \quad (5.19c)$$

where γ = Angle between the x_1 axis and $\underline{\Omega}$

Values for Ω_0, T_0 and γ used in this example were as follows:

Ω_0 = 0.72552 rad/sec

T_0 = 2 sec

$\gamma = 30^\circ$

The rigid body response for $t > T_0$ in such a situation would be for the angular velocity vector to precess about the x_1 axis with a constant precession rate λ [35]. For rigid bodies with $I_{22} = I_{33} > I_{11}$, the angular velocities are as follows for $t > T_0$:

$$\Omega_1 = \Omega_0 \cos\gamma = \text{constant} \quad (5.20a)$$

$$\Omega_2 = \Omega_0 \sin\gamma \sin\lambda\,(t-T_0) \quad (5.20b)$$

The effect of the control forces on the rotation angle is illustrated in Fig. 13. When a control force is applied, the motion will eventually damp out and the average angular velocity will approach zero. As seen in Fig. 13, the larger the control force, the smaller the rotation angle. Figures 14 and 15 show the tip displacements and the angular velocity as a function of time. Note that the amplitudes of vibration decrease with time as the control forces are applied as would be expected. One thing should also be noted in Fig. 15. At $t = T_0 = 2$ sec the applied moment which is turning the spacecraft is suddenly released. This sudden change or discontinuity in applied moment results in a discontinuity in the accelerations which shows up as a "kink" in the angular velocity at $t = 2$ sec. No "kink" is seen in the displacements since the velocities are all continuous.

In this example it has been demonstrated that it is indeed necessary to take into account the deformations of the spacecraft to accurately analyze the motion.

Another way of determining the effect of offset is to see how unsymmetrical the motion is. In Fig. 11 is plotted the tip displacement of both left and right beams for $I_R = 10^4$ slug-ft^2, $m_R = 100$ slug and $r_G = 15$ ft. The displacements can be seen to be almost the same for each beam indicating that at least for the $\underline{\Omega}(t)$ given in eq. (5.16) the motion is almost symmetrical.

Next, the effects of these changes on the rotation of the body axes are considered. The effects on the rotation angle of increasing the rigid inertia has already been considered in Section 5.2. The effects of increased offset are illustrated in Fig. 12 which gives the rotation angle as a function of time for $r_G = 0$ and 15 ft. Note that for both cases the average angular velocity is the same but that the period is larger for the larger offset.

5.3.2 The Effect of Control Forces

In this section the effect of control forces applied at the tips of the beams are considered. These forces are proportional to the tip velocity:

$$\underline{F}_C = - K_T \underline{V}_T \tag{5.17}$$

where K_T = Control constant

$\underline{V}_T$ = Beam tip velocity

Note that

$$\underline{V}_T = \underline{\Omega} \times \underline{r}_T + \underline{\dot{u}}_T \tag{5.18}$$

$\underline{r}_T$ = Position vector of beam tip

$\underline{\dot{u}}_T$ = Elastic velocity of beam tip

Three different values of control constants are considered, $K_T = 0$, 5, and 20 Lb-sec/ft. For all three cases, the rigid mass and inertia were $m_R = 500$ slugs and $I_R = 5(10)^4$ slug-ft^2 with an offset of $r_G = 5$ ft. Once again, a time step of 0.1 sec was used in the numerical integration.

5.3.1 Parametric Studies

For all the problems in this part, the beam properties were kept constant and only the properties of the central rigid mass were varied. The way these changes affect the frequency of vibration of the beams can thus be determined.

The equations of motion were solved using a time step of $\Delta t = 0.1$ sec. and one element to represent each beam. The resulting beam periods of vibration are summarized in table 5. Note that the period increases as the size of the rigid mass increases. As the rigid inertia grows smaller in comparison to the inertia of the beam, the problem approaches that of a free-free beam vibrating in its second mode shape. For a 200 ft. length beam, the linear second mode frequency results in a period of 2.2 seconds. As the rigid inertia grows very large in comparison to the beam inertia, the problem approaches that of a cantilever beam attached to a very large rigid mass. The linear period for a 100 ft. cantilever is 6.4 seconds. In Table 5, the periods will vary between these two extremes.

Now, what about the effect of the offset? As can be seen in Table 5, for a given rigid inertia as the offset increases so also does the period. However, notice that the change in period is much less as the rigid inertia increases. Also, to determine the effects of varying the rigid mass while keeping the rigid rotary inertia constant, the following was done. For $I_R = 10^4$ slug-ft^2 and $r_G = 15$ ft, rigid masses of $m_R = 100$, 500, and 1000 slugs were used. The resulting periods were all the same value of $T = 3.3$ sec. indicating that m_R has little effect on the period. What was affected by m_R was the translation of the body axes. These, however, were very small and never exceeded one foot and thus had very little effect on the rest of the motion.

5.3 Example 2 - Rotating Spacecraft with an Offset Center of Mass and Applied Control Forces

In this example a simple spacecraft consisting of two slender aluminum beams attached to a central rigid mass is analyzed (Fig. 10). The rigid mass has a mass moment of inertia of I_R, a mass of m_R, and a width of $2r_c$. A set of body axes, x_1, x_2 and x_3 are fixed in the spacecraft and rotate with it. The centerlines of the beams are originally aligned along the x_1 axis and the center of mass of the spacecraft is offset a distance r_G along the x_2 axis.

The spacecraft is originally at rest but at time t = 0 a moment is applied to the spacecraft for T_o seconds such that a given angular velocity is achieved. This angular velocity was chosen so that the rigid mass would rotate through a given angle in the x_1 - x_2 plane and then come smoothly to rest at $t = T_o$. After T_o seconds, the applied moment is released and the angular velocity becomes a free variable. The particular form chosen for the angular velocity was as follows:

$$\underline{\Omega}(t) = \begin{cases} \frac{\Omega_o}{2}\left[1 + \sin \pi \left(\frac{2t}{T_o} - \frac{1}{2}\right)\right] \text{ rad/sec} & 0 \leq t \leq T_o \\ \text{Free Variable} & t > T_o \end{cases} \tag{5.16}$$

For all the problems solved in this example, $\Omega_o = \pi/20$ rad/sec and $T_o = 2$ seconds. Note that if $r_G = 0$ the problem is symmetric and only one half of the spacecraft need be modeled. However, if $r_G \neq 0$, then in general the motion will not be symmetric and the entire spacecraft will need to be modeled.

The results of this example are divided into two parts. In the first part, a parametric study is done in which the effects of varying the rigid mass and inertia as well as the center of mass offset are studied. In the second part, the effect of applied control forces is examined. For both cases, eq. (5.16) is used during the "spin-up" period of motion.

Also note that the larger I_R is in comparison to I_B, the closer Ω_{Avg} will be to the rigid body angular velocity Ω_0.

Now eq. (5.15) can be used to explain the behavior of the beam in figures 8 and 9. At t = 1.0 sec the beam is moving away from the body axis and thus $H_{D_0} < 0$. At t = 3.3 sec. the beam has reached its maximum displacement relative to the body axis and thus $H_{D_0} \simeq 0$. At t = 7.0 sec. the beam is leading the rigid body motion and $H_{D_0} > 0$. Thus the average angular velocities pictured in figure 8 are as predicted by eq. (5.15). Similar results are obtained in figure 9 except that with a larger inertia ratio, all the averge angular velocities are closer to Ω_0 as predicted again by eq. (5.15).

where I_B = Mass moment of inertia of the beam about the shaft centerline

Also, let

$$H_D = \underline{H}^T \dot{\underline{q}} \tag{5.11}$$

The value of I_B will change only slightly as the beam vibrates and for the purposes of this discussion it is sufficient to consider it to be a constant. The conservation of angular momentum requires that

$$(I_R + I_B)\ \Omega_o + H_{D_o} = (I_R + I_B)\ \Omega + H_D \tag{5.12}$$

where $H_{D_o} = (H_D)_{t=T_{MOM}}$

Solving for Ω,

$$\Omega = \Omega_o + \left(\frac{1}{I_R + I_B}\right)(H_{D_o} - H_D) \tag{5.13}$$

The angular velocity will be constantly changing, but what will its average value be? Taking a time average of eq. (5.13),

$$\Omega_{Avg} = \Omega_o + \left(\frac{1}{I_R + I_B}\right)\left[H_{D_o} - (H_D)_{Avg}\right] \tag{5.14}$$

Since the beam vibrates about the equilibrium position, $(H_D)_{Avg}$ will be small and can be negleccted. Thus,

$$\Omega_{Avg} = \Omega_o + \left(\frac{1}{I_R + I_B}\right) H_{D_o} \tag{5.15}$$

So if

$H_{D_o} < 0$ then $\Omega_{Avg} < \Omega_o$

$H_{D_o} > 0$ then $\Omega_{Avg} > \Omega_o$

$H_{D_o} = 0$ then $\Omega_{Avg} = \Omega_o$

The results for case 2 are presented in figures 8 and 9, which show the variation of the rotation angle of the body axes with time. In figure 8, $I_R/I_B = 0.5$ and in figure 9 $I_R/I_B = 1.0$. For both cases, $T_{MOM} = 1.0, 3.3$, and 7.0 seconds. In both figures, the "average" angular velocity is greater than Ω_o for $T_{MOM} = 7$ and less than Ω_o for $T_{MOM} = 1.0$ while for $T_{MOM} = 3.3$ it is about the same as Ω_o. Note also that all the angular velocities are closer to Ω_o for the larger inertia ratio in figure 9 than in figure 8.

In order to understand the behavior of the beam in figures 8 and 9, consider what happens when the moment support is released at $t = T_{MOM}$ and the angular velocity becomes a free variable. For $t > T_{MOM}$, there is no longer an applied moment turning the shaft and the angular momentum will remain constant. The angular momentum $\underline{H}_A$ is determined as follows:

$$\underline{H}_A = \int_V \rho(\underline{r} \times \frac{d\underline{r}}{dt})\, dv \tag{5.6}$$

But
$$\frac{d\underline{r}}{dt} = \underline{\Omega} \times \underline{r} + \dot{\underline{u}} \tag{5.7}$$

Substituting eq. (5.7) as well as eq. (2.14) into eq. (5.6) and rearranging,

$$\underline{H}_A = - (\int_V \rho\, \underline{\bar{r}}^2\, dv)\, \underline{\Omega} + (\int_V \rho\, \underline{\bar{r}}\, \underline{N}^*\, dv)\dot{\underline{q}} \tag{5.8}$$

Using eqs. (2.29) and (2.30) results in

$$\underline{H}_A = \underline{I}\, \underline{\Omega} + \underline{H}^T\, \dot{\underline{q}} \tag{5.9}$$

For this particular problem, $\underline{H}_A$, $\underline{I}$ and $\underline{\Omega}$ are scalars and

$$I = I_R + I_B \tag{5.10}$$

Case 2 - $\underline{\Omega}(t)$ free for $t > T_{MOM}$

$$\underline{\Omega}(t) = \begin{cases} \Omega_0 \left[6 \left(\frac{t}{T_0}\right)^5 - 15 \left(\frac{t}{T_0}\right)^4 + 10 \left(\frac{t}{T_0}\right)^3\right] \text{ rad/sec} & 0 \leq t \leq T_0 \\ \Omega_0 \text{ rad/sec} & T_0 \leq t \leq T_{MOM} \\ \text{Unknown variable} & t \geq T_{MOM} \end{cases}$$

For both cases, values of $\Omega_0 = \pi/10$ rad/sec and $T_0 = 1$ sec were used. The equations of motion were integrated using a time step of $\Delta t = 0.1$ sec and one beam element was used.

The results for case 1 are shown in figures 6 and 7. Figure 6 shows the angular displacement of the tip of the beam as it rotates. This is the angle between the inertial x_1 axis and a line drawn from the origin of the body axis to the tip of the beam at time t. The body axes and inertial axes coincide at t = 0. In figure 7 is pictured the orientation of the deformed beam at different times. The dashed lines represent the positions of the x_1 body axis at the given times and coincides with the motion of a rigid beam. The solid lines are the shapes of the deformed beam and the arrows represent the displacement of the beam tip.

The linear natural frequency for this beam as given in Table 1 is $\omega_1 =$ 0.547 rad/sec which corresponds to a period of 11.5 sec. Note that $\omega_1 > \Omega_0$ and thus it would be expected that the beam would complete about 1.7 vibration cycles about the rigid body position during the 20.5 sec. it takes for the shaft to complete one rotation. As can be seen in figures 6 and 7, this is exactly what the beam does. For the first 6 seconds it lags behind the rigid body motion, then for the next 6 seconds it leads the rigid body motion completing a cycle in 12 seconds. Thus the beam vibrates back and forth about the rigid body motion.

5.2 Example 1 - A Beam Rotating About a Fixed Axis

In this example a thin uniform aluminum beam is fixed to a shaft which is rotating about its centerline with an angular velocity Ω. The shaft has a mass moment of inertia of I_R about its centerline which is fixed so that no translations occur. The radius of the shaft is negligible compared to the length of the beam. A set of body axes x_1, x_2 and x_3 are fixed in the shaft and rotate with it. At time $t = 0$ the beam and shaft are at rest and the beam is aligned along the x_1 axis. The situation is illustrated in figure 5.

Two different cases are considered. In case 1 the angular velocity $\underline{\Omega}$ is a specified function of time for all time. The only unknowns are the nodal displacements and velocities which can be found using eq. (2.75) with $\underline{\Omega}$ and $\dot{\underline{\Omega}}$ given and $\underline{V}_0 = \dot{\underline{V}}_0 = \underline{0}$. For case 2, the angular velocity is specified only for $t \leq T_{MOM}$ after which it becomes a free variable. The time period $0 \leq t \leq T_{MOM}$ is the "spin up" period during which the beam is accelerated from rest to a given angular velocity. For $t > T_{MOM}$, the angular velocity becomes an unknown variable and eq. (2.28) must be used to solve for it. For each case, the angular velocity during the spin up period is a smooth polynomial. The two cases can be summarized as follows:

Case 1 - $\underline{\Omega}(t)$ given for all time

$$\underline{\Omega}(t) = \begin{cases} \Omega_0 \left[6 \left(\frac{t}{T_0}\right)^5 - 15 \left(\frac{t}{T_0}\right)^4 + 10 \left(\frac{t}{T_0}\right)^3\right] \text{ rad/sec} & 0 \leq t \leq T_0 \\ \Omega_0 \text{ rad/sec} & t \geq T_0 \end{cases}$$

$$\underline{F}_B = -\left(\int_{v_e} \rho\ \underline{N}^{*T}\ dv\right) \frac{\mu_o \underline{R}_o}{R_o^{\ 3}} \tag{5.2}$$

or

$$\underline{F}_B = -\left(\frac{\mu_o}{R_o^{\ 3}}\right) \underline{P}\ \underline{R}_o \tag{5.3}$$

The moment due the gravitational gradient can be shown [34] to be as follows:

$$\underline{M}_G = \frac{\mu_o M}{R_o^{\ 3}} \overline{\underline{R}}_o\ \underline{r}_G - \frac{3\mu_o}{R_o^{\ 5}} \int_v \rho\ (\underline{R}_o^T\ \underline{r})(\overline{\underline{R}}_o\ \underline{r})\ dv \tag{5.4}$$

where

$$\underline{r}_G = \frac{1}{M} \int_v \rho\ \underline{r}\ dv \tag{5.5}$$

Note that $\underline{r}_G$ is the instantaneous location of the center of mass.

body case and the elastic cases are pictured in figure 21. Note that for $E = E_0$, the response time is still about 5 seconds but that because of the elasticity of the beams, the peak overshoot is near 10%. Also, it takes about 12 seconds before the orientation does not vary more than 1% from 20°. The more flexible beam with $E = \frac{1}{2} E_0$ still has a peak overshoot of 10% but the rise time is increased to 5.8 seconds and it takes even longer for the rotation to settle down to within 1% of θ_{Ref}. Figure 22 shows the actual orientation of the spacecraft for $E = E_0$ at $t = 5$ seconds. The beam tip lateral displacement are plotted in Figure 23. Note that both figures illustrate the large deformations which occur.

5.6 Example 5 - Gravity Gradient Stabilization of a Spacecraft in a Circular Earth Orbit

The previous example examined spacecraft with fairly high rates of rotation during relatively short time periods. This example considers a slowly turning spacecraft over a time period which is a significant percentage of the orbital period. Consider the spacecraft pictured in figures 24 and 25 which consists of a single long slender beam attached to a rigid mass. The spacecraft is in a 200 mile altitude circular Earth orbit and at time t = 0 the beam axis is at an angle $\beta = 45^\circ$ to the orbital radius vector $\underline{R}_0$. The spacecraft is rotating with an initial angular velocity $\omega_0 = \sqrt{\mu_0/R_0^3} = 1.1512(10^{-3})$ rad/sec. and thus $\dot{\beta} = 0$. The gravitational gradient causes a moment (eq. (5.4)) which tends to align the beam axis with the orbital radius vector. A control moment M_c is applied at point 0 in the rigid mass as follows:

$$M_c = -L_\beta \dot{\beta} \tag{5.25}$$

where L_β = Control constant

In order to determine the values of L_β to use, consider the rigid body problem with small β.

$$\ddot{\beta} + 2\mu p \dot{\beta} + p^2 \beta = 0 \tag{5.26}$$

where

$$p^2 = \frac{3\mu_0}{R_0^3} \left(\frac{I_{22} - I_{11}}{I_{33}}\right) \tag{5.27}$$

$$\mu = \frac{L_\beta}{2pI_{33}} \tag{5.28}$$

With $\mu = 1$, the system becomes critically damped, thus for an underdamped system, choose

$$L_\beta < 2pI_{33} \tag{5.29}$$

The spacecraft is in a 200 mile high orbit and thus the orbital period is 5458 sec. Two different sizes of rigid mass are considered:

<u>Case 1</u>	<u>Case 2</u>
m_R = 5000 slugs	m_R = 1500 slugs
$I_{R_1} = 10^4$ ft-lb-sec^2	$I_{R_1} = 10^4$ ft-lb-sec^2
$I_{R_2} = 10^8$ ft-lb-sec^2	$I_{R_2} = 2.43\ (10^6)$ ft-lb-sec^2
$I_{R_3} = 3(10^8)$ ft-lb-sec^2	$I_{R_3} = 3(10^6)$ ft-lb-sec^2

The size and material properties of the beam are identical for each case. The problems were tested using both a one and two element model with a time step of $\Delta t = 10$ seconds.

Figures 26 and 27 show the results for case 1 for both free vibration (no control forces) and a control moment with $L_B = 4.5(10^4)$ ft-lb-sec. Note that even though fig. 25 indicates that large elastic displacements in the beam are occuring, the motion of the rigid mass is almost the sames as that for a rigid body. Thus, for such a large rigid mass, the elastic displacements of the beam have little effect on the variation of the angle β.

The results for case 2 are pictured in figs. 28 and 29. For no control forces, the elastic deformations in this case do have an effect on β, even though it generally follows the rigid body case. With the control force added, however, the motion for β is nearly indentical to the rigid body case.

CHAPTER VI

CONCLUSIONS

The numerical results obtained in Chapter V indicate that the method developed here is capable of determining the time response of unrestrained flexible structures which are undergoing large elastic deformations coupled with gross nonsteady rigid body translational and rotational motions with respect to an inertial reference. The use of an implicit-explicit split operator numerical integration scheme has resulted in stable solutions for all the problems tested. In addition, the example problems indicate that the method is capable of analyzing problems which include the effect of control forces. Although only beam elements have been used in this work, the equations in Chapter II are quite general and will apply for more complicated elements such as plates and shells. Also, the method can be used to solve problems which include more complicated types of motions such as spacecraft deployments involving rotations and relative velocities between different spacecraft parts.

Table 1

Natural Frequencies of a Linear Cantilever Beam Modelled by One 3-Node Timoshenko Element
L/t = 100

Shear Factor β	ω_1	ω_2 (Rad/Sec)	ω_3	ω_4
1.0	0.5470	4.502	8417	11,287
0.5	0.5470	4.499	5956	7,981
0.1	0.5470	4.478	2677	3,570
0.01	0.5448	4.259	891	1,132

Table 2

Natural Frequencies of a Linear Cantilever Beam Modelled by Two 3-Node Timoshenko Elements
L/t = 100

Shear Factor β	ω_1	ω_2	ω_3	ω_4 (Rad/Sec)	ω_5	ω_6	ω_7	ω_8
1.0	0.5222	3.533	11.88	49.85	5271	9900	11,287	11,294
0.5	0.5528	3.549	11.87	49.39	3763	7007	7,981	7,988
0.1	0.5311	3.524	11.74	46.10	1808	3157	3,570	3,582
0.01	0.5312	3.411	10.62	29.94	905	1073	1,132	1,173

TABLE 3

Summary of Newton-Raphson Iteration Scheme

1. Predict quantities for first iteration, i=1

$$\underline{q}_{G_i}^{n+1} = \underline{q}_G^{n}$$

$$\dot{\underline{q}}_{G_i}^{n+1} = \dot{\underline{q}}_G^{n}$$

$$\ddot{\underline{q}}_{G_i}^{n+1} = -\frac{4}{\Delta t}\dot{\underline{q}}_G^{n} - \ddot{\underline{q}}_G^{n}$$

$$\tilde{\underline{q}}_{G_i}^{n+1} = \underline{q}_G^{n} + \Delta t\,\dot{\underline{q}}_G^{n} + \frac{(\Delta t)^2}{4}\ddot{\underline{q}}_G^{n}$$

$$\tilde{\dot{\underline{q}}}_{G_i}^{n+1} = \dot{\underline{q}}_G^{n} + \frac{\Delta t}{2}\ddot{\underline{q}}_G^{n}$$

2. Form Modified Stiffness Matrix and Force Vector

$$\underline{K}^{*}_{G_i} = \underline{K}_{GE}\,(\underline{q}_{G_i}^{n+1}) + \frac{4}{(\Delta t)^2}\underline{M}_G\,(\underline{q}_{G_i}^{n+1})$$

$$\underline{F}^{*}_{G_i} = \underline{F}_G\,(\tilde{\underline{q}}_{G_i}^{n+1}, \tilde{\dot{\underline{q}}}_{G_i}^{n+1}) - \underline{M}_G\,(\underline{q}_{G_i}^{n+1})\,\ddot{\underline{q}}_{G_i}^{n+1}$$

3. Solve for incremental displacements

$$\Delta\underline{q}_{G_i}^{n+1} = \underline{K}^{*-1}_{G_i}\,\underline{F}^{*}_{G_i}$$

4. Update or correct the displacements, velocities and accelerations

$$\underline{q}_{G_{i+1}}^{n+1} = \underline{q}_{G_i}^{n+1} + \Delta\,\underline{q}_{G_i}^{n+1}$$

$$\ddot{\underline{q}}_{G_{i+1}}^{n+1} = \frac{4}{(\Delta t)^2}(\underline{q}_{G_i}^{n+1} - \underline{q}_G^{n}) - \frac{4}{\Delta t}\dot{\underline{q}}_G^{n} - \ddot{\underline{q}}_G^{n}$$

TABLE 3

$$\dot{\underline{q}}_{G_{i+1}}^{n+1} = \dot{\underline{q}}_G^{n} + \frac{\Delta t}{2} (\ddot{\underline{q}}_{G_{i+1}}^{n+1} + \ddot{\underline{q}}_G^{n})$$

$$\tilde{\underline{q}}_{G_{i+1}}^{n+1} = \underline{q}_{G_{i+1}}^{n+1}$$

$$\tilde{\dot{\underline{q}}}_{G_{i+1}}^{n+1} = \dot{\underline{q}}_{G_{i+1}}^{n+1}$$

5. Check to see if iterations have converged

$$\left\| \frac{\Delta \underline{q}_{G_i}}{\underline{q}_{G_{i+1}}^{n+1} - \underline{q}_G^{n}} \right\| \overset{?}{\leq} \text{Tol}$$

If yes, go to step 6

If no, i = i + 1 and go to step 2

6. Update angular orientation (see Table 4)
7. $t_{n+1} = t_{n+1} + \Delta t$
8. If $t_{n+1} \leq t_{max}$, go to step 1

   If $t_{n+1} > t_{max}$, stop

TABLE 4

SPACECRAFT ANGULAR ORIENTATION DETERMINATION

1. Update the space-three angles

   If $\theta \approx 90^{\circ}$, Go to step 4

   Otherwise, use eq. (4.39) and (4.40)

   $$\underline{\theta}_{n+1} = \underline{\theta}_n + \frac{\Delta t}{2} \underline{M}_{\theta} (\underline{\Omega}_n + \underline{\Omega}_{n+1})$$

2. Calculate $\underline{C}_D$ using eqs. (4.45)

3. Calculate Euler Angles

   a) If $|C_{33}| = 1$, go to step 3c

   otherwise

   $\theta = \cos^{-1} (C_{33}) \quad 0 < \theta < \pi$

   b) Let $\alpha = \cos^{-1} \left(- \frac{C_{32}}{\sin \theta}\right) \qquad 0 \leq \alpha \leq \pi$

   $\beta = \cos^{-1} \left(\frac{C_{32}}{\sin \theta}\right) \qquad 0 \leq \beta \leq \pi$

   Then

   $$\psi = \begin{cases} \alpha \text{ if } C_{13} \geq 0 \\ 2\pi - \alpha \text{ if } C_{13} < 0 \end{cases}$$

   and

   $$\phi = \begin{cases} \beta \text{ if } C_{31} \geq 0 \\ 2\pi - \beta \text{ if } C_{31} < 0 \end{cases}$$

   stop

   c) $$\theta = \begin{cases} 0 \text{ if } C_{33} = 1 \\ \pi \text{ if } C_{33} = -1 \end{cases}$$

TABLE 4

$$\phi = 0$$

$$\alpha = \cos^{-1}(C_{22}) \qquad 0 \leq \alpha \leq \pi$$

$$\psi = \begin{cases} \alpha \text{ if } C_{21} \geq 0 \\ 2\pi - \alpha \text{ if } C_{21} < 0 \end{cases}$$

stop

4. Update Euler Angles

Use eqs. (4.41) and (4.42)

$$\underline{\Theta}_{n+1} = \underline{\Theta}_n + \frac{\Delta t}{2} \underline{M}_\theta (\underline{\Omega}_n + \underline{\Omega}_{n+1})$$

5. Calculate $\underline{C}_D$ using eqs. (4.46)

6. Calculate Space-Three Angles

a) If $|C_{13}| = 1$, go to step 6c

Otherwise,

$$\theta_2 = \sin^{-1}(C_{31}) \qquad -\frac{\pi}{2} \leq \theta_2 \leq \frac{\pi}{2}$$

b) Let $\alpha = \sin^{-1}\left(\frac{C_{32}}{\cos\theta_2}\right) \qquad -\frac{\pi}{2} \leq \alpha \leq \frac{\pi}{2}$

$$\beta = \sin^{-1}\left(\frac{C_{21}}{\cos\theta_2}\right) \qquad -\frac{\pi}{2} \leq \beta \leq \frac{\pi}{2}$$

Then,

$$\theta_1 = \begin{cases} \alpha \text{ if } C_{33} \geq 0 \\ \pi - \alpha \text{ if } C_{33} > 0 \end{cases}$$

$$\theta_3 = \begin{cases} \beta \text{ if } C_{11} \geq 0 \\ \pi - \beta \text{ if } C_{11} < 0 \end{cases}$$

Stop

TABLE 4

c) $\theta_3 = 0$

$$\theta_2 = \begin{cases} -\frac{\pi}{2} & \text{if } C_{31} = 1 \\ \frac{\pi}{2} & \text{if } C_{31} = -1 \end{cases}$$

Let $\alpha = \sin^{-1}(-C_{32}) \qquad -\frac{\pi}{2} \le \alpha \le \frac{\pi}{2}$

Then

$$\theta_1 = \begin{cases} \alpha & \text{if } C_{22} \ge 0 \\ \pi-\alpha & \text{if } C_{22} < 0 \end{cases}$$

Stop

TABLE 5

Period of Vibration of the Beams for Various Rigid Body Inertias

	offset r_6 (Ft)		
	0	5	15
$I_R \times (10^4)$, m_R	Period of Vibration (sec)		
1.0, 100	2.7	2.8	3.3
2.5, 250	3.3	3.4	3.9
5.0, 500	4.1	4.2	4.5
20, 2000	6.3	6.4	6.4

Figure 1

Reference Axes for an Unrestrained Deformable Body

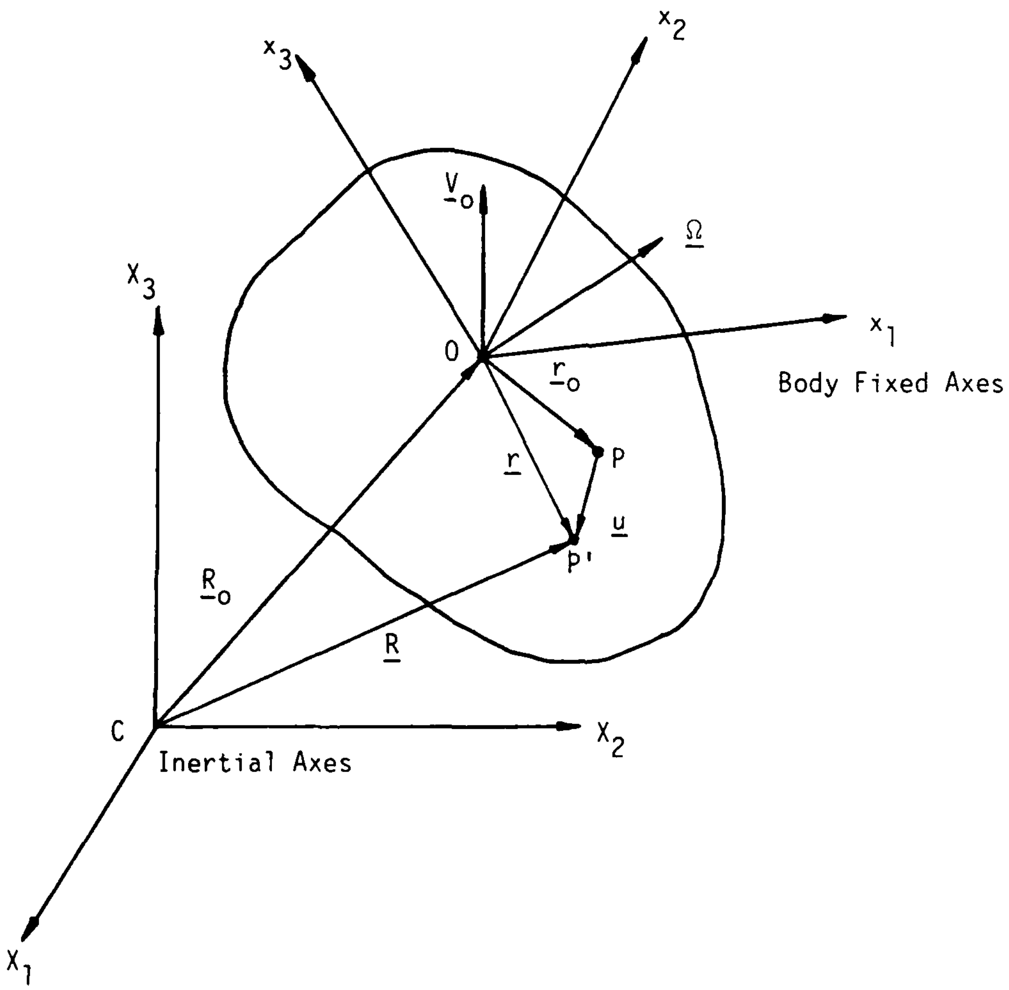

Figure 2

Beam Large Displacement Geometry

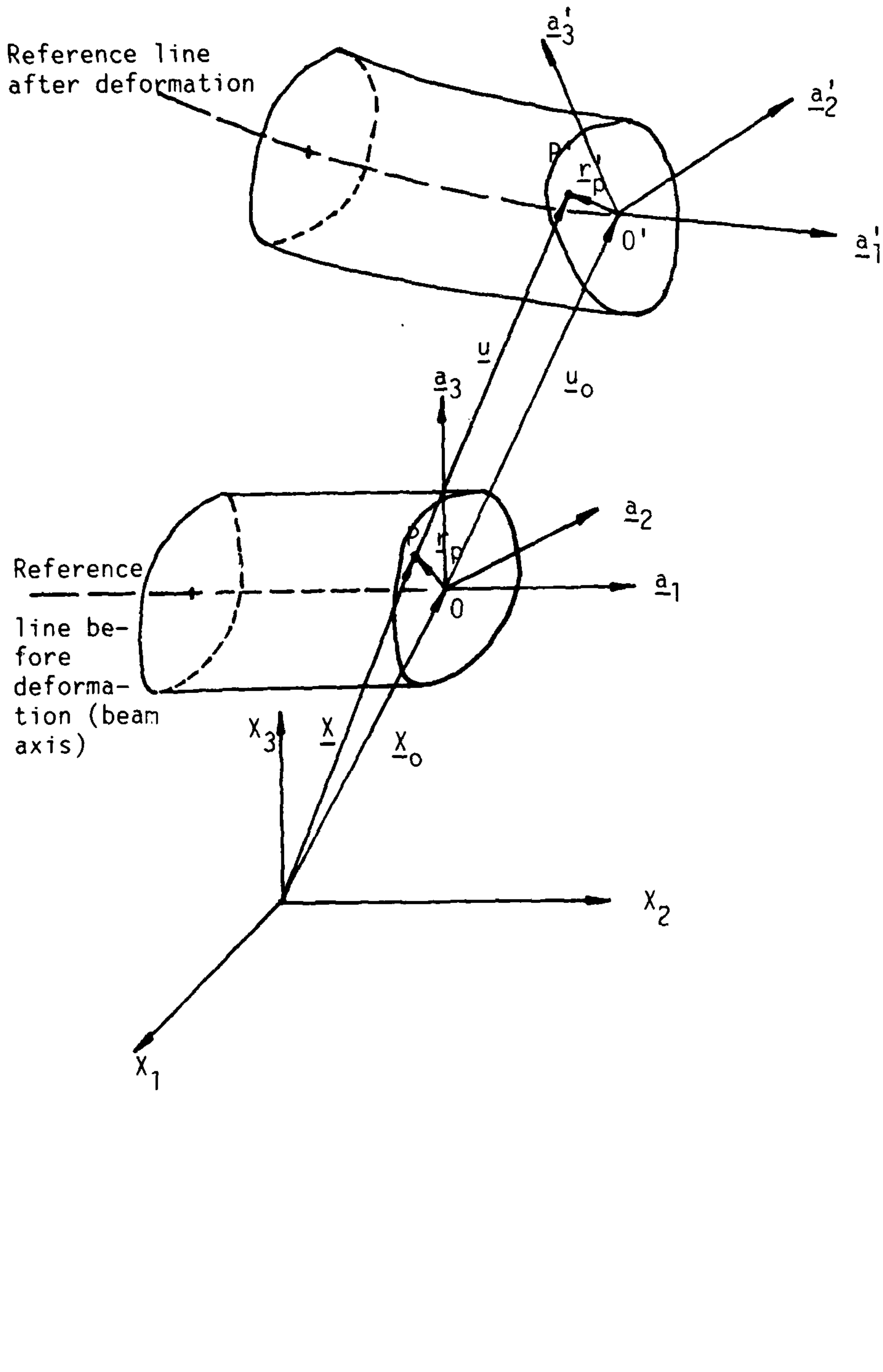

AD-A151 176 DEVELOPMENT OF A DYNAMIC FINITE ELEMENT MODEL FOR UNRESTRAINED FLEXIBLE S..(U) MARYLAND UNIV COLLEGE PARK DEPT OF AEROSPACE ENGINEERING E R CHRISTENSEN ET AL. OCT 84 AFOSR-TR-85-0183 AFOSR-82-0296 2/2

UNCLASSIFIED F/G 12/1 NL

END

FILMED

DTIC

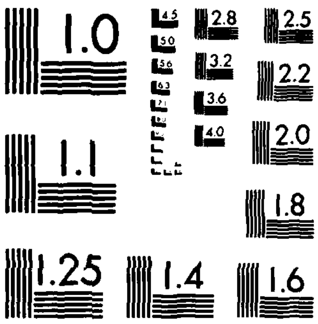

MICROCOPY RESOLUTION TEST CHART
NATIONAL BUREAU OF STANDARDS-1963-A

Figure 3
Rotation Angles

(a) Euler Angles

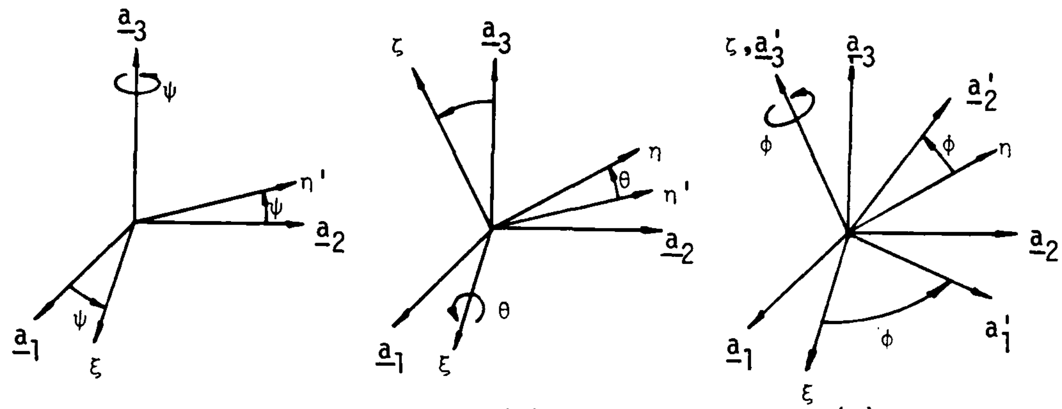

(1) Rotate ψ about x_3

(2) Rotate θ about ξ

(3) Rotate ϕ about ζ

(b) Space - Three: 1-2-3 Angles

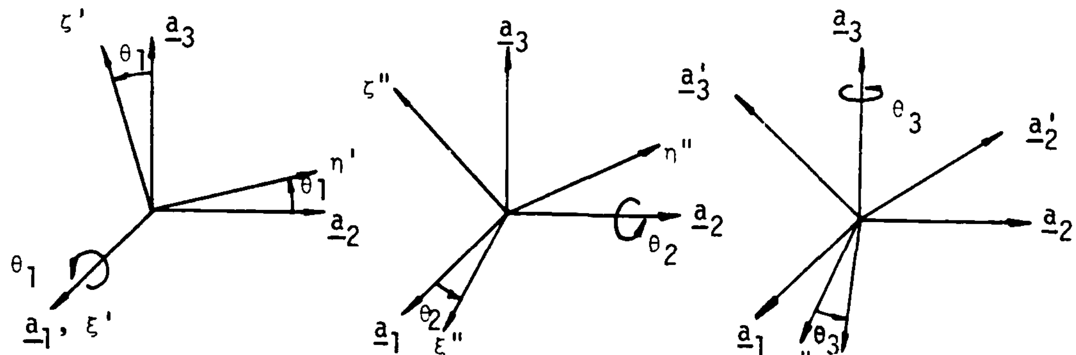

(1) Rotate θ_1 about $\underline{a}_1$

(2) Rotate θ_2 about $\underline{a}_2$

(3) Rotate θ_3 about $\underline{a}_3$

Figure 3

(c) Body - Three: 1-2-3

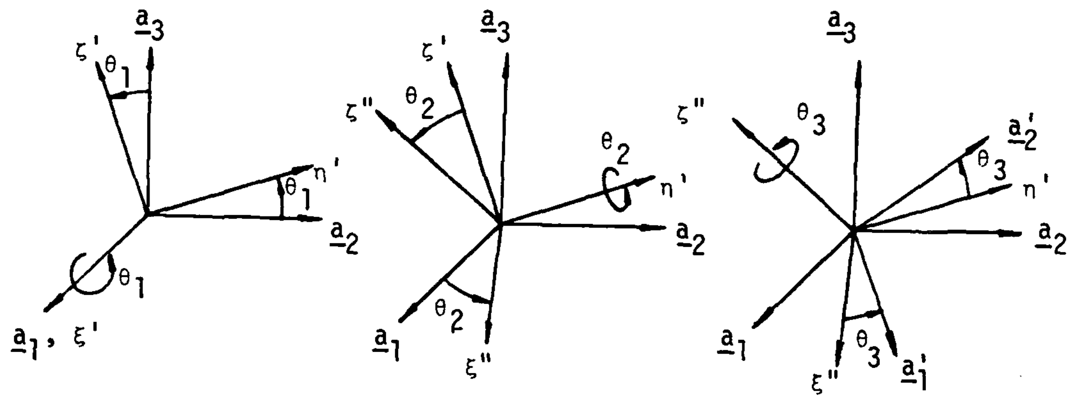

(1) Rotate θ_1 about $\underline{a}_1$

(2) Rotate θ_2 about η'

(3) Rotate θ_3 about ζ''

Figure 4

The Three Node Eighteen Degree of Freedom Beam Element

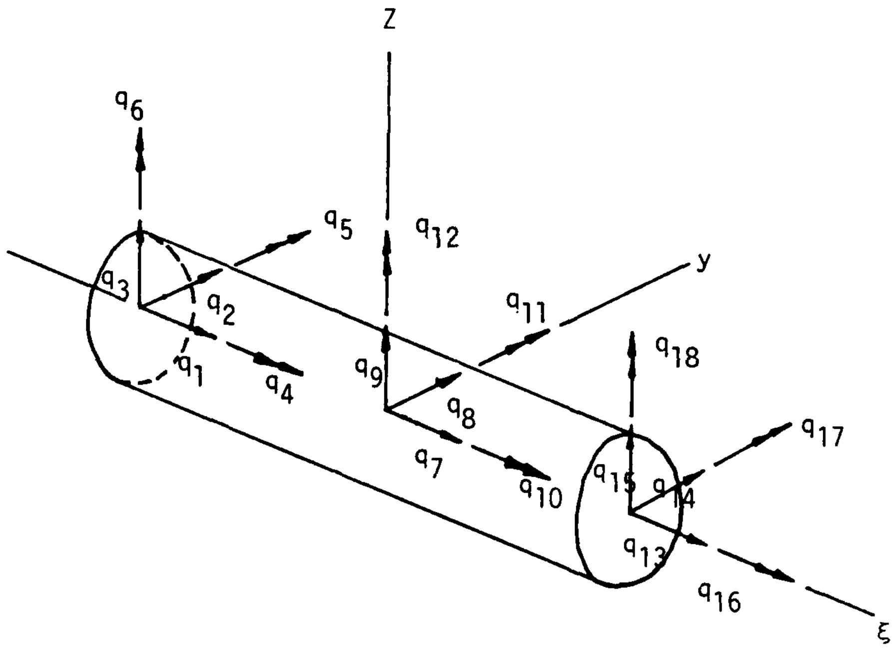

Figure 5

Example 1 - Beam Rotating About a Fixed Axis

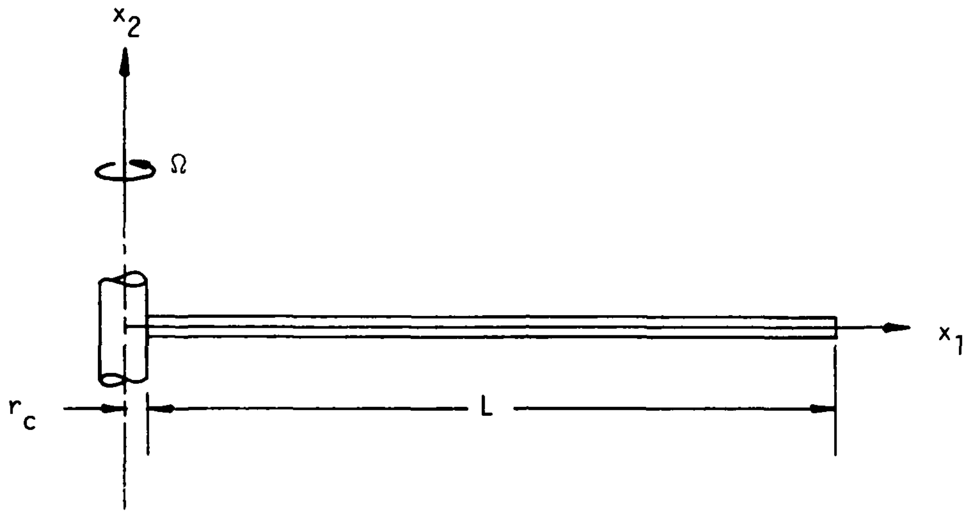

$r_c << L$

$L = 100$ ft.

$A = 1$ ft²

$I_{yy} = 0.08333$ ft^4

$I_{zz} = 0.08333$ ft^4

$\rho = 5.22$ slug/ft³

$E = 1.44(10^8)$ lb/ft²

$G = 5.54(10^7)$ lb/ft²

Figure 6

Angle of Beam Tip for Rotating Beam

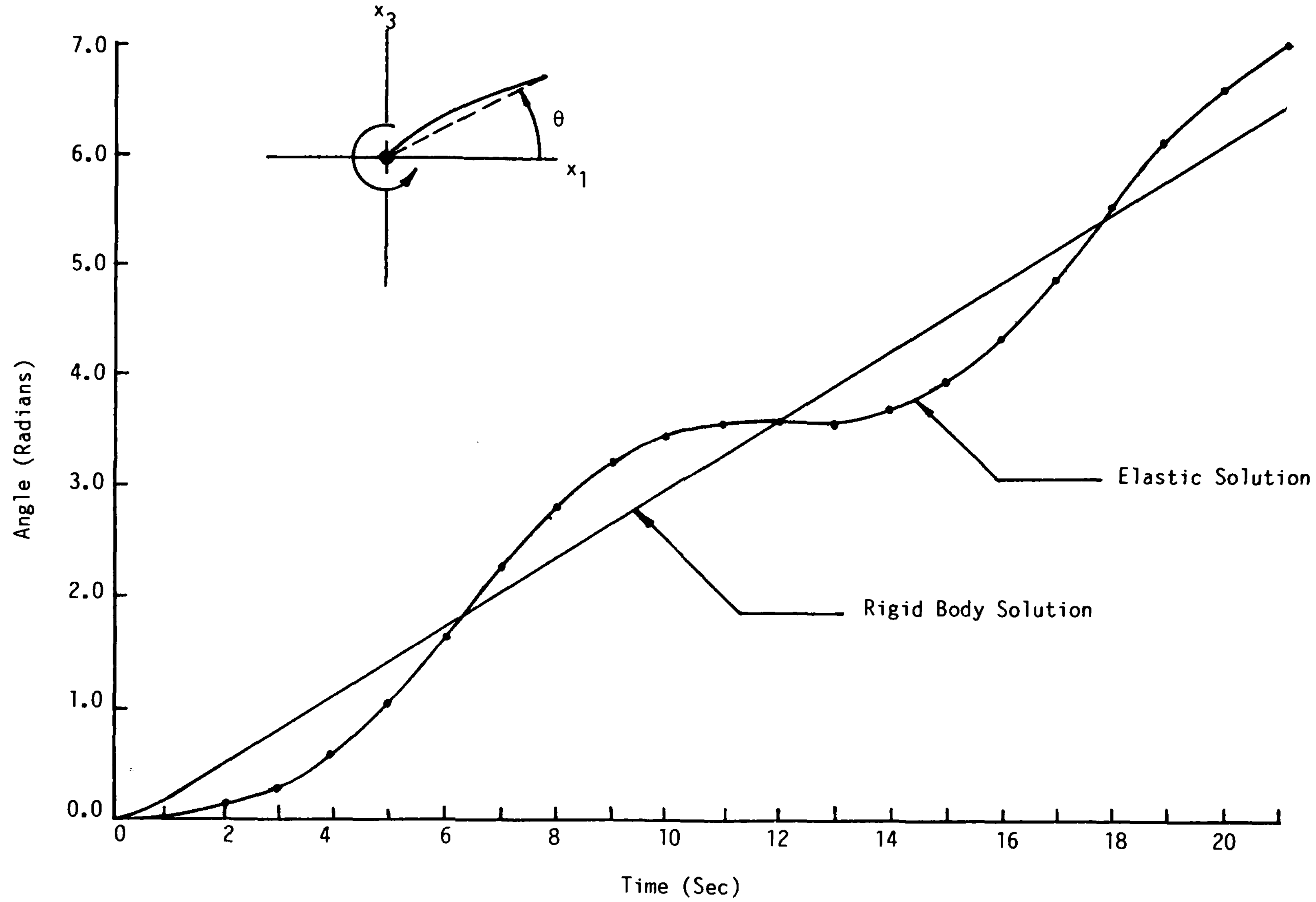

Figure 7

Large Displacements of a Rotating Beam

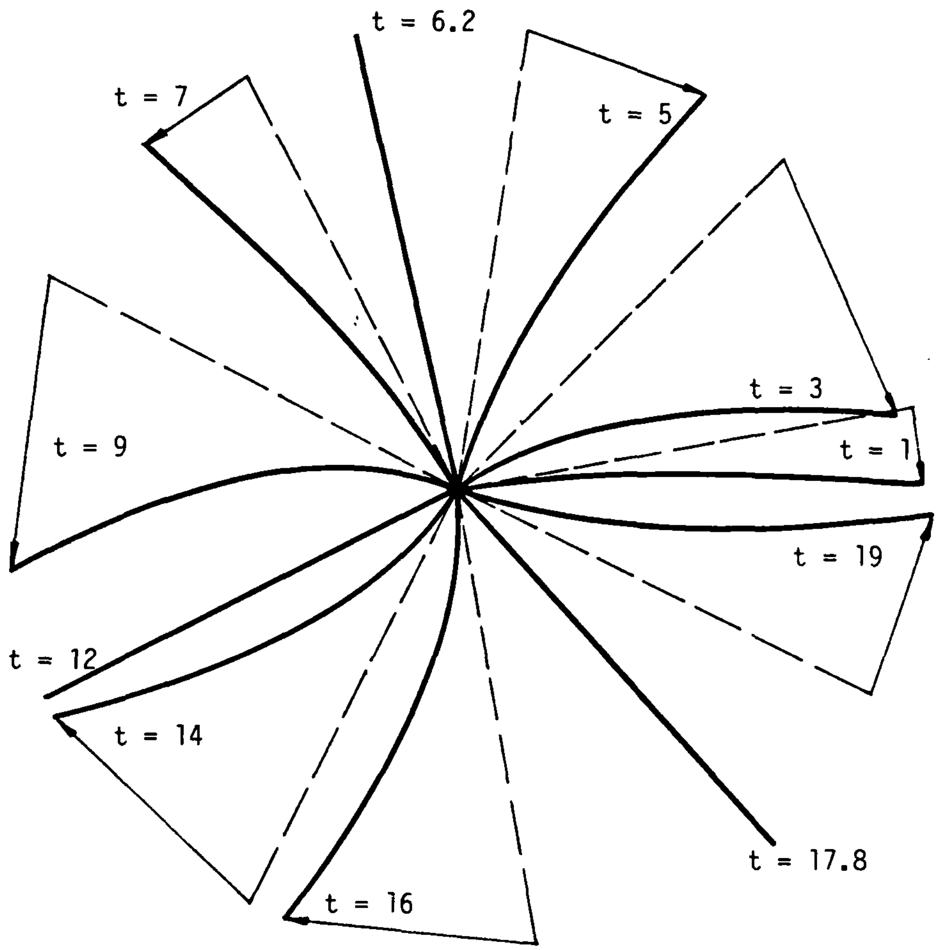

Figure 8

Body Axis Rotation Angle

Case 2

$I_R/I_B = 0.5$

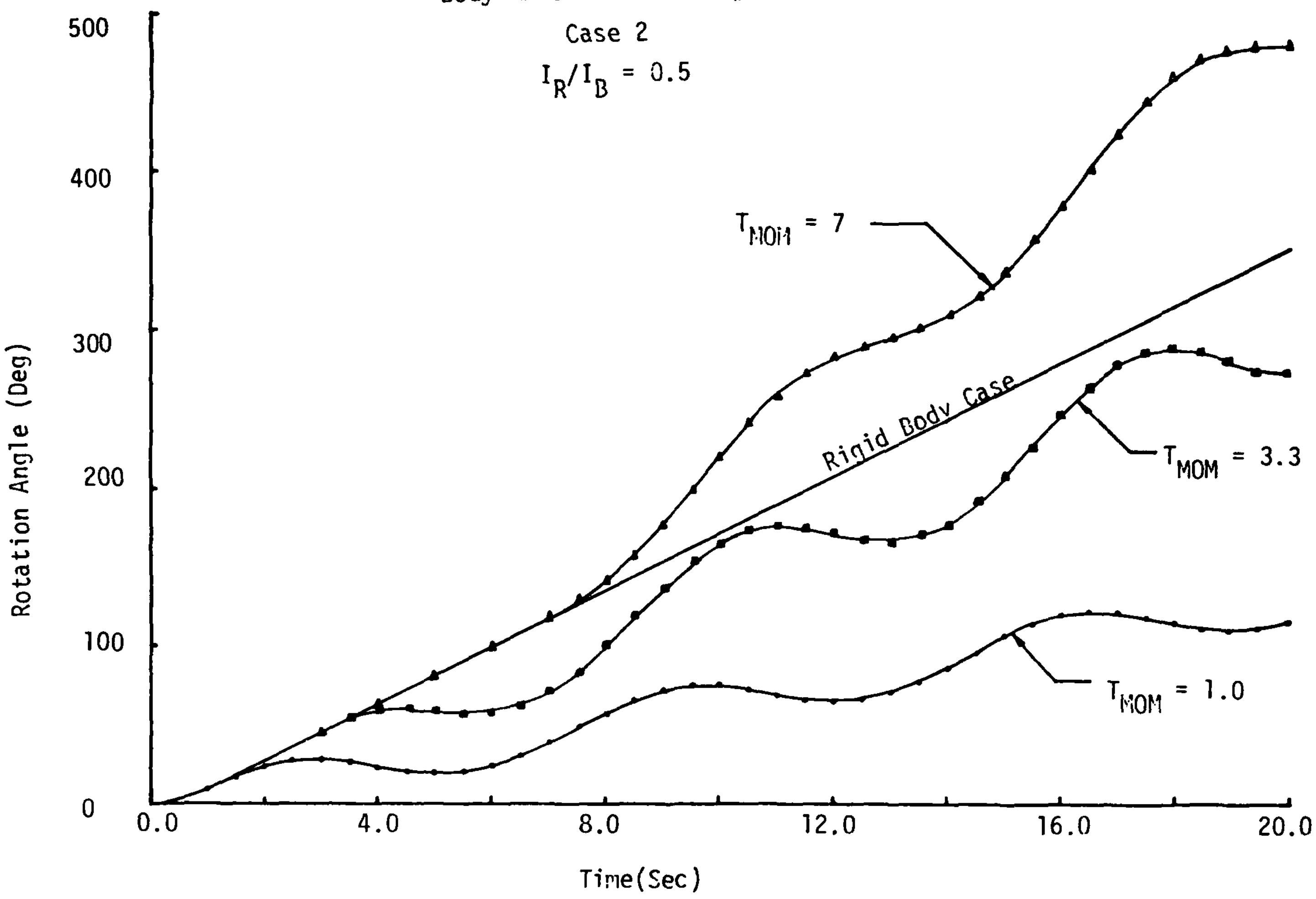

Figure 9

Body Axis Rotation Angle
Case 2
$I_R/I_B = 1.0$

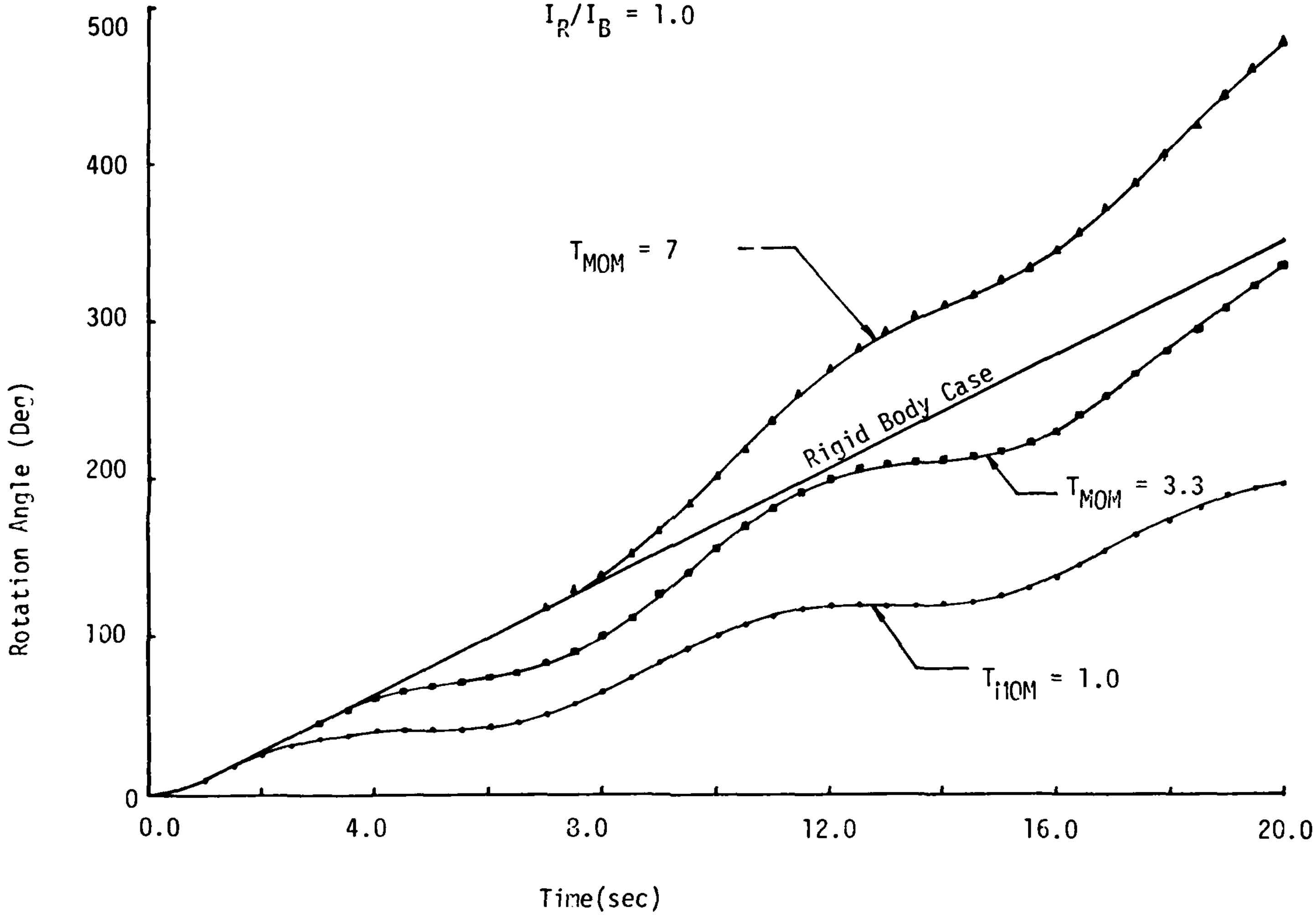

Figure 10

Example 2 - A Rotating Spacecraft With an Offset Center of Mass and Control Forces

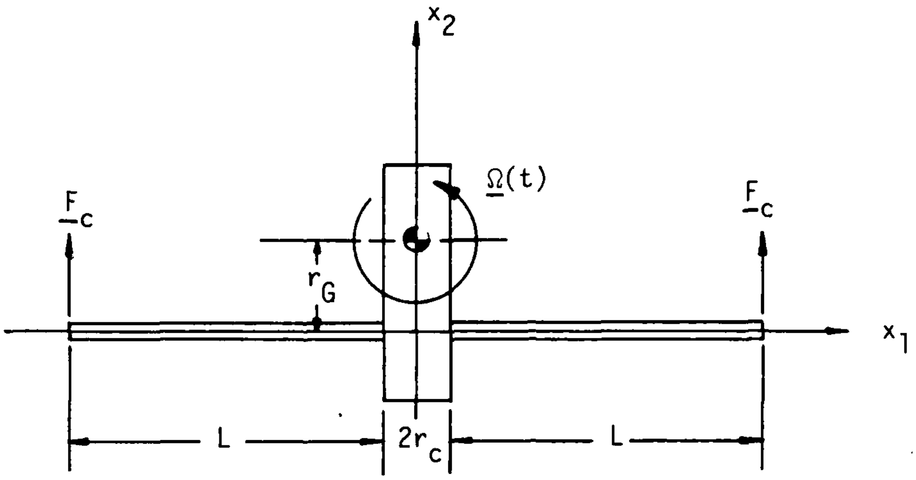

Beam Properties:

$L = 100$ ft.

$A = 6.55(10^{-2})$ ft²

$I_{yy} = I_{zz} = 8.18(10^{-3})$ ft^4

$\rho = 5.22$ slug/ft³

$E - 1.44(10^8)$ lb/ft³

$G = 5.54(10^7)$ lb/ft³

$r_c = 5$ ft.

Figure 11

Beam Tip Displacements for an Offset of 15 Ft.

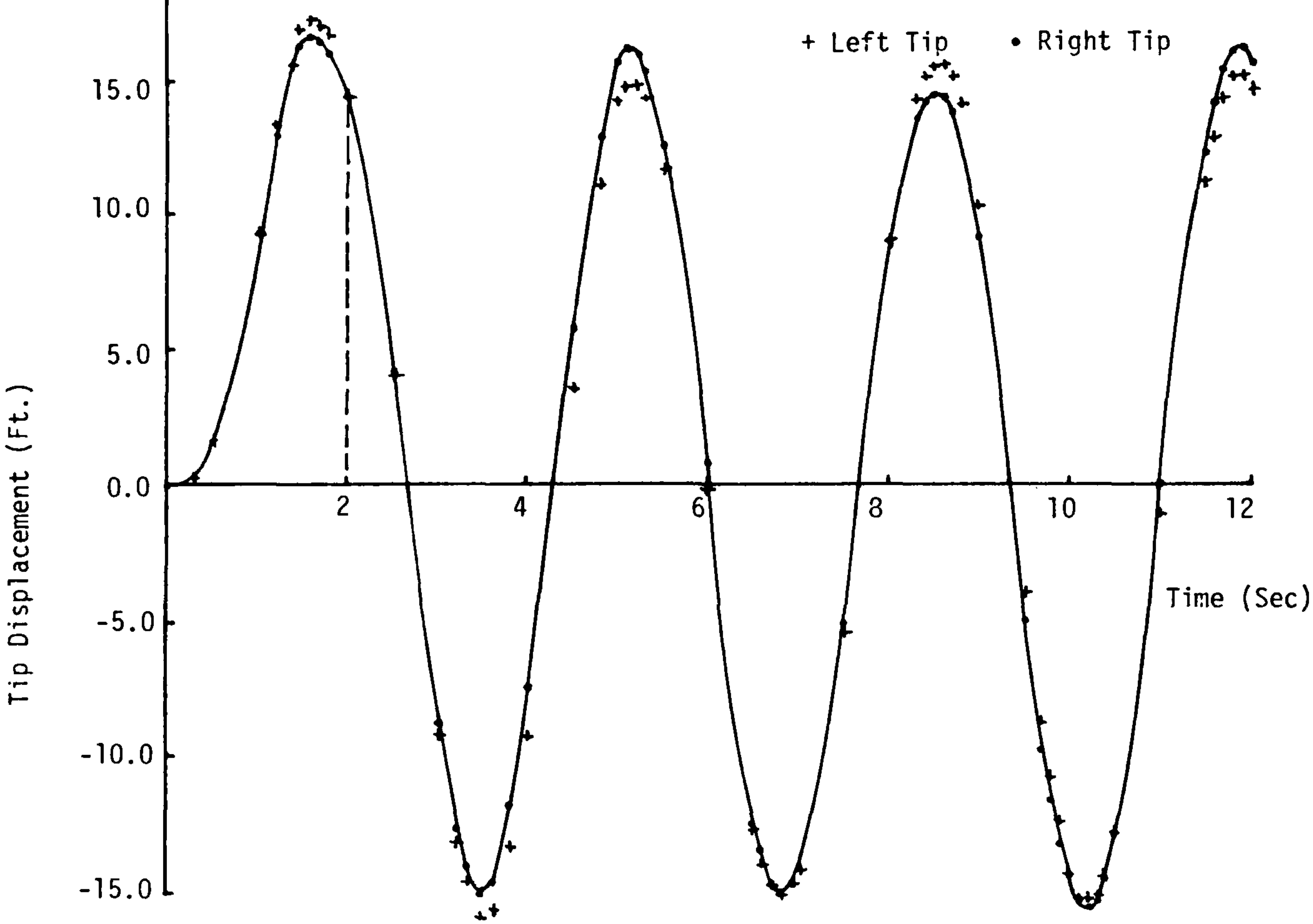

Figure 12

Body Axis Rotation Angle For Two Different Offsets

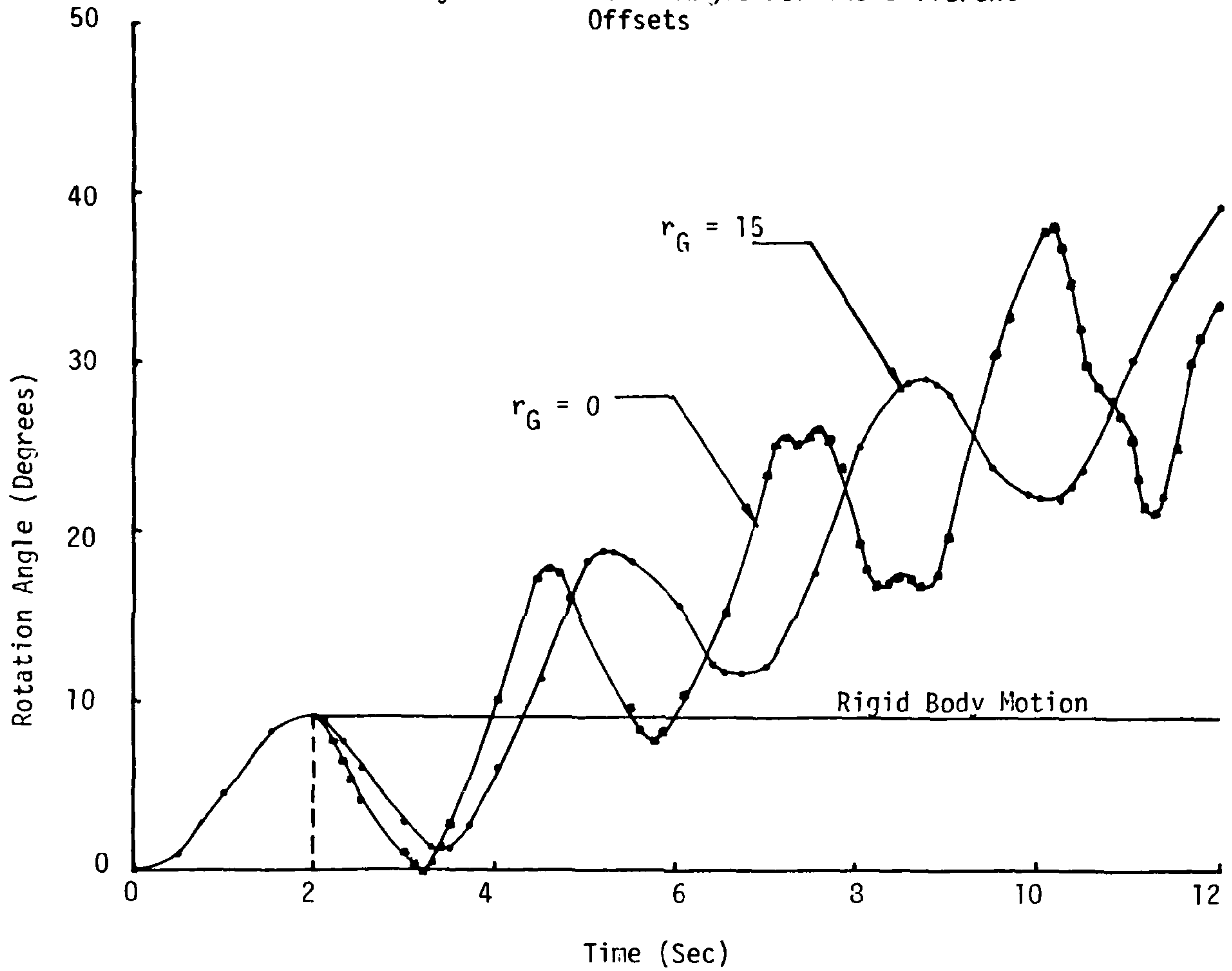

Figure 13

Body Axis Rotation Angle

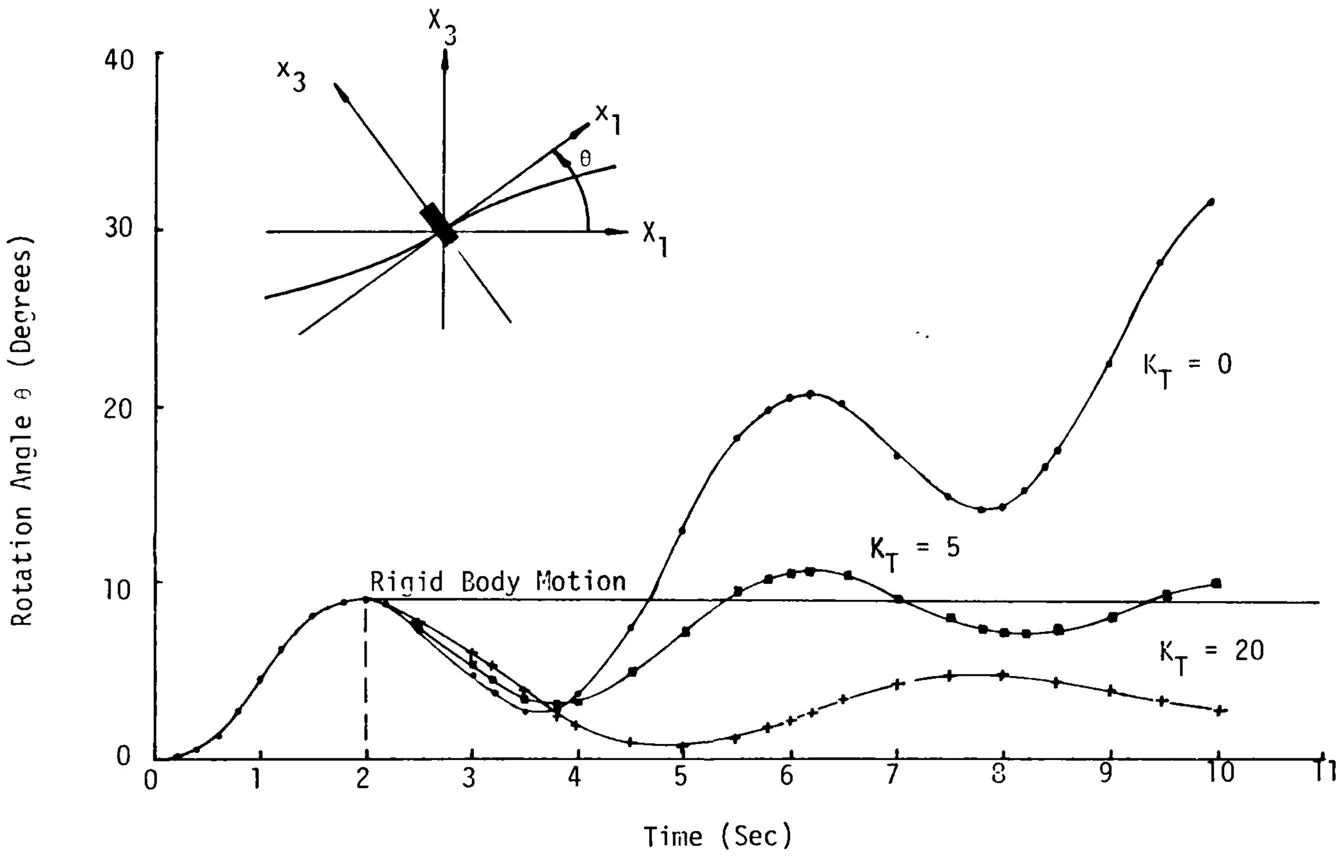

Figure 27

Beam Tip Displacement - Case 1

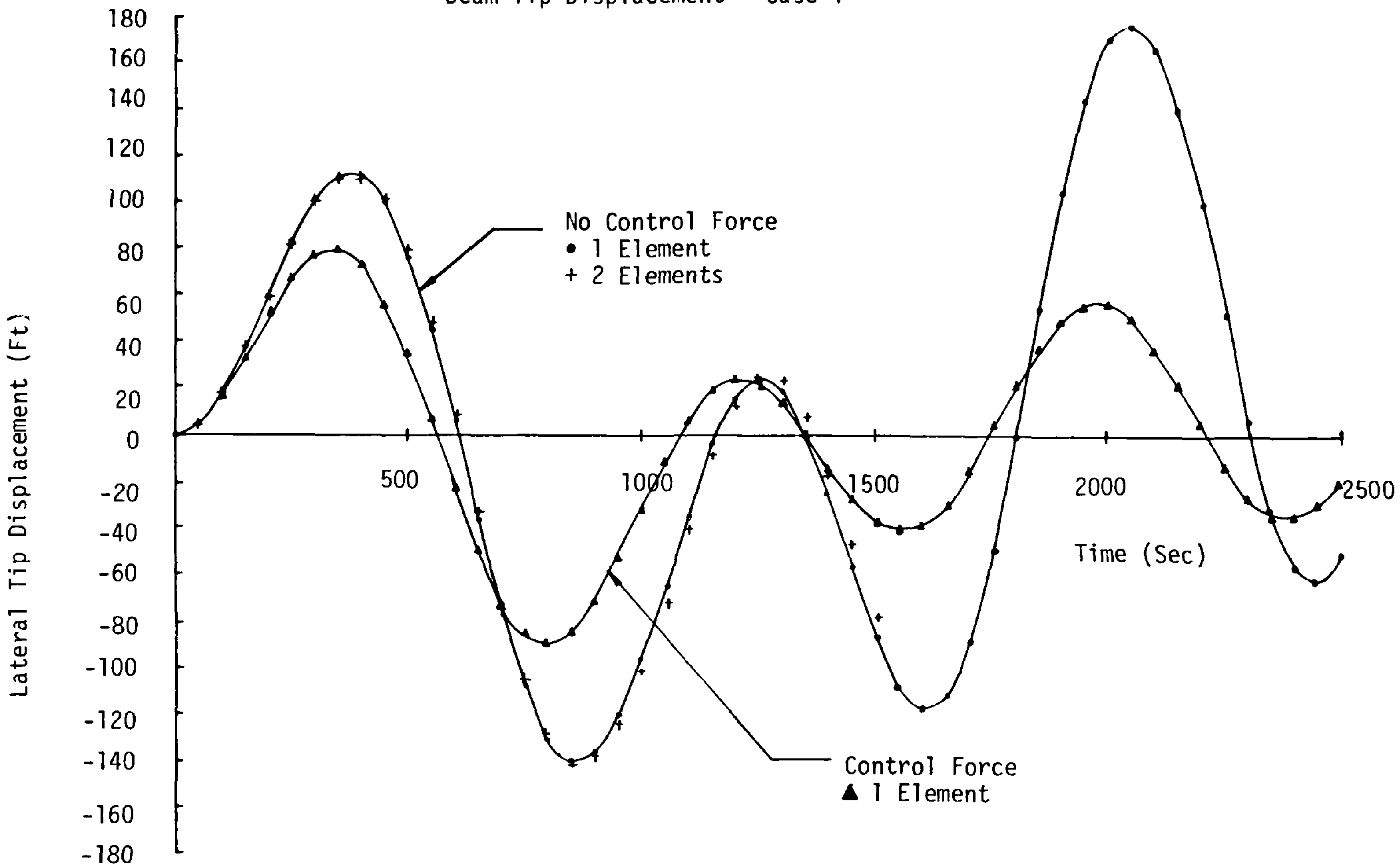

Figure 26

Rotation Angle β - Case 1

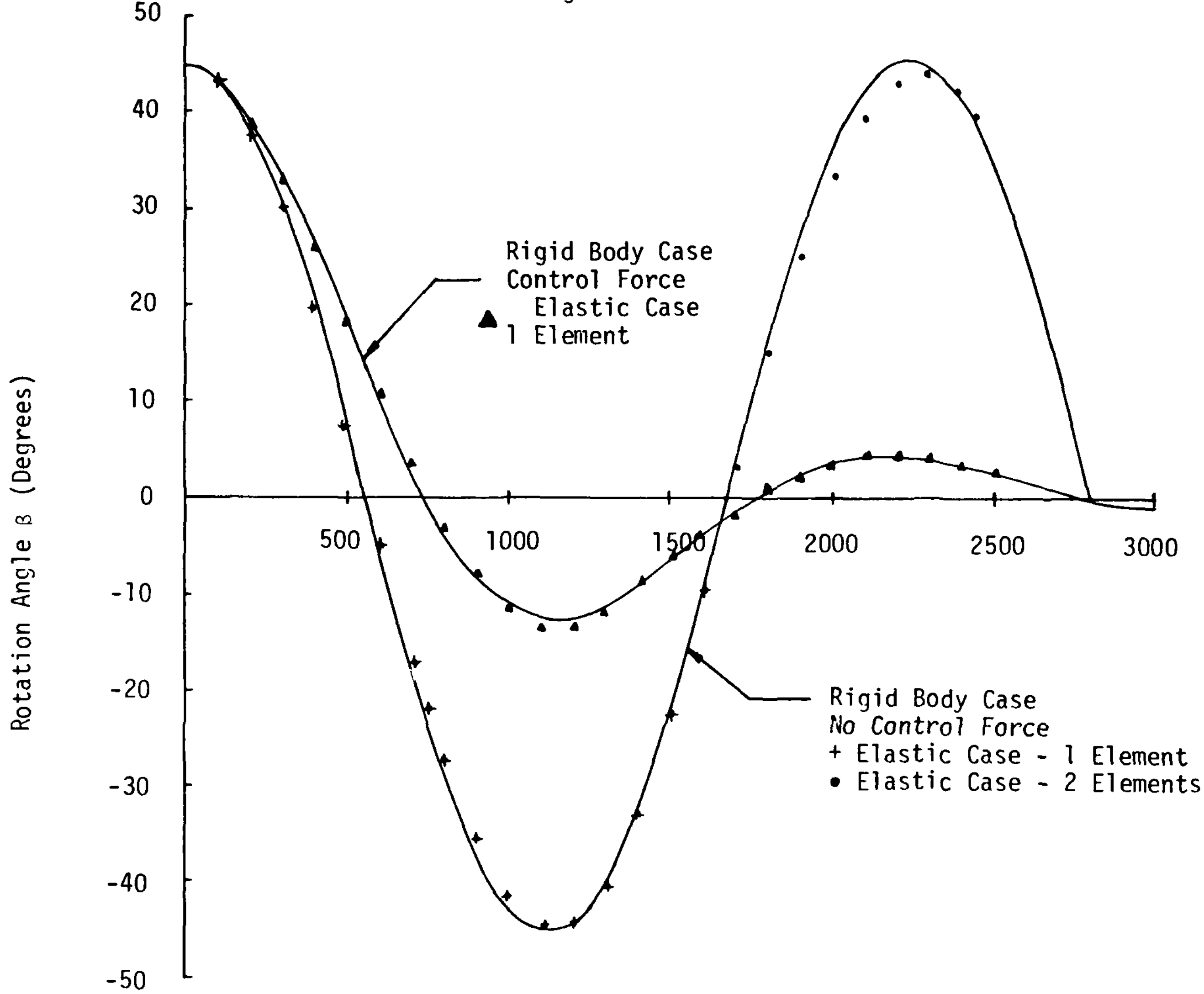

Figure 25

Spacecraft Geometry

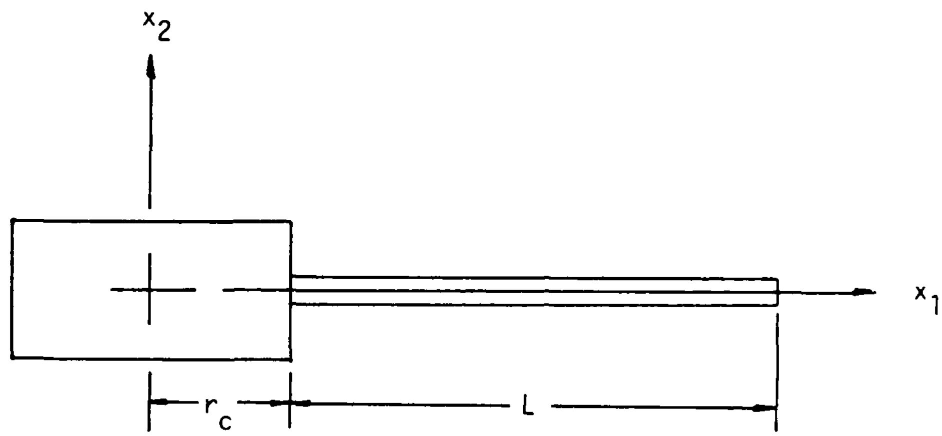

<u>Beam Properties:</u>

$L = 450$ ft.

$A = 6.545(10^{-2})$ ft²

$I_{yy} = I_{zz} = 4.092(10^{-4})$ ft^4

$\rho = 5.22$ slug/ft³

$E = 1.44(10^8)$ lb/ft²

$G = 5.54(10^7)$ lb/ft²

$r_c = 50$ ft.

<u>Rigid Mass Properties</u>

See Text

Figure 24

Example 5 - Gravity Gradient Stabilization

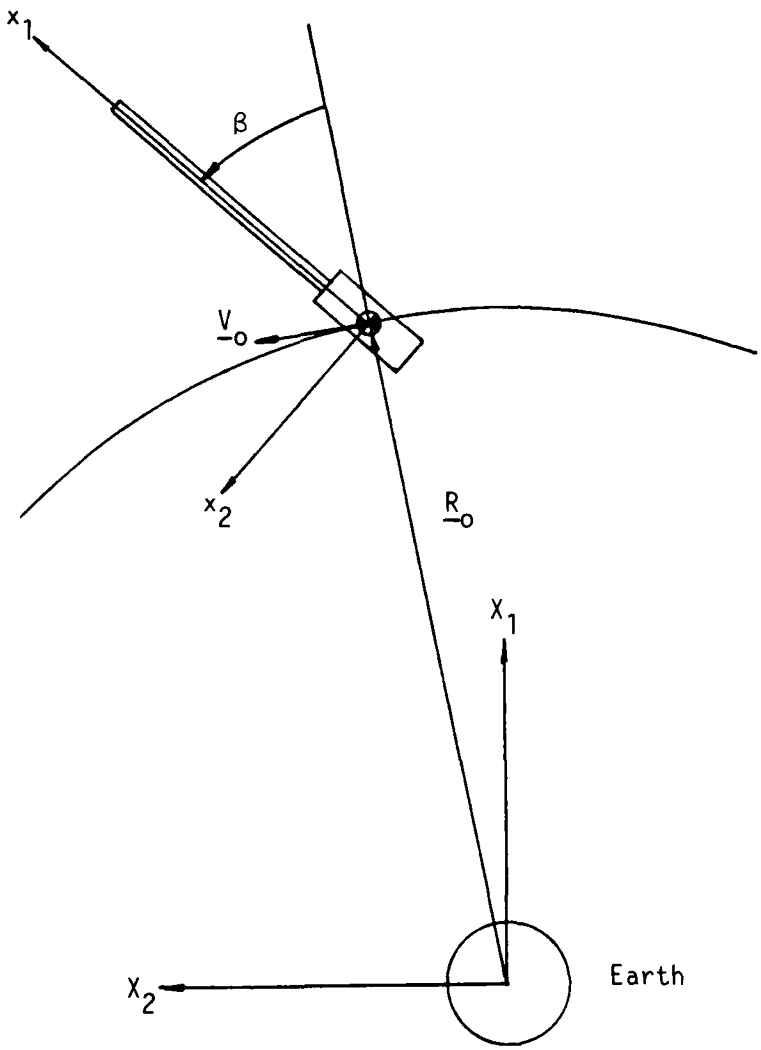

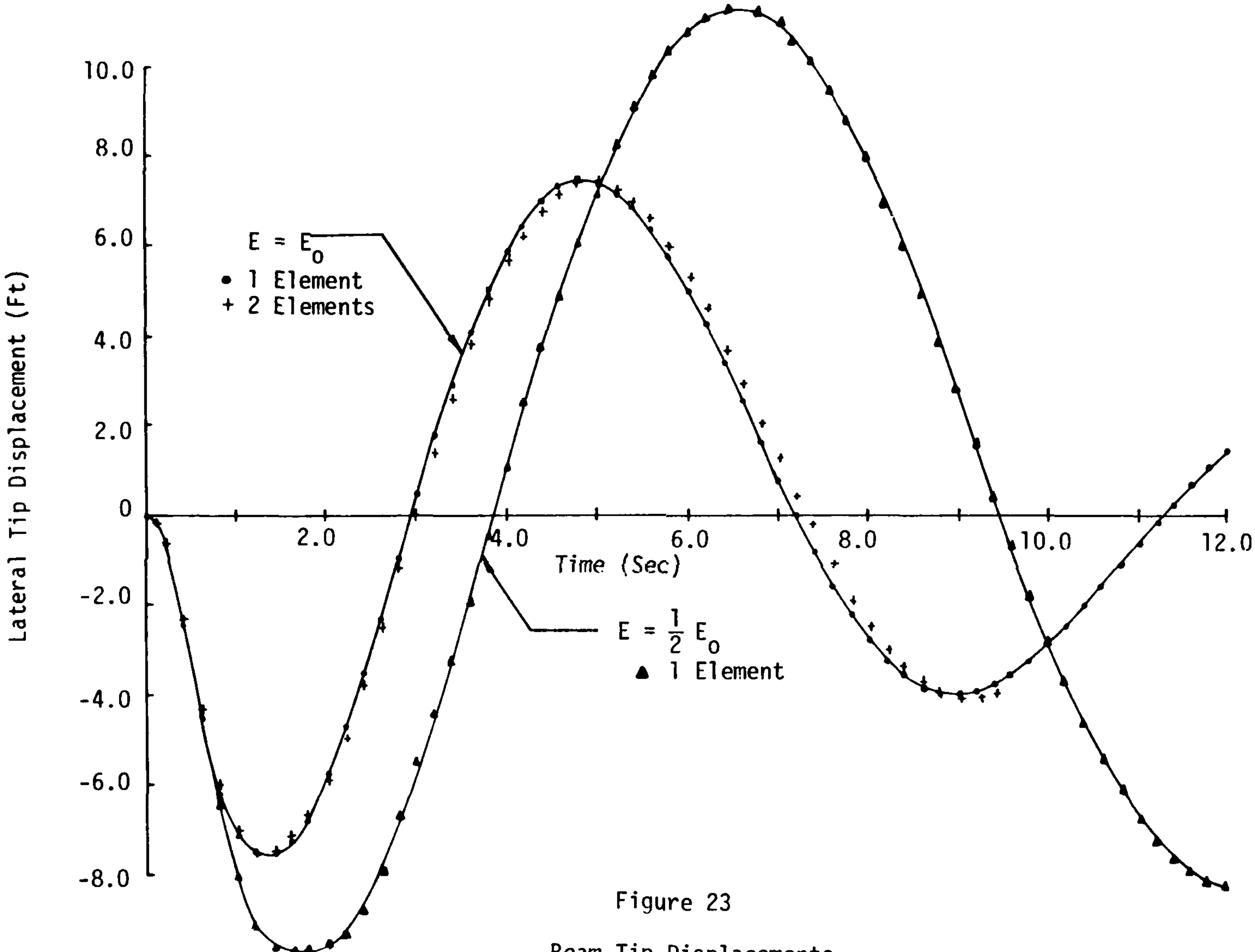

Figure 23

Beam Tip Displacements

Figure 22

Spacecraft Orientation at t = 5 Sec

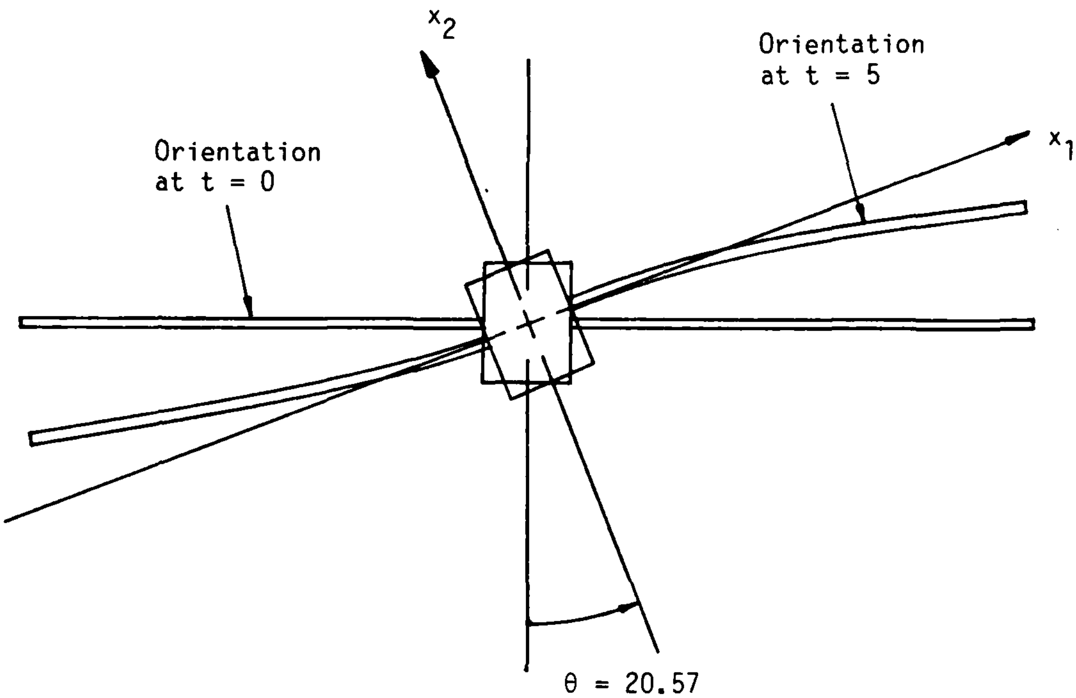

Figure 21

Body Axis Rotation Angle θ

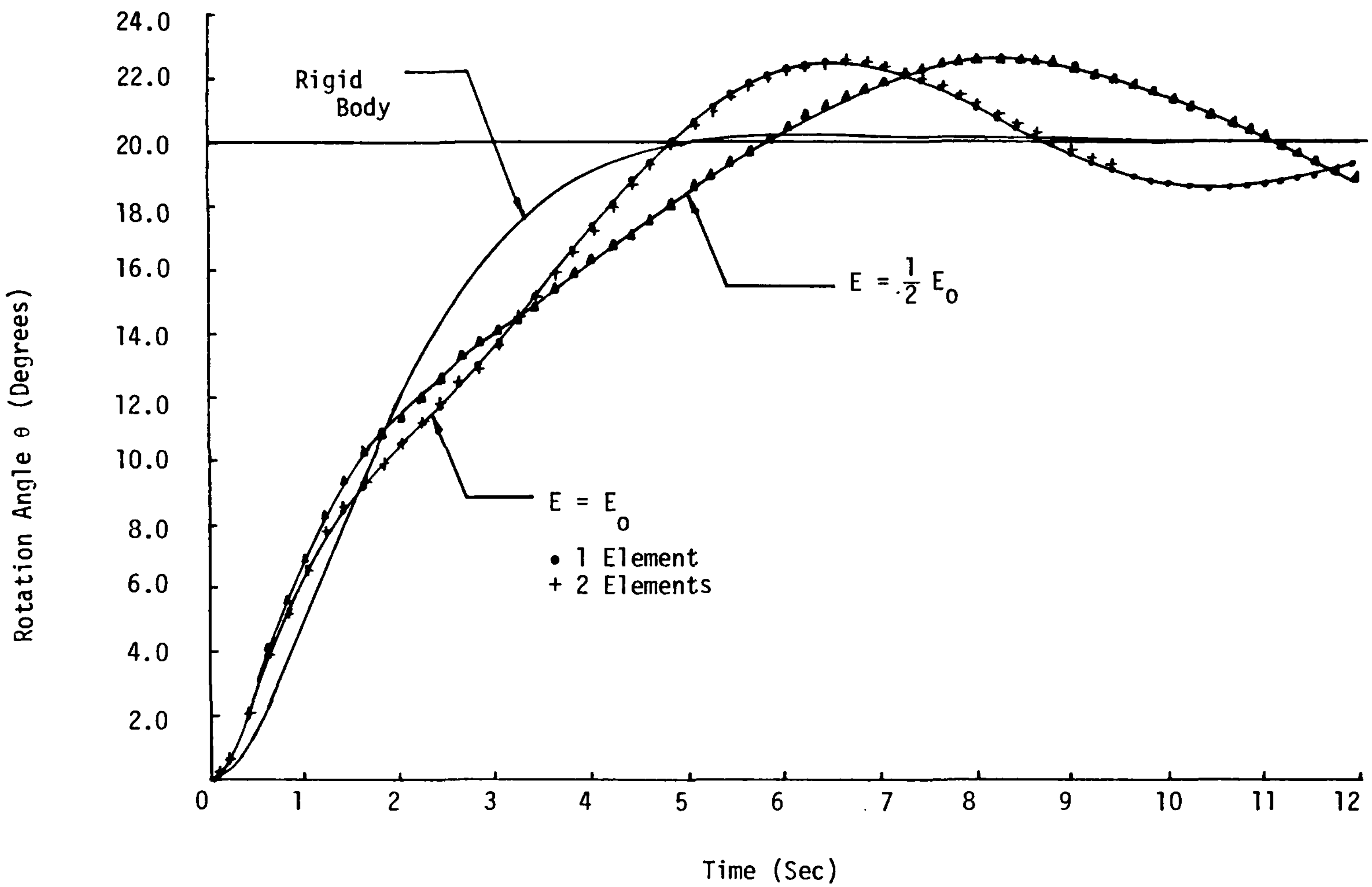

Figure 20

Example 4 - Spacecraft Rotating to a Specified Orientation

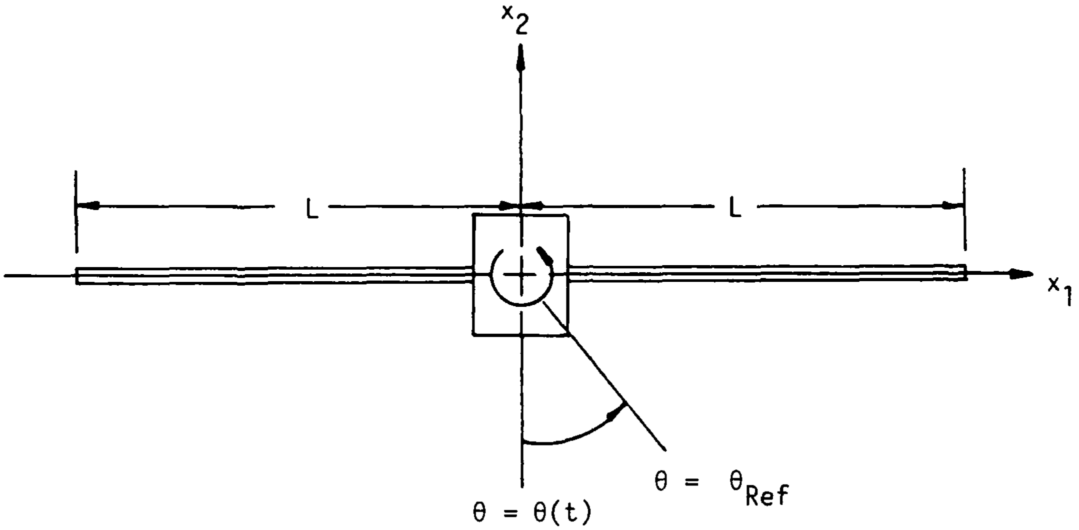

Beam Parameters:

$L = 50$ ft

$A = 0.02182\ ft^2$

$I_{yy} = I_{zz} = 3.0419(10^{-4})\ ft^4$

$\rho = 5.22$ slug/ft³

$E_o = 1.44(10^8)$ lb/ft³

$G_o = 5.54(10^7)$ lb/ft³

Rigid Mass Parameters:

$m_R = 50$ slugs

$I_{R_{11}} = I_{R_{22}} = 10^3$ slug-ft²

$I_{R_{33}} = 2.5(10^3)$ slug-ft²

Figure 19

Ω_3 Component of Angular Velocity

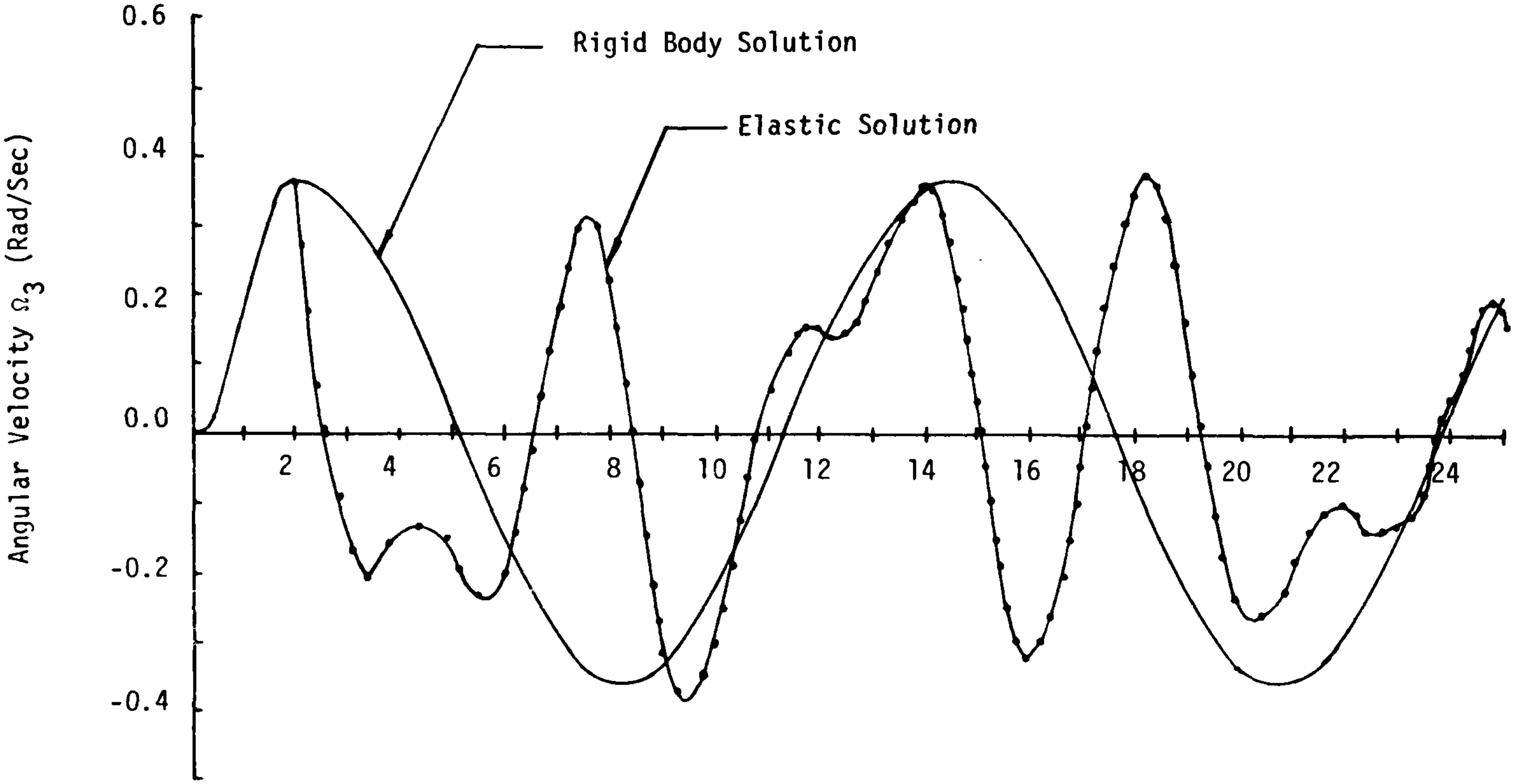

Figure 18

Ω_2 Component of Angular Velocity

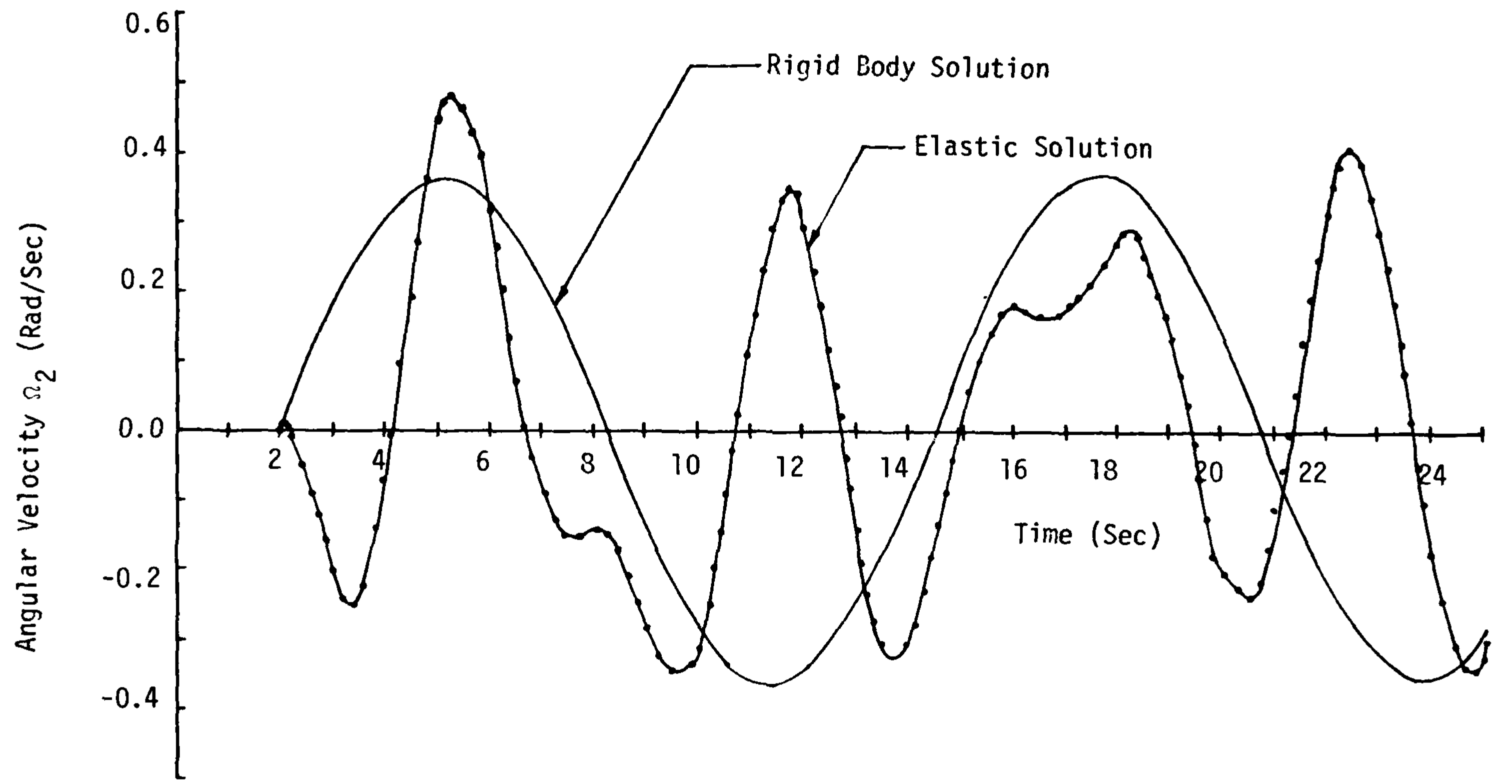

Figure 17

Ω_1 Component of Angular Velocity

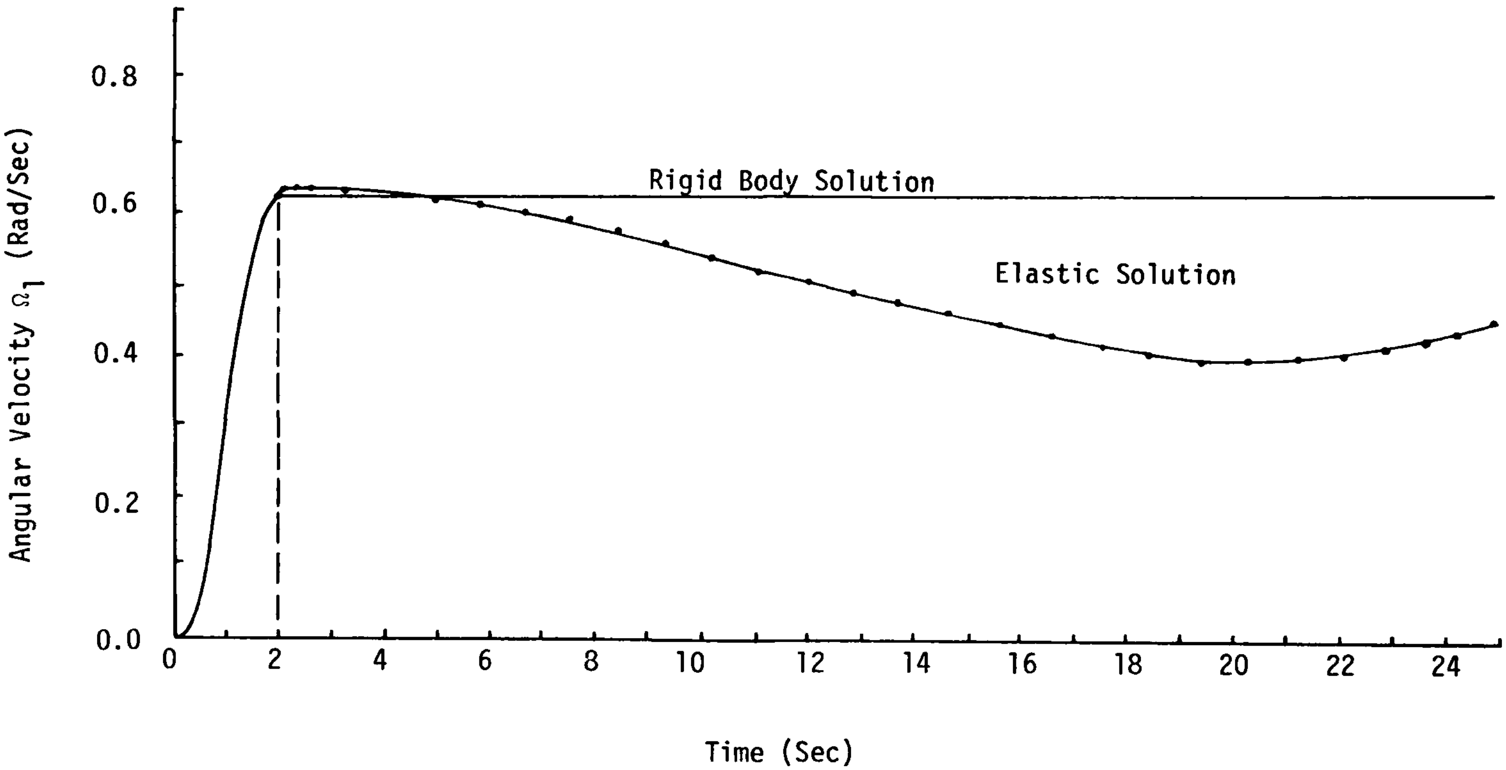

Figure 16

Example 3 - Three Dimensional Precessing Spacecraft

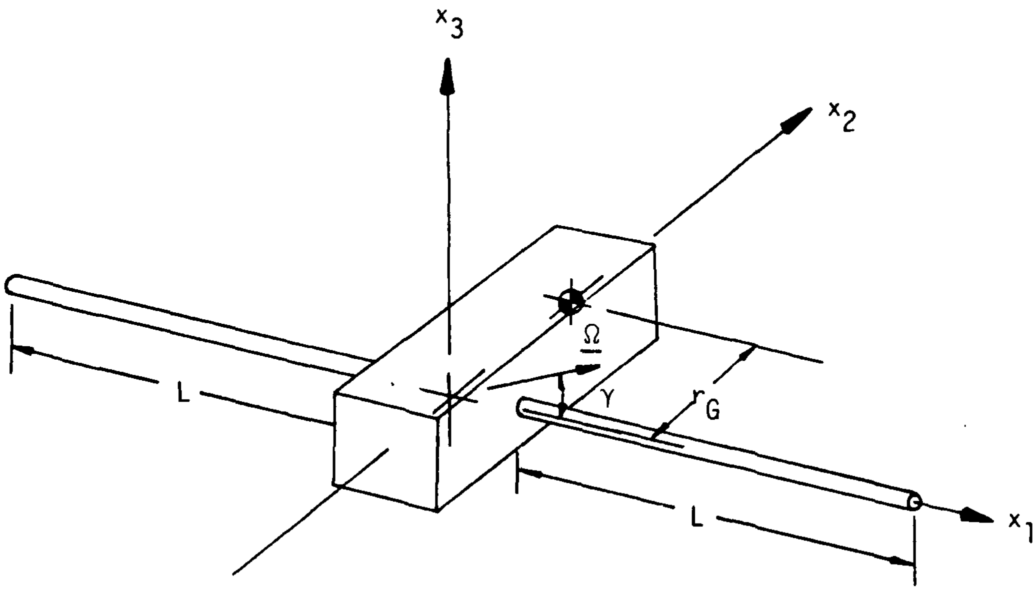

Beam Properties:

$L = 100$ ft.

$A = 0.0654$ ft²

$I_{yy} = I_{zz} = 0.008185$ ft^4

$\rho = 5.22$ slug/ft³

$E = 1.44(10^8)$ lb/ft²

$G = 5.54(10^7)$ lb/ft²

$r_G = 5.0$ ft.

Rigid Mass Properties:

$I_{R_{11}} = 6.1(10^4)$ slug-ft²

$I_{R_{22}} = 5.0(10^4)$ slug-ft²

$I_{R_{33}} = 4.829175(10^4)$ slug-ft²

$m_R = 500$ slugs

Figure 15

Body Axis Angular Velocity

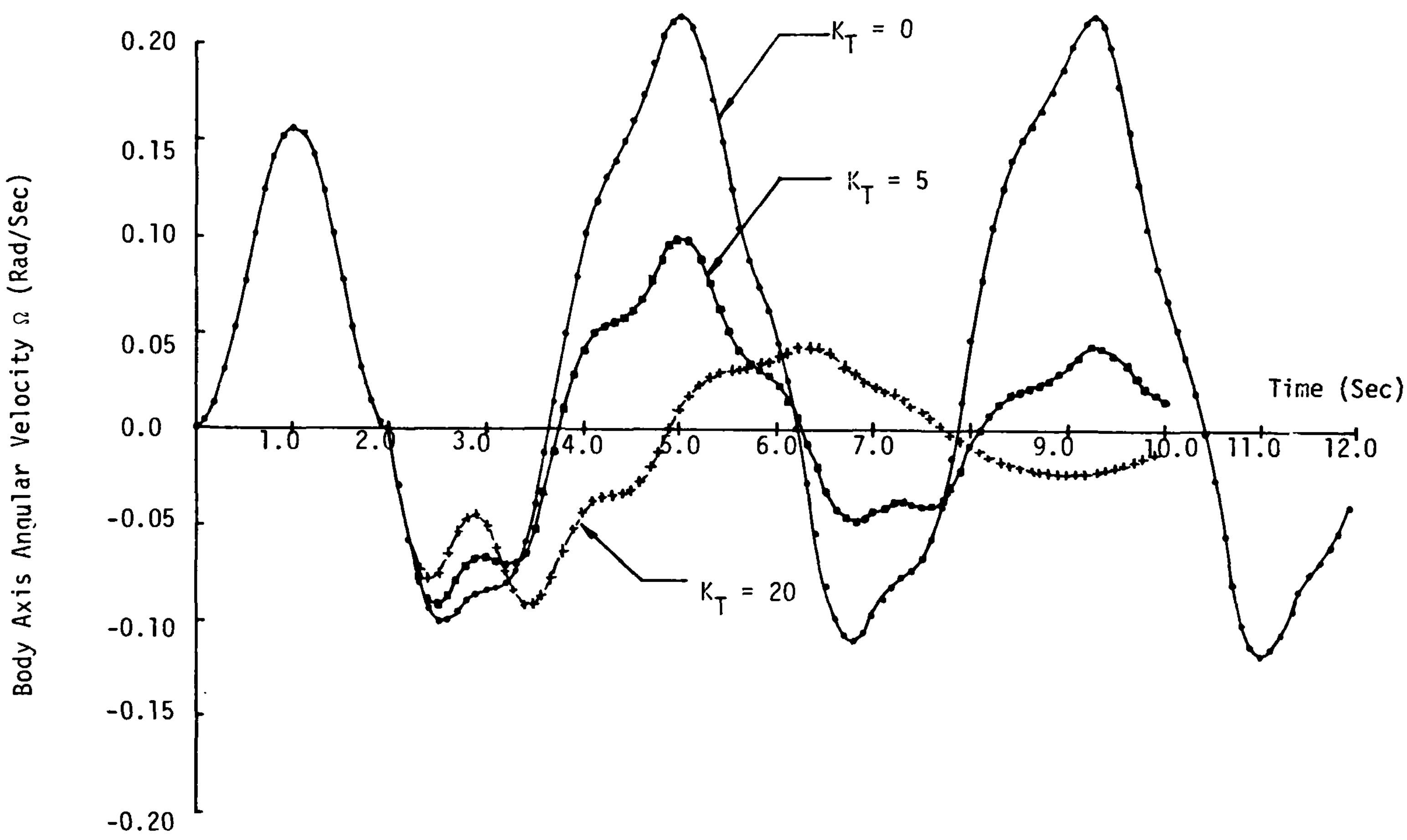

Figure 14

Lateral Tip Displacement of the Right Beam

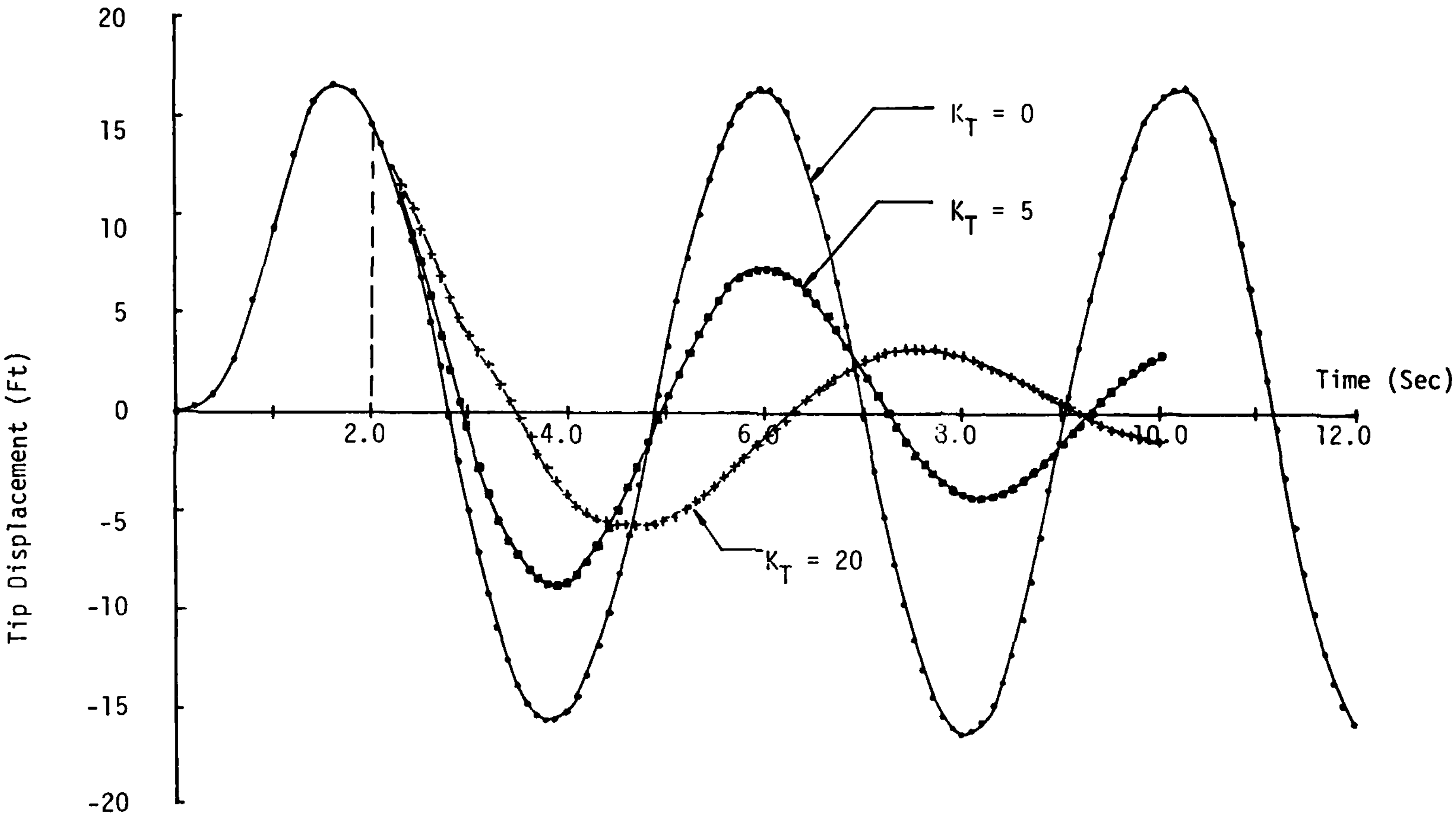

Figure 28

Rotation Angle β - Case 2

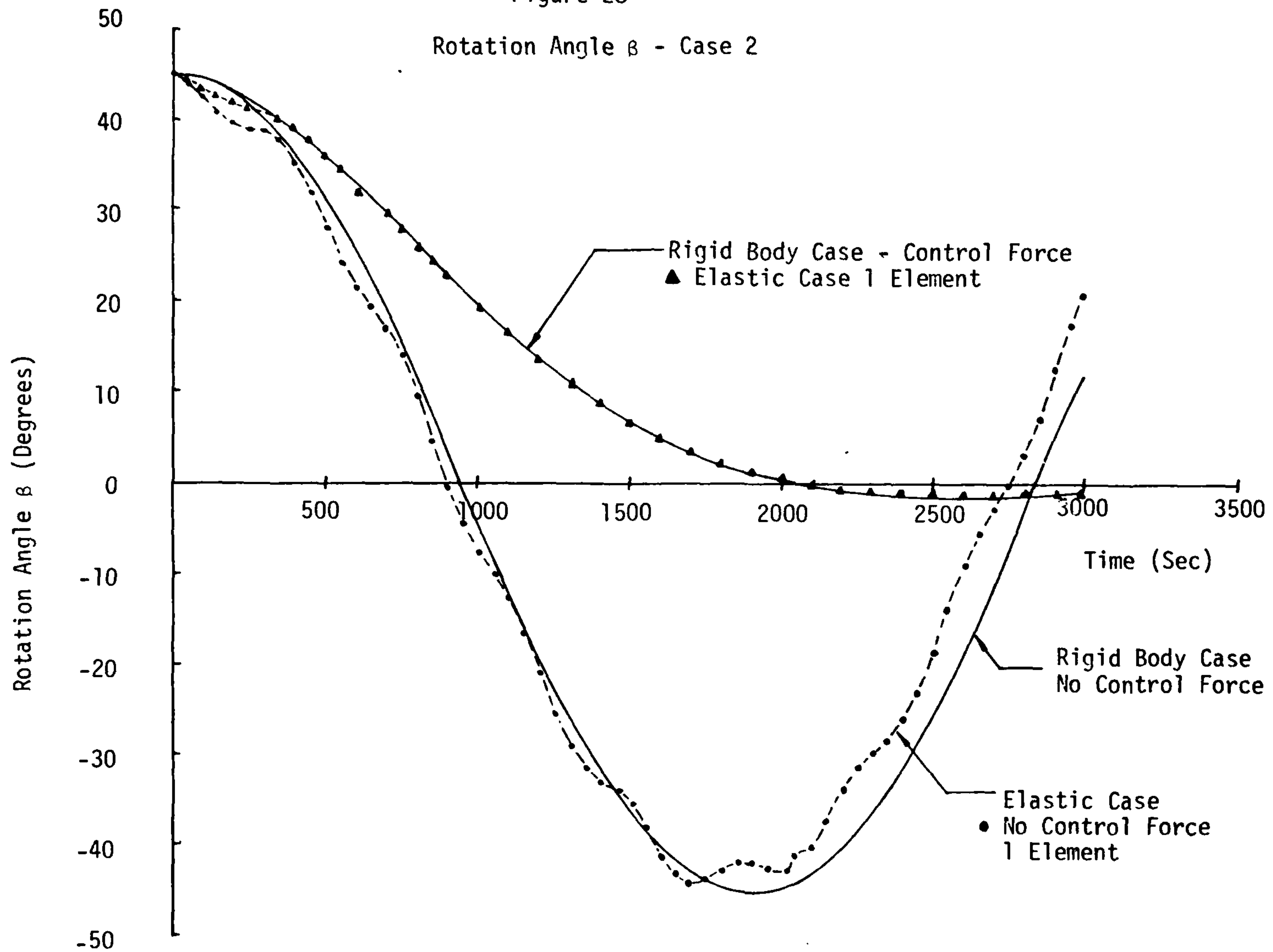

Figure 29

Beam Tip Displacement - Case 2
1 Element
No Control Force

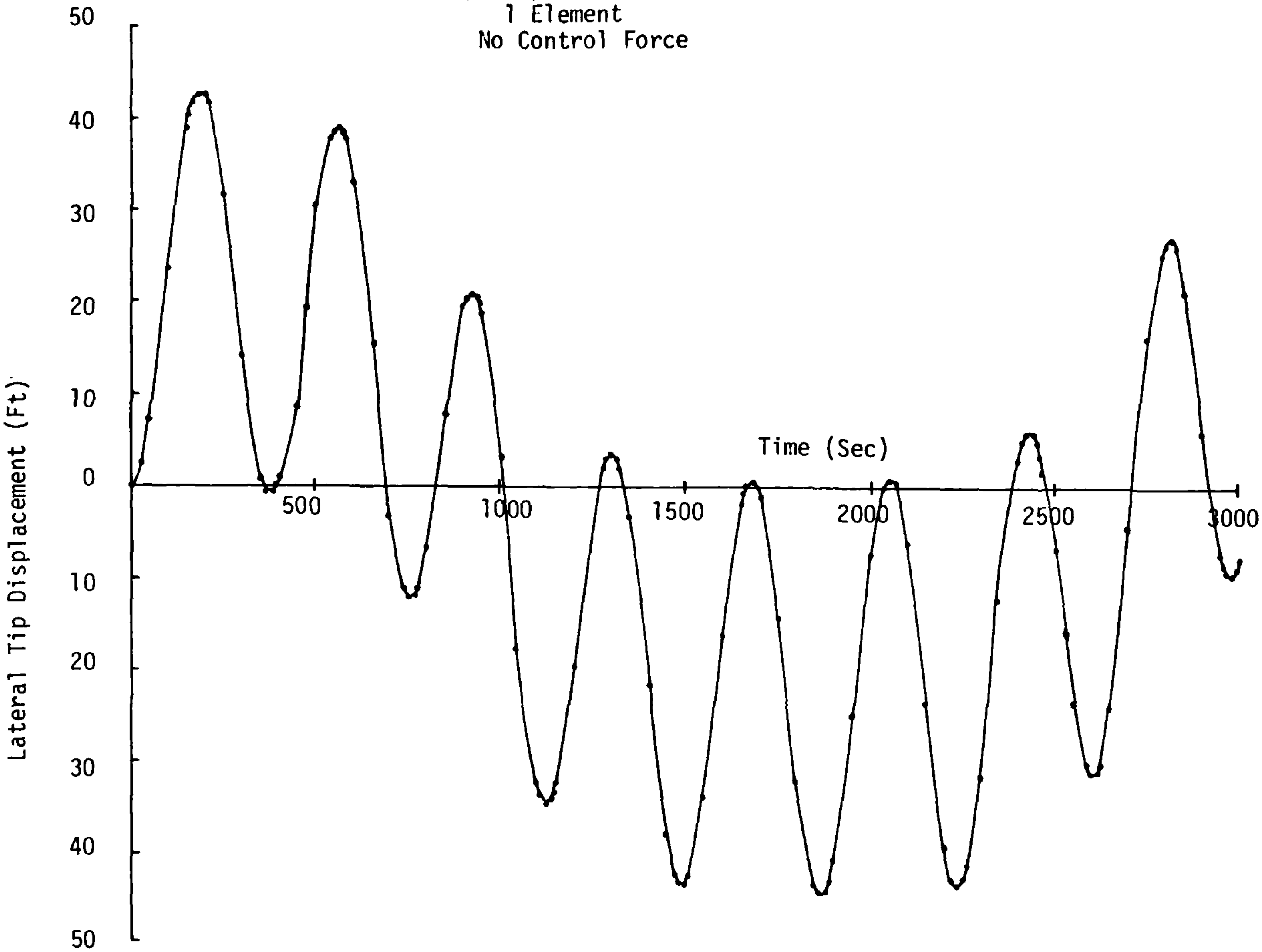

APPENDIX A - ORIENTATION MATRICES AND VECTORS

Let $\underline{a}_1$, $\underline{a}_2$, and $\underline{a}_3$ be a set of mutually orthogonal axes fixed in the undeformed beam, centered at the centroid of the cross-section with $\underline{a}_1$ tangent to the longitudinal axis of the beam. Also, ${}^o\theta_1$ ${}^o\theta_2$, and ${}^o\theta_3$ represent the space-three 1-2-3 orientation angles of the beam. Let d_{ij} and e_{ij} be the ij^{th} element of the matrices $\underline{D}$ and $\underline{E}$ respectively. Then these elements are as follows for $k = 1,2,3$.

$$d_{k1} = (\sin{}^o\theta_2 \cos{}^o\theta_1 \cos{}^o\theta_3 + \sin{}^o\theta_1 \sin{}^o\theta_3)\, a_{1k} + (\sin{}^o\theta_2 \sin{}^o\theta_3 \cos{}^o\theta_1 - \sin{}^o\theta_1 \cos{}^o\theta_3)\, a_{2k} + \cos{}^o\theta_1 \cos{}^o\theta_2\, a_{3k} \tag{A1}$$

$$d_{k2} = \sin{}^o\theta_1 \cos{}^o\theta_2 \cos{}^o\theta_3\, a_{1k} + \sin{}^o\theta_1 \sin{}^o\theta_3 \cos{}^o\theta_2\, a_{2k} - \sin{}^o\theta_2 \sin{}^o\theta_1\, a_{3k} \tag{A2}$$

$$d_{k3} = -(\sin{}^o\theta_1 \sin{}^o\theta_2 \sin{}^o\theta_3 + \cos{}^o\theta_1 \cos{}^o\theta_3)\, a_{1k} + (\sin{}^o\theta_1 \sin{}^o\theta_2 \cos{}^o\theta_3 - \sin{}^o\theta_3 \cos{}^o\theta_1)\, a_{2k} \tag{A3}$$

$$e_{k1} = (-\sin{}^o\theta_1 \sin{}^o\theta_2 \cos{}^o\theta_3 + \sin{}^o\theta_3 \cos{}^o\theta_1)\, a_{1k} - (\sin{}^o\theta_1 \sin{}^o\theta_2 \sin{}^o\theta_3 + \cos{}^o\theta_1 \cos{}^o\theta_3)\, a_{2k} - \sin{}^o\theta_1 \cos{}^o\theta_2\, a_{3k} \tag{A4}$$

$$e_{k2} = \cos{}^o\theta_1 \cos{}^o\theta_2 \cos{}^o\theta_3\, a_{1k} + \cos{}^o\theta_1 \sin{}^o\theta_3 \cos{}^o\theta_2\, a_{2k} - \sin{}^o\theta_2 \cos{}^o\theta_1\, a_{3k} \tag{A5}$$

$$e_{k3} = (-\cos{}^o\theta_1 \sin{}^o\theta_2 \sin{}^o\theta_3 + \sin{}^o\theta_1 \cos{}^o\theta_3)\, a_{1k} + (\cos{}^o\theta_1 \sin{}^o\theta_2 \cos{}^o\theta_3 + \sin{}^o\theta_1 \sin{}^o\theta_3)\, a_{2k} \tag{A6}$$

Also, the change in directional axes is as follows:

For k = 1,2,3

$$({}^{\circ}a_2' - a_2)_k = (\sin{}^{\circ}\theta_1 \sin{}^{\circ}\theta_2 \cos{}^{\circ}\theta_3 - \cos{}^{\circ}\theta_1 \sin{}^{\circ}\theta_3)\, a_{1k} + (\sin{}^{\circ}\theta_1 \sin{}^{\circ}\theta_2 \sin{}^{\circ}\theta_3 + \cos{}^{\circ}\theta_1 \cos{}^{\circ}\theta_3 - 1)\, a_{2k} + \sin{}^{\circ}\theta_1 \cos{}^{\circ}\theta_2\, a_{3k} \tag{A7}$$

$$({}^{\circ}a_3' - a_3)_k = (\cos{}^{\circ}\theta_1 \sin{}^{\circ}\theta_2 \cos{}^{\circ}\theta_3 + \sin{}^{\circ}\theta_1 \sin{}^{\circ}\theta_3)\, a_{1k} + (\cos{}^{\circ}\theta_1 \sin{}^{\circ}\theta_2 \sin{}^{\circ}\theta_3 - \sin{}^{\circ}\theta_1 \cos{}^{\circ}\theta_3)\, a_{2k} + (\cos{}^{\circ}\theta_1 \cos{}^{\circ}\theta_2 - 1)\, a_{3k} \tag{A8}$$

Note that eqs. (A7) and (A8) are related to the $\underline{D}$ and $\underline{E}$ matrices as follows:

$$\frac{\partial}{\partial {}^{\circ}\theta_i} ({}^{\circ}a_2' - a_2)_k = d_{ik} \qquad i,k = 1,2,3 \tag{A9}$$

$$\frac{\partial}{\partial {}^{\circ}\theta_i} ({}^{\circ}a_3' - a_3)_k = e_{ik} \qquad i,k = 1,2,3 \tag{A10}$$

Finally, the transformation matrix $\underline{T}$ between local and global stresses and strains is as follows:

$$\underline{T} = \begin{bmatrix} a_{11}^2 & a_{12}^2 & a_{13}^2 & 2a_{11}a_{12} & 2a_{11}a_{13} & 2a_{12}a_{13} \\ 2a_{11}a_{21} & 2a_{12}a_{22} & 2a_{13}a_{23} & a_{11}a_{22}+a_{12}a_{21} & a_{11}a_{23}+a_{13}a_{21} & a_{12}a_{23}+a_{13}a_{22} \\ 2a_{11}a_{31} & 2a_{12}a_{32} & 2a_{13}a_{33} & a_{11}a_{32}+a_{12}a_{31} & a_{11}a_{33}+a_{13}a_{31} & a_{12}a_{33}+a_{13}a_{32} \end{bmatrix} \tag{A11}$$

APPENDIX B

ELEMENTS OF MATRICES OF WHICH THE STIFFNESS MATRIX IS COMPOSED

The $\underline{D}^k$ Matrix

$$\underline{D}^k = \underline{D}_o^k(\xi) + y\,\underline{D}_y^k(\xi) + z\,\underline{D}_z^k(\xi) \qquad k = 1,2,3$$

The $\underline{D}_o^k$, $\underline{D}_y^k$, and $\underline{D}_z^k$ are partitioned into three 3 x 6 submatrices as follows:

$$\underline{D}_o^k = [(\underline{D}_o^k)_1 \ (\underline{D}_o^k)_2 \ (\underline{D}_o^k)_3] \tag{B1}$$

$$\underline{D}_y^k = [(\underline{D}_y^k)_1 \ (\underline{D}_y^k)_2 \ (\underline{D}_y^k)_3] \tag{B2}$$

$$\underline{D}_z^k = [(\underline{D}_z^k)_1 \ (\underline{D}_z^k)_2 \ (\underline{D}_z^k)_3] \tag{B3}$$

Now, let $(d_{rs})_i$ and $(e_{rs})_i$ be the elements of the $\underline{D}_i$ ad $\underline{E}_i$ matrices respectively (see Appendix A) and N_i be the ith shape function, then for i,k = 1,2,3

$$(\underline{D}_0^1)i = \begin{bmatrix} \frac{\partial N_i}{\partial \xi} & 0 & 0 & 0 & 0 & 0 \\ 0 & 0 & 0 & N_i(d_{11})_i & N_i(d_{12})_i & N_i(d_{13})_i \\ 0 & 0 & 0 & N_i(e_{11})_i & N_i(e_{12})_i & N_i(e_{13})_i \end{bmatrix} \tag{B4}$$

$$(\underline{D}_0^2)_i = \begin{bmatrix} 0 & \frac{\partial N_i}{\partial \xi} & 0 & 0 & 0 & 0 \\ 0 & 0 & 0 & N_i(d_{21})_i & N_i(d_{22})_i & N_i(d_{23})_i \\ 0 & 0 & 0 & N_i(e_{21})_i & N_i(e_{22})_i & N_i(e_{23})_i \end{bmatrix} \tag{B5}$$

$$(\underline{D}_0^3)_i = \begin{bmatrix} 0 & 0 & \frac{\partial N_i}{\partial \xi} & 0 & 0 & 0 \\ 0 & 0 & 0 & N_i(d_{31})_i & N_i(d_{32})_i & N_i(d_{33})_i \\ 0 & 0 & 0 & N_i(e_{31})_i & N_i(e_{32})_i & N_i(e_{33})_i \end{bmatrix} \tag{B6}$$

$$(\underline{D}_y^k)_i = \begin{bmatrix} 0 & 0 & 0 & \frac{\partial N_i}{\partial \xi}(d_{k1})_i & \frac{\partial N_i}{\partial \xi}(d_{k2})_i & \frac{\partial N_i}{\partial \xi}(d_{k3})_i \\ 0 & 0 & 0 & 0 & 0 & 0 \\ 0 & 0 & 0 & 0 & 0 & 0 \end{bmatrix} \tag{B7}$$

$$(\underline{D}_z^k)_i = \begin{bmatrix} 0 & 0 & 0 & \frac{\partial N_i}{\partial \xi}(e_{k1})_i & \frac{\partial N_i}{\partial \xi}(e_{k2})_i & \frac{\partial N_i}{\partial \xi}(e_{k3})_i \\ 0 & 0 & 0 & 0 & 0 & 0 \\ 0 & 0 & 0 & 0 & 0 & 0 \end{bmatrix} \tag{B8}$$

The $\underline{D}_\varepsilon$ Matrix

First, rewrite eqs. (3.64)-(3.66) as follows for k = 1,2,3:

$$\frac{\partial\, {}^{o}u_k}{\partial \xi} = h_{o_k} + y\, h_{oy_k} + z\, h_{oz_k} \tag{B9}$$

$$\frac{\partial\, {}^{o}u_k}{\partial y} = h_{y_k} \tag{B10}$$

$$\frac{\partial\, {}^{o}u_k}{\partial z} = h_{z_k} \tag{B11}$$

where

$$h_{o_k} = \sum_{i=1}^{3} \frac{\partial N_i}{\partial \xi} ({}^{\circ}u_{ok})_i \tag{B12}$$

$$h_{oy_k} = \sum_{i=1}^{3} \frac{\partial N_i}{\partial \xi} ({}^{\circ}a'_{2k} - a_{2k})_i \tag{B13}$$

$$h_{oz_k} = \sum_{i=1}^{3} \frac{\partial N_i}{\partial \xi} ({}^{\circ}a'_{3k} - a_{3k})_i \tag{B14}$$

$$h_{yk} = \sum_{i=1}^{3} N_i(\xi)\ ({}^{\circ}a'_{2k} - a_{2k})_i \tag{B15}$$

$$h_{zk} = \sum_{i=1}^{3} N_i(\xi)\ ({}^{\circ}a'_{3k} - a_{3k})_i \tag{B16}$$

Let the inverse of the Jacobian matrix be represented as follows:

$$\underline{J}^{-1} = \begin{bmatrix} L_{11} & L_{12} & L_{13} \\ L_{21} & L_{22} & L_{23} \\ L_{31} & L_{32} & L_{33} \end{bmatrix} \tag{B17}$$

Note that $\underline{J}^{-1}$ will be a constant. Thus the derivatives $\{\frac{\partial^{\circ}u}{\partial X}\}$ can be written using eq. (55) as follows:

$$\frac{\partial^{\circ}u_k}{\partial X_j} = {}^{\circ}\ell_{kj} + y\ {}^{y}\ell_{kj} + z\ {}^{z}\ell_{kj} \qquad k,j = 1,2,3 \tag{B18}$$

$${}^{\circ}\ell_{kj} = L_{j1}\ h_{ok} + L_{j2}\ h_{yk} + L_{j3}\ h_{zk} \tag{B19}$$

$${}^{y}\ell_{kj} = L_{j1}\ h_{oy_k} \tag{B20}$$

$${}^{z}\ell_{kj} = L_{j1}\ h_{oz_k} \tag{B21}$$

Finally, by substituting the derivatives in eq. (B18) into the expressions for $\underline{D}_\varepsilon$ given in eq. (3.52), the elements of $\underline{D}_{\varepsilon o}$, $\underline{D}_{\varepsilon y}$, and $\underline{D}_{\varepsilon z}$ can be given as follows:

$$\underline{D}_{\varepsilon o} = \begin{bmatrix} 1+{}^{o}\ell_{11} & 0 & 0 & {}^{o}\ell_{21} & 0 & 0 & {}^{o}\ell_{31} & 0 & 0 \\ 0 & {}^{o}\ell_{12} & 0 & 0 & 1+{}^{o}\ell_{22} & 0 & 0 & {}^{o}\ell_{32} & 0 \\ 0 & 0 & {}^{o}\ell_{13} & 0 & 0 & {}^{o}\ell_{23} & 0 & 0 & 1+{}^{o}\ell_{33} \\ {}^{o}\ell_{12} & 1+{}^{o}\ell_{11} & 0 & 1+{}^{o}\ell_{22} & {}^{o}\ell_{21} & 0 & {}^{o}\ell_{32} & {}^{o}\ell_{31} & 0 \\ {}^{o}\ell_{13} & 0 & 1+{}^{o}\ell_{11} & {}^{o}\ell_{23} & 0 & {}^{o}\ell_{21} & 1+{}^{o}\ell_{33} & 0 & {}^{o}\ell_{31} \\ 0 & {}^{o}\ell_{13} & {}^{o}\ell_{12} & 0 & {}^{o}\ell_{23} & 1+{}^{o}\ell_{22} & 0 & 1+{}^{o}\ell_{33} & {}^{o}\ell_{32} \end{bmatrix} \tag{B22}$$

$$\underline{D}_{\varepsilon y} = \begin{bmatrix} {}^{y}\ell_{11} & 0 & 0 & {}^{y}\ell_{21} & 0 & 0 & {}^{y}\ell_{31} & 0 & 0 \\ 0 & {}^{y}\ell_{12} & 0 & 0 & {}^{y}\ell_{22} & 0 & 0 & {}^{y}\ell_{32} & 0 \\ 0 & 0 & {}^{y}\ell_{13} & 0 & 0 & {}^{y}\ell_{23} & 0 & 0 & {}^{y}\ell_{33} \\ {}^{y}\ell_{12} & {}^{y}\ell_{11} & 0 & {}^{y}\ell_{22} & {}^{y}\ell_{21} & 0 & {}^{y}\ell_{32} & {}^{y}\ell_{31} & 0 \\ {}^{y}\ell_{13} & 0 & {}^{y}\ell_{11} & {}^{y}\ell_{23} & 0 & {}^{y}\ell_{21} & {}^{y}\ell_{33} & 0 & {}^{y}\ell_{31} \\ 0 & {}^{y}\ell_{13} & {}^{y}\ell_{12} & 0 & {}^{y}\ell_{23} & {}^{y}\ell_{22} & 0 & {}^{y}\ell_{33} & {}^{y}\ell_{32} \end{bmatrix} \tag{B23}$$

$$\underline{D}_{\varepsilon z} = \begin{bmatrix} {}^{z}\ell_{11} & 0 & 0 & {}^{z}\ell_{21} & 0 & 0 & {}^{z}\ell_{31} & 0 & 0 \\ 0 & {}^{z}\ell_{12} & 0 & 0 & {}^{z}\ell_{22} & 0 & 0 & {}^{z}\ell_{32} & 0 \\ 0 & 0 & {}^{z}\ell_{13} & 0 & 0 & {}^{z}\ell_{23} & 0 & 0 & {}^{z}\ell_{33} \\ {}^{z}\ell_{12} & {}^{z}\ell_{11} & 0 & {}^{z}\ell_{22} & {}^{z}\ell_{21} & 0 & {}^{z}\ell_{32} & {}^{z}\ell_{31} & 0 \\ {}^{z}\ell_{13} & 0 & {}^{z}\ell_{11} & {}^{z}\ell_{23} & 0 & {}^{z}\ell_{21} & {}^{z}\ell_{33} & 0 & {}^{z}\ell_{31} \\ 0 & {}^{z}\ell_{13} & {}^{z}\ell_{12} & 0 & {}^{z}\ell_{23} & {}^{z}\ell_{22} & 0 & {}^{z}\ell_{33} & {}^{z}\ell_{32} \end{bmatrix} \tag{B24}$$

APPENDIX C

DETAILS OF MATRICES AND VECTORS USED IN THE MOMENTUM EQUATIONS

LINEAR MOMENTUM EQUATION

The Element $\underline{P}$ Matrix (18x3)

$$\underline{P}_e = \int_{V_e} \rho \, \underline{N}^{*T} \, dV \qquad \text{(C1)}$$

Substituting eqs. (3.18) and (3.13) into eq. (C1) and carrying out the volume integral results in the following 18 x 3 matrix for P:

$$\underline{P}_e^T = \frac{\rho A \ell}{6} [\underline{I}_3 \;\; 0 \;\; 4\underline{I}_3 \;\; 0 \;\; \underline{I}_3 \;\; 0] \qquad \text{(C2)}$$

where ℓ = Beam element length

$\underline{I}_3$ = 3 x 3 Indentity Matrix

$\underline{0}$ = 3 x 3 Null Matrix

The $\underline{G}$ Matrix (3X3)

$$\underline{G}^T = + \int_v \rho \, \underline{\overline{r}} \, dv = + \int_v \rho(\underline{\overline{r}}_0 + {}^\circ\underline{\overline{u}} + \Delta\underline{\overline{u}}) \, dv \qquad \text{(C3)}$$

$$\underline{G}^T = \int_v \rho \, \underline{\overline{r}}_0 \, dv + \int_v \rho \, {}^\circ\underline{\overline{u}} \, dv + \int_v \rho \, \Delta\underline{\overline{u}} \, dv \qquad \text{(C4)}$$

Now,

$$\underline{G}_0^T = \int_v \rho \, \underline{\overline{r}}_0 \, dv = \text{Matrix of Center of Mass Position at } t = 0 \qquad \text{(C5)}$$

In many cases $\underline{G}_0 = 0$. Substituting eqs. (3.14), (3.17), (3.18)-(3.21) into eq. (C4) and integrating over the volume results in the following:

$$\underline{G}^T = \underline{G}_o^T + M\,\overline{\underline{u}}_G \tag{C6}$$

where M = Total Mass

$$\underline{u}_G = \frac{1}{M}\int_V \rho(^{\circ}\underline{u} + \Delta\underline{u})dv = \frac{1}{M}\,\underline{P}^T\,(^{\circ}\underline{q} + \Delta\underline{q}) \tag{C7}$$

Note that $\underline{u}_G$ is the change in the center of mass from the initial undeformed state. Eq. (C6) can be simplified to eq. (C8). Note also that the use of the $\underline{P}$ matrix is after its assembly.

$$\underline{G}^T = M\,\overline{\underline{r}}_G \tag{C8}$$

where

$$\overline{\underline{r}}_G = \overline{\underline{r}}_{G_o} + \overline{\underline{u}}_G \tag{C9}$$

$$\underline{r}_{G_o} = \frac{1}{M}\int_V \rho\,\underline{r}_o\,dv \tag{C10}$$

<u>The $\underline{f}_c$ Force Vector (3x1)</u>

$$\underline{f}_c = \overline{\underline{\Omega}}^2\int_V \rho\,\underline{r}\,dv = \overline{\underline{\Omega}}^2\int_V \rho(\underline{r}_o + {}^{\circ}\Delta\underline{u} + \Delta\underline{u})\,dv \tag{C11}$$

Using eq. (C7) and (C10), eq. (C11) becomes

$$\underline{f}_c = M\,\overline{\underline{\Omega}}^2\,\underline{r}_G \tag{C12}$$

<u>ANGULAR MOMENTUM EQUATION</u>

<u>The $\underline{I}_T$ Matrix (3x3)</u>

$$\underline{I}_T = -\int_V \rho\,\overline{\underline{r}}^2\,dv = -\int_{V_R} \rho\,\overline{\underline{r}}^2\,dv - \sum_{i=1}^{N}\int_{V_i} \rho\,\overline{\underline{r}}^2\,dv \tag{C13}$$

In these integrals, V_R represents an integral over any rigid parts of the body and the summation is over all the elements. The position vector of a general point in the cross section of the i^{th} element can be written as follows:

$$\underline{r} = {}^\circ\underline{r} + y\,{}^\circ\underline{a}_2' + z\,{}^\circ\underline{a}_3' \tag{C14}$$

where $${}^\circ\underline{r} = {}^\circ\underline{r}_o + {}^\circ\underline{u}_o \tag{C15}$$

As before, ${}^\circ\underline{r}_o$ represents the undeformed position vector of the centerline of the beam element and ${}^\circ\underline{u}_o$ is the initial displacement vector of the centerline. The $\Delta\underline{u}$ vector is neglected in these integrals since it is small and the terms are of second order. Using eqs. (3.12) and (3.14), $^\circ r$ is written as follows:

$${}^\circ\underline{r} = \sum_{j=1}^{3} N_j(\xi)({}^\circ\underline{r}_o + {}^\circ\underline{u}_o)_j \tag{C16}$$

where $${}^\circ\underline{u}_{oj}^T = [{}^\circ q_{o6j-5} \;\; {}^\circ q_{o6j-4} \;\; {}^\circ q_{o6j-3}] \tag{C17}$$

Note that ${}^\circ\underline{u}_{oj}$ are the x_1, x_2, and x_3 displacements of the jth node. Similar expressions exist for ${}^\circ\underline{a}_2'$ and ${}^\circ\underline{a}_3'$ as follows:

$${}^\circ\underline{a}_2' \quad \sum_{j=1}^{3} N_j(\xi)\; {}^\circ\underline{a}_{2j}' \tag{C18}$$

$${}^\circ\underline{a}_3' = \sum_{i=1}^{3} N_j(\xi)\; {}^\circ\underline{a}_{3j}' \tag{C19}$$

The ${}^\circ\underline{a}_{2j}'$ and ${}^\circ\underline{a}_{3j}'$ terms can be evaluated using eqs. (A7) and (A8).

Thus, the finite element approximation to $\underline{r}$ is found by substituting eqs. (C16)-(C19) into eq. (C14):

$$\underline{r} = \sum_{j=1}^{3} N_j(\xi)\ ({}^{\circ}\underline{r}_o + {}^{\circ}\underline{u}_o + y{}^{\circ}\underline{a}_2' + z{}^{\circ}\underline{a}_3')_j \tag{C20}$$

If eq. (C14) is substituted into eq. (C13) and the area integrals carried out, then

$$\underline{I}_T = \underline{I}_R - \sum_{i=1}^{N} [\rho A_i \int_{L_i} {}^{\circ}\underline{\tilde{r}}^2\, d\ell + \rho\, I_{zz_i} \int_{L_i} ({}^{\circ}\underline{\tilde{a}}_2')^2\, d\ell + \rho\, I_{yy_i} \int_{L_i} ({}^{\circ}\underline{\tilde{a}}_3')^2\, d\ell] \tag{C21}$$

The $\underline{I}_R$ matrix is the inertia matrix for the rigid parts of the structure which is found in the usual way. The integrals along the length of the beam in eq. (C21) are evaluated numerically. They can be done exactly using three point Gaussian integration:

$$\int_{L_i} {}^{\circ}\underline{\tilde{r}}^2\, d\ell = \frac{\ell_i}{2} \sum_{k=1}^{3} {}^{\circ}\underline{\tilde{r}}^2(\xi_k)\ H_k \tag{C22}$$

$$\int_{L_i} {}^{\circ}\underline{\tilde{a}}_r'^{\,2}\, d\ell = \frac{\ell_i}{2} \sum_{k=1}^{3} {}^{\circ}\underline{\tilde{a}}'^{\,2}\ (\xi_k)\ H_k \qquad r = 2,3 \tag{C23}$$

The ${}^{\circ}\underline{\tilde{r}}(\xi_k)$ and ${}^{\circ}\underline{\tilde{a}}'^{\,2}(\xi_k)$ matrices can be evaluated by using eqs. (C16) - (C19) with $\xi = \xi_k$.

<u>The Element $\underline{H}$ Matrix (18x3)</u>

$$\underline{H}_T = \int_{V_e} \rho\, \underline{\tilde{r}}\, \underline{N}^*\, dV \tag{C24}$$

Substitute eqs. (3.18) and (C14) into (C24) and integrate to obtain the following for the i^{th} element:

$$\underline{H}^T = \rho A_i \int_{L_i} {}^\circ\underline{\overline{r}}^2 \, \underline{N}_o^* \, d\ell + \rho \, I_{zz_i} \int_{L_i} {}^\circ\underline{\overline{a}}_2' \, \underline{N}_y^* \, d\ell + \rho \, I_{yy_i} \int_{L_i} {}^\circ\underline{\overline{a}}_3' \, \underline{N}_z^* \, d\ell \tag{C25}$$

Once again eq. (C25) is evaluated numerically as follows:

$$\underline{H}^T = \frac{\rho \ell_i}{2} \sum_{k=1}^{3} [A_i {}^\circ\underline{\overline{r}}(\xi_k) \underline{N}_o^*(\xi_k) + I_{zz_i} {}^\circ\underline{\overline{a}}_2'(\xi_k) \underline{N}_y^*(\xi_k) + I_{yy_i} {}^\circ\underline{\overline{a}}_3'(\xi_k) \underline{N}_z^*(\xi_k)] H_k \tag{C26}$$

The $\underline{H}$ matrix is assembled in the usual way.

<u>The $\underline{M}_{cent}$ Vector (3x1)</u>

$$\underline{M}_{cent} = \int_v \rho \, \underline{\overline{r}} \, \underline{\overline{\Omega}}^2 \, \underline{r} \, dv = \int_{v_R} \rho \, \underline{\overline{r}} \, \underline{\overline{\Omega}}^2 \, \underline{r} \, dv + \sum_{i=1}^{N} \int_{v_i} \rho \, \underline{\overline{r}} \, \underline{\overline{\Omega}}^2 \, \underline{r} \, dv \tag{C27}$$

Let $$\underline{M}_{cent_R} = \int_{v_R} \rho \, \underline{\overline{r}} \, \underline{\overline{\Omega}}^2 \, \underline{r} \, dv \tag{C28}$$

It can be shown [34] that the eq. (C28) is equivalent to the following:

$$(M_{cent_R})_1 = I_{R_{12}} \, \Omega_1 \Omega_3 - I_{R_{13}} \, \Omega_1 \Omega_2 - I_{R_{23}} \, (\Omega_2^2 - \Omega_3^2) - (I_{R_{22}} - I_{R_{33}}) \, \Omega_2 \Omega_3 \tag{C29}$$

$$(M_{cent_R})_2 = I_{R_{23}} \, \Omega_1 \Omega_2 - I_{R_{12}} \, \Omega_2 \Omega_3 - I_{R_{13}} \, (\Omega_3^2 - \Omega_1^2) - (I_{R_{33}} - I_{R_{11}}) \, \Omega_3 \Omega_1 \tag{C30}$$

$$(M_{cent_R})_3 = I_{R_{13}}\ \Omega_2\Omega_3 - I_{R_{23}}\ \Omega_1\Omega_3 - I_{R_{12}}\ (\Omega_1^2-\Omega_2^2) - (I_{R_{11}}-I_{R_{22}})\ \Omega_1\Omega_2 \tag{C31}$$

Note that $I_{R_{ij}}$ are the inertias of the rigid parts of the structure. The rest of M_{cent} is found as in the previous sections, i.e., substituting eq. (C14) into eq. (C27) and integrating. Thus,

$$\underline{M}_{cent} = \underline{M}_{cent_R} + \sum_{i=1}^{N} \frac{\rho \ell_i}{2} \{ \sum_{k=1}^{3} [A_i\ {}^\circ\overline{\underline{r}}_o(\xi_k)\ \overline{\underline{\Omega}}^2\ {}^\circ\underline{r}(\xi_k)$$

$$+ I_{zz_i}\ {}^\circ\overline{\underline{a}}_2'(\xi_k)\overline{\underline{\Omega}}\,{}^\circ\underline{a}_2'(\xi_k) + I_{yy_i}\ {}^\circ\overline{\underline{a}}_3'(\xi_k)\overline{\underline{\Omega}}^2\,{}^\circ\overline{\underline{a}}_3'(\xi_k)]H_k\} \tag{C32}$$

The $\underline{M}_{cor}$ Vector (3x1)

$$\underline{M}_{cor} = \sum_{i=1}^{N} 2\int_{V_i} \rho\ \overline{\underline{r}}\ \overline{\underline{\Omega}}\ \dot{\underline{u}}\ dv \tag{C33}$$

Within an element, $\dot{\underline{u}}$ can be found using eq. (2.14):

$$\dot{\underline{u}} = \underline{N}^*\dot{\underline{q}} = (\underline{N}_o^* + y\ \underline{N}_y^* + z\ \underline{N}_z^*)\ \dot{\underline{q}} = \dot{\underline{u}}_o + y\dot{\underline{u}}_y + z\dot{\underline{u}}_z \tag{C34}$$

where

$$\dot{\underline{u}}_o = \underline{N}_o^*\ \dot{\underline{q}} \tag{C35}$$

$$\dot{\underline{u}}_y = \underline{N}_y^*\ \dot{\underline{q}} \tag{C36}$$

$$\dot{\underline{u}}_z = \underline{N}_z^*\ \dot{\underline{q}} \tag{C37}$$

Substituting eqs. (C35) - (C37) as well as eq. (C14) into eq. (C33) an integrating results in the following expression for $\underline{M}_{cor}$:

$$\underline{M}_{cor} = \sum_{i=1}^{N} \rho \ell_i \left\{ \sum_{k=1}^{3} \left[A_i \; {}^{\circ}\underline{\overline{r}}(\xi_k) \; \underline{\overline{\Omega}\dot{u}}_o(\xi_k) \right.\right.$$

$$\left.\left. + I_{zz_i} \; {}^{\circ}\underline{\overline{a}}_2'(\xi_k) \underline{\overline{\Omega}\dot{u}}_y(\xi_k) + I_{yy_i} \; {}^{\circ}\underline{\overline{a}}_3'(\xi_k) \underline{\overline{\Omega}\dot{u}}_z(\xi_k) \right] H_k \right\} \quad (C38)$$

APPENDIX D

DETAILS OF THE MATRICES AND VECTORS RESULTING FROM THE INERTIA TERM IN THE PRINCIPLE OF VIRTUAL WORK

The Element Mass Matrix $\underline{M}$ (18x18)

$$\underline{M} = \int_{V_e} \rho \, \underline{N}^{*T} \, \underline{N}^{*} \, dv \tag{D1}$$

Substitute eq. (3.18) into eq. (D1), evaluate the matrix products and integrate over the area to obtain

$$\underline{M} = \underline{M}_o + \underline{M}_y + \underline{M}_z \tag{D2}$$

where

$$\underline{M}_o = \rho A \int_L \underline{N}_o^{*T} \, \underline{N}_o^{*} \, d\ell \tag{D3}$$

$$\underline{M}_y = \rho I_{zz} \int_L \underline{N}_y^{*T} \, \underline{N}_y^{*} \, d\ell \tag{D4}$$

$$\underline{M}_z = \rho I_{yy} \int_L \underline{N}_z^{*T} \, \underline{N}_z^{*} \, d\ell \tag{D5}$$

These integrals can be evaluated analytically using the expressions for $\underline{N}_o^{*}$, $\underline{N}_y^{*}$ and $\underline{N}_z^{*}$ in eqs. (3.19) - (3.21). The results are as follows:

$$
\underline{M}_o = \frac{\rho A \ell}{30}
\begin{bmatrix}
4\underline{I}_3 & \underline{0} & 2\underline{I}_3 & \underline{0} & -\underline{I}_3 & \underline{0} \\
 & \underline{0} & \underline{0} & \underline{0} & \underline{0} & \underline{0} \\
 & & 15\underline{I}_3 & \underline{0} & 2\underline{I}_3 & \underline{0} \\
 & & & \underline{0} & \underline{0} & \underline{0} \\
 & \text{SYMMETRIC} & & & 4\underline{I}_3 & \underline{0} \\
 & & & & & \underline{0}
\end{bmatrix}
\qquad (D6)
$$

$$
\underline{M}_y = \frac{\rho I_{zz} \ell}{30}
\begin{bmatrix}
\underline{0} & \underline{0} & \underline{0} & \underline{0} & \underline{0} & \underline{0} \\
 & 4\underline{D}_1^T\underline{D}_1 & \underline{0} & 2\underline{D}_1^T\underline{D}_2 & \underline{0} & -\underline{D}_1^T\underline{D}_3 \\
 & & \underline{0} & \underline{0} & \underline{0} & \underline{0} \\
 & & & 16\underline{D}_2^T\underline{D}_2 & \underline{0} & 2\underline{D}_2^T\underline{D}_3 \\
 & \text{SYMMETRIC} & & & \underline{0} & \underline{0} \\
 & & & & & 4\underline{D}_3^T\underline{D}_3
\end{bmatrix}
\qquad (D7)
$$

$$
\underline{M}_y = \frac{\rho I_{yy} \ell}{30}
\begin{bmatrix}
\underline{0} & \underline{0} & \underline{0} & \underline{0} & \underline{0} & \underline{0} \\
 & 4\underline{E}_1^T\underline{E}_1 & \underline{0} & 2\underline{E}_1^T\underline{E}_2 & \underline{0} & -\underline{E}_1^T\underline{E}_3 \\
 & & \underline{0} & \underline{0} & \underline{0} & \underline{0} \\
 & & & 16\underline{E}_2^T\underline{E}_2 & \underline{0} & 2\underline{E}_2^T\underline{E}_3 \\
 & \text{SYMMETRIC} & & & \underline{0} & \underline{0} \\
 & & & & & 4\underline{E}_3^T\underline{E}_3
\end{bmatrix}
\qquad (D8)
$$

where $\underline{I}_3$ = 3 x 3 Identity Matrix

$\underline{0}$ = 3 x 3 Null Matrix

The Element Gyroscopic Matrix $\underline{C}$

$$\underline{C} = 2\int_{V_e} \rho\, \underline{N}^{*T}\, \underline{\bar{\Omega}}\, \underline{N}^{*}\, dv \tag{D9}$$

Using es. (3.18) in Eq. (D9) and evaluating the integral as above results in:

$$\underline{C} = \underline{C}_o + \underline{C}_y + \underline{C}_z \tag{D10}$$

$$\underline{C}_o = \frac{\rho A \ell}{15}\begin{bmatrix} 4\underline{\bar{\Omega}} & \underline{0} & 2\underline{\bar{\Omega}} & \underline{0} & -\underline{\bar{\Omega}} & \underline{0} \\ & \underline{0} & \underline{0} & \underline{0} & \underline{0} & \underline{0} \\ & & 16\underline{\bar{\Omega}} & \underline{0} & \overline{2\underline{\bar{\Omega}}} & \underline{0} \\ & \text{SYMMETRIC} & & \underline{0} & \underline{0} & \underline{0} \\ & & & & 4\underline{\bar{\Omega}} & \underline{0} \\ & & & & & \underline{0} \end{bmatrix} \tag{D11}$$

$$\underline{C}_y = \frac{\rho I_{zz} \ell}{15}\begin{bmatrix} \underline{0} & \underline{0} & \underline{0} & \underline{0} & \underline{0} & \underline{0} \\ & 4\underline{D}_1^T\underline{\bar{\Omega}}\underline{D}_1 & \underline{0} & 2\underline{D}_1^T\underline{\bar{\Omega}}\underline{D}_2 & \underline{0} & -\underline{D}_1^T\underline{\bar{\Omega}}\underline{D}_3 \\ & & \underline{0} & \underline{0} & \underline{0} & \underline{0} \\ & \text{SYMMETRIC} & & 16\underline{D}_2^T\underline{\bar{\Omega}}\underline{D}_2 & \underline{0} & 2\underline{D}_2^T\underline{\bar{\Omega}}\underline{D}_3 \\ & & & & \underline{0} & \underline{0} \\ & & & & & 4\underline{D}_3^T\underline{\bar{\Omega}}\underline{D}_3 \end{bmatrix} \tag{D12}$$

$$\underline{C}_z = \frac{\rho I_{yy} \ell}{15}\begin{bmatrix} \underline{0} & \underline{0} & \underline{0} & \underline{0} & \underline{0} & \underline{0} \\ & 4\underline{E}_1^T\underline{\bar{\Omega}}\underline{E}_1 & \underline{0} & 2\underline{E}_1^T\underline{\bar{\Omega}}\underline{E}_2 & \underline{0} & -\underline{E}_1^T\underline{\bar{\Omega}}\underline{E}_3 \\ & & \underline{0} & \underline{0} & \underline{0} & \underline{0} \\ & \text{SYMMETRIC} & & 16\underline{E}_2^T\underline{\bar{\Omega}}\underline{E}_2 & \underline{0} & 2\underline{E}_2^T\underline{\bar{\Omega}}\underline{E}_3 \\ & & & & \underline{0} & \underline{0} \\ & & & & & 4\underline{E}_3^T\underline{\bar{\Omega}}\underline{E}_3 \end{bmatrix} \tag{D13}$$

The element Force Vector Due to Centrifugal Force $\underline{F}_c$

$$\underline{F}_c = \int_{V_e} \rho\, \underline{N}^{*T}\, \overline{\underline{\Omega}}^2\, (\underline{r}_o + \underline{u}_o)\, dv \tag{D14}$$

But by using eq. (C14) and (C15),

$$\underline{r}_o + \underline{u}_o = {}^{\circ}\underline{r}_o + {}^{\circ}\underline{u}_o + y^{\circ}\underline{a}_2' + z^{\circ}\underline{a}_3' \tag{D15}$$

As in Appendix C, use numerical integration to evaluate eq. (D14):

$$\underline{F}_c = \frac{\rho \ell}{2} \sum_{k=1}^{3} [A\, \underline{N}_o^{*T}(\xi_k)\, \overline{\underline{\Omega}}^2\, {}^{\circ}\underline{r}(\xi_k) + I_{zz}\, \underline{N}_y^{*T}(\xi_k)\, \overline{\underline{\Omega}}^2\, {}^{\circ}\underline{a}_2'(\xi_k)$$

$$+ I_{yy}\, \underline{N}_z^{*T}(\xi_k)\, \overline{\underline{\Omega}}^2\, {}^{\circ}\underline{a}_3'(\xi_k)]\, H_k \tag{D16}$$

REFERENCES

1. Ashley, H., and Bisplinghoff, R. L., Principles of Aeroelasticity, John Wiley and Sons, Inc., N.Y., 1962.

2. Ashley, H., "Observations on the Dynamic Behavior of Large Flexible Bodies in Orbit," AIAA Journal, Vol. 5., No. 3, 1967, pp. 460-469.

3. McDonough, T. B., "Forumulation of the Global Equations of Motion of a Deformable Body," AIAA Journal, Vol. 14, No. 5, May 1976, pp. 656-660.

4. Fraejis de Veubeke, B., "The Dynamics of Flexible Bodies," Int. J. Eng., Sci., Vol. 14, 1976, pp. 895-913.

5. Kane, T. R., and Levinson, D. A., "Formulation of Equations of Motion for Complex Spacecraft," Journal of Guidance and Control, Vol. 3, No. 2, March-April 1980, pp. 99-112.

6. Kane, T. R. and Levinson, D. A., "Simulation of Large Motions of Nonuniform Beams in Orbit," The Journal of Astronautical Sciences, Vol. 29, No. 3, July-September 1981, pp. 213-244.

7. Santini, P., "Stability of Flexible Spacecrafts," Acta Astronautica, Vol. 3, 1976, pp. 685-731.

8. Likins, P. W., "Finite Element Appendage Equations for Hybrid Coordinate Dynamic Analysis," Int'l Journal of Solids and Structures, Vol. 8, No. 5, 1972, pp. 709-731.

9. Tsing, Gan-Tai, "Dynamical Equations of Spacecraft With Controlled Flexible Appendages Using Finite Element Approach," AIAA Paper No. 74-1261, October 1974.

10. Newton, J. K. and Farrell, J. L., "Natural Frequencies of a Flexible Gravity-Gradient Satellite," Journal of Spacecraft and Rockets, Vol. 5, No. 5, 1968, pp. 560-569.

11. Grote, P. B., McMunn, J. C. and Gluck, R., "Equations of Motion of Flexible Spacecraft," Journal of Spacecraft and Rockets, Vol. 8, No. 6, 1971, pp. 561-567.

12. Kumar, V. K. and Bainum, P. M., "Dynamics of a Flexible Body in Orbit," Journal of Guidance and Control, Vol. 3, No. 1, 1980, pp. 90-91.

13. Sellapan, R. and Bainum, P. M., "Modal Control of the Planar Motion of a Long Flexible Beam in Orbit," Acta Astronautica, Vol. 7, 1980, pp. 19-36.

14. Davis, R. M., Yong, K. and Blair, W. E., "Dynamic Behavior of an Extremely Flexible Gravity-Gradient Depole Satellite," AAS Paper No. 75-091, 1975.

15. Smart, D. R., Gill, K. F., Gething, J. M. and Holt, J. A., "Dynamic Analysis of Flexible Space Vehicles Having Uncoupled Control Axes," Aeronautical Journal, December 1974, pp. 560-569.

16. Austin, F., and Pan, H. H., "Planar Dynamics of Free Rotating Beams with Tip Masses," AIAA Journal, Vol. 8, No. 4, 1970, pp. 726-733.

17. Hughes, P. C., "Attitude Dynamics of a Three-Axis Stabilized Satellite with a Large Flexible Solar Array," Journal of the Astronautical Sciences, Vol. XX, No. 3, 1972, pp. 166-189.

18. Bathe, K. J. and Wilson, E. L., Numberical Methods in Finite Element Analysis, Prentice-Hall, 1976.

19. Gupta, K. K., "Development of a Unified Numerical Procedure for Free Vibration Analysis of Structures," Int. J. Num. Meth. Eng., Vol. 17, 1981, pp. 187-198.

20. Meirovitch, L., "A New Method of Solution of the Eigenvalue Problem for Gyroscopic Systems," AIAA Journal, Vol. 12, 1974, pp. 1339-1342.

21. Goudreau, G. L. and Taylor, R. L., "Evaluation of Numerical Integration Methods in Elastodynamics," Computer Methods in Applied Mechanics and Engineering, Vol. 2, 1972, pp. 69-97.

22. Felippa, C. A. and Park, K. C., "Direct Time Integration Methods in Nonlinear Structural Dynamics," Computer Methods in Applied Mechanics and Engineering, Vol. 17, 1979, pp. 277-313.

23. McNamara, J. F., "Solution Schemes for Problems of Nonlinear Structural Dynamics," Journal of Pressure Vessel Technology, May 1974, pp. 96-102.

24. Trujillo, D. M., "An Unconditionally Stable Explicit Algorithm for Structural Dynamics," International Journal for Numerical Methods in Engineering, Vol. 11, 1977, pp. 1579-1592.

25. Hughes, T. J. R., Pister, K. S. and Taylor, R. L., "Implicit-Explicit Finite Elements in Nonlinear Transient Analysis," Computer Methods in Applied Mechanics and Engineering," Vol. 17/18, March 1979, pp. 159-182.

26. Belytschko, T. and Mullen, R., "Staibility of Explicit-Implicit Mesh Partition in Time Integration," International Journal for Numerical Methods in Engineering," Vol. 12, 1978, pp. 1575-1586.

27. Cescotto, S., Frey, F., and Fonder, G., "Total and Updated Lagrangian Description in Nonlinear Structural Analysis: A Unified Approach," Energy Methods in Finite Element Analysis, edited by Glowinski, R., Rodin, E. Y., and Zienkiewicz, O. C., John Wiley & Sons, 1978.

28. Zienkiewicz, O. C., The Finite Element Method in Engineering Science, McGraw-Hill, 1971.

29. Zienkiewicz, O. C., Too, J. and Taylor, R. L., "Reduced Integration Technique in General Analysis of Plates and Shells," International Journal for Numerical Methods in Engineering, Vol. 3, 1971, pp. 275-290.

30. Hughes, T. J. R., Cohen, M. and Haroun, M., "Reduced and Selective Integration Techniques in the Finite Element Analysis of Plates," Nuclear Engineering and Design, Vol. 4, 1978, pp. 203-222.

31. Krieg, R. D., "Unconditional Stability in Numerical Time Integration Methods," Journal of Applied Mechanics, Vol. 40, 1973, pp. 417-421.

32. Fu, C. C., "On the Stability of Explicit Methods for the Numerical Integrations of the Equations of Motion in Finite Element Methods," International Journal for Numerical Methods in Engineering, Vol. 4, 1972, pp. 95-107.

33. Newmark, N. M., "A Method of Computation for Structural Dynamics," Proceedings of the ASCE, Vol. 85, No. EM3, 1959, pp. 67-94.

34. Kane, T. R., Likins, P. W., Levinson, D. A., Spacecraft Dynamics, McGraw-Hill, 1983.

35. Kaplan, M. H., Modern Spacecraft Dynamics and Control, John Wiley and Sons, 1976.

END

FILMED

4-85

DTIC